Volume 48, December 2014

New Mexico Journal Of Science

WATER, ENERGY, AND THE ENVIRONMENT

Kurt S. J. Anderson
Editor

THE NEW MEXICO ACADEMY OF SCIENCE

Volume 48, December 2014
The New Mexico Journal of Science

WATER, ENERGY, AND THE ENVIRONMENT

The *New Mexico Journal of Science* is a publication of the New Mexico Academy of Science. Each issue of the Journal, which has been published since 1906, usually contains research papers and review articles deemed of interest to the scientists, educators, and citizens of New Mexico. Some volumes have addressed topics of social or economic interest to the state while others have emphasized scientific areas in which New Mexico is particularly active. This year's *Journal* deviates somewhat from that tradition.

This volume of the *New Mexico Journal of Science* is subtitled "Water, Energy, and the Environment". The first part contains abstracts for the oral and poster papers presented at the New Mexico Academy of Science Research Symposium which was held in Albuquerque, New Mexico on 1 November 2014. These presentations represent some of the scientific research being conducted by undergraduate and graduate students at New Mexico's colleges and universities. The New Mexico Academy of Science also oversees a New Mexico Junior Academy of Science program that sponsors an annual statewide scientific paper competition for students in New Mexico's high schools. The final part of this *Journal* contains a selection of research papers from this competition.

We wish to acknowledge the several organizations which co-sponsored the 2014 Research Symposium: the New Mexico Alliance for Minority Participation (NM AMP), the New Mexico Experimental Program to Stimulate Competitive Research (NM EPSCoR), and the New Mexico Partnership for Math and Science Education (NMPMSE). The Editor also wishes to acknowledge the assistance of Ms. Natalie Willoughby of NM EPSCoR in preparing this volume of the *Journal*.

The *New Mexico Journal of Science* is published in an electronic-only format; it can be freely downloaded from the Academy's website at http://www.nmas.org. This enables the Academy to reach a much wider readership without incurring the considerable costs associated with the production and mailing of paper copies.

Kurt S. J. Anderson, Editor
New Mexico Journal of Science

Professor of Astronomy, Emeritus
Department of Astronomy
New Mexico State University
kurt@nmsu.edu

TABLE OF CONTENTS

ABOUT THE SYMPOSIUM

The 2014 New Mexico Academy of Science Research Symposium ("Where Science, Education, and Research Meet") was held in Albuquerque on 1 November 2014. The Symposium was sponsored by the New Mexico Academy of Science (NMAS), the New Mexico Alliance for Minority Participation (NM AMP), the New Mexico Experimental Program to Stimulate Competitive Research (NM EPSCoR), and the New Mexico Partnership for Math and Science Education (NMPMSE). The Symposium schedule included twenty-five oral presentations and 31 poster offerings from the students and faculty of New Mexico's universities and colleges. Dr. Abraham Ellis provided the luncheon keynote address. Abstracts of these presentations are included in this annual volume of the NMAS New Mexico Journal of Science.

The Symposium closed with the presentation of awards for what were judged to be the best undergraduate and graduate posters and with the New Mexico Academy of Science's two annual awards for Outstanding Science Teaching.

KEYNOTE ADDRESS

Dr. Abraham Ellis, Sandia National Laboratory

Renewable Energy Potential and Technical Challenges

New Mexico has significant potential for development of renewable energy resources like wind and solar. These are more sustainable than the alternatives from an environmental point of view, as they do not consume water or produce emissions locally. However, how much wind and solar can be developed in New Mexico considering cost to connect to the grid and deliver to load and the challenges associated with managing variability and uncertainty of the output? In this presentation, we will discuss what we have learned from rapid deployment of wind and solar generation over the last decade, and how the industry and technology has evolved to get ready for an even more significant wave of photovoltaic and wind deployment in the future. We will discuss how Smart Grid technologies such as storage (batteries) can help.

About Keynote Speaker

Abraham Ellis received his BS, MS, and PhD degrees in electrical engineering, specializing in power systems and renewable, from New Mexico State University. Dr. Ellis has over 15 years experience in power system analysis and simulation to support bulk system planning and operations. He worked for 8 years as lead transmission planner for Public Service Company of New Mexico, where he led integration and interconnection study activities for conventional and renewable generation. Dr. Ellis joined Sandia in 2008 as a Principal Member of Technical Staff, and currently serves as acting manager for the PV and Distributed Applications Department. He is the technical lead for renewable systems integration at Sandia. Dr. Ellis chairs the Renewable Modeling Task Force (REMTF) of the Western Electricity Coordinating Council (WECC), is a senior member of IEEE, and is actively involved in a number of activities related to renewable energy integration and modeling, under IEEE, NERC, UWIG, IEC and WECC.

ABOUT THE SPONSORS

The New Mexico Academy of Science

Founded in 1902, the New Mexico Academy of Science has been in continuous existence since 1915. The Academy is a member of the National Association of Academies of Science (NAAS) and an affiliate of the American Association for the Advancement of Science (AAAS). The New Mexico Academy of Science works with teachers, state agencies, and the legislature to establish appropriate standards for the teaching of the sciences. The Academy can also act as a resource center, providing scientific advice and expertise to these groups and others. The Academy Goals are to foster scientific research and scientific cooperation, increase public awareness of the role of science in human progress and human welfare, and promote science education in New Mexico. Membership is open to any person or organization engaged in or interested in scientific research, scientific education, or the goals and activities of the Academy. Visit www.nmas.org to learn more about NMAS.

New Mexico Experimental Program to Stimulate Competitive Research

The New Mexico Experimental Program to Stimulate Competitive Research (NM EPSCoR) is funded by the National Science Foundation (NSF) to build the state's capacity to conduct research. Faculty and students from New Mexico universities and colleges are working to realize the state's potential for sustainable energy development, and cultivating a well-qualified Science, Technology, Engineering and Mathematics (STEM) workforce while supporting a culture of innovation and entrepreneurship. The infrastructure and activities of the Energize New Mexico grant are designed to support shared-use equipment, engage new research and community college faculty, and support the STEM pipeline by training teachers, undergraduate and graduate students, and post-doctoral fellows. Research findings will be communicated broadly through new partnerships with New Mexico's museum network, a citizen-centric web portal, and vibrant, experiential programs targeting K-12 students. Visit www.nmepscor.org to learn more about NM EPSCoR.

The New Mexico Alliance for Minority Participation

Established in 1993 with major funding from the NSF, the New Mexico AMP program is a partnership of the state's two- and four-year colleges and universities, with a primary goal of increasing the number of B.S. degrees awarded to under-represented students in New Mexico. NM AMP supports students with scholarships; research assistantships; professional development; and enhanced teaching, learning, and mentoring experiences. Program activities are designed to attend to individual student retention, development, and progression; support student progression to the STEM workforce and graduate school; and promote the replication of best practices, both within New Mexico and nationally. Since program inception, New Mexico has seen increases in the number of science degrees earned by under-represented students at the state's public 4-year universities, thereby increasing diversity in STEM. To learn more, visit www.nmsu.edu/~nmamp/.

The New Mexico Partnership for Math & Science Education

The New Mexico Partnership for Math and Science Education (NMPMSE) is a clearinghouse and network for STEM education initiatives in New Mexico. The statewide membership organization aims to promote coherence and quality of STEM education initiatives through dissemination of information, networking, coordination, and collaboration so that New Mexico will become a leader in STEM education. Key activities of NMPMSE include: providing a forum for communication among state government, K-12 & higher education, non-profit organizations and projects, and private organizations interested in STEM education; coordinating STEM education projects and activities in New Mexico; and providing opportunities for people and projects to communicate and work collaboratively.

CONCURRENT SESSIONS (A) AT A GLANCE

Bioalgal Energy Development

Moderator: Jayne Aubelle, New Mexico Museum of Natural History & Science

A review on treating dairy manure effluents using microalgae cultivated on an Algal Turf Scrubber®
Juchao Yan, Eastern New Mexico University

Hydrothermal liquefaction with algae biofuel
Julian Bojorquez, New Mexico Tech

Recovery and reuse of nutrients released by hydrothermal liquefaction of algal biomass
Thinesh Selvaratnam, New Mexico State University

Increasing productivity of algae culture to supply bio-crude oil production
Tim Torres II, University of New Mexico

Solar Energy Development

Moderator: Kurt Anderson, New Mexico State University

Computational studies of electronic coupling involving σ-pathways in donor-bridge-acceptor systems
Ranjana Dangi, University of New Mexico

Photons to formate: Utilizing Earth-abundant materials for mitigating CO and generating solar fuels
Michael Heagy, New Mexico Tech

Making the most of the sun, part II
JT Goodart, Grants High School

A molecular breakwater-like tetrapod for organic solar cells
Jianzhong Yang, University of New Mexico

Engineering and Energy

Moderator: Michaela Buenemann, New Mexico State University

Energy, water and New Mexico: Challenges and constraints
Bruce Thomson, University of New Mexico

Sustainable energy for sustainable water: Solar heat driven desalinating system for providing clean and safe water for rural areas
Vladislav Sevostianov, Las Cruces High School

Water runoff energy collection
Samuel Pearson, Santa Fe Community College

Osmotic power development
Cassandra Sanchez & Kelsy Waggaman, New Mexico Tech

CONCURRENT SESSIONS (B) AT A GLANCE

Water And Energy

Moderator: Kurt Anderson, New Mexico State University

Positive impacts on groundwater resources subsequent to wildfire in the Lincoln National Forest in New Mexico
Marco Wikstrom, University of New Mexico and John Shomaker & Associates, Inc.

The occurrence and mobility of uranium and co-occurring constituents in soil at an abandoned mine waste site in northeastern Arizona
Johanna Blake, University of New Mexico

Community-based student research experience projects
Nader Vadiee, Southwestern Indian Polytechnic Institute

Method development of speciation and characterization techniques for uranium in water
Samantha Saville, New Mexico Tech

Solar Chemistry

Moderator: Shanalyn Kemme, Sandia National Laboratory

High intra-chain order improves doping efficiency in J-aggregate poly(3-hexylthiophene) aggregate nanofibers
Martin Kirk, University of New Mexico

Unpaired electrons as reporters of excited state interactions
Benjamin Stein, University of New Mexico

The role of differential covalency in the excited state lifetimes of platinum donor-acceptor complexes
Logan Giles, University of New Mexico

Spectroscopic studies of donor-acceptor excited state lifetimes
Jing Yang, University of New Mexico

The influence of structure-directing cations on fluorescent MOFs
Carlos Ordoñez, New Mexico Highlands University

Ecosystems

Moderator: Hartono Sumali, Sandia National Laboratory

The impact of invasive Bullfrogs on the demographics of Northern Leopard Frogs in northern New Mexico
Robert Ortega, New Mexico Highlands University

Metapopulation structure of two sympatric garter snake species (*Thamnophis elegans* and *Thamnophis cyrtopsis*) in the Mora River watershed
Lisa McBride, New Mexico Highlands University

Effects of forest fire on submerged aquatic macrophytes: Ecosystem engineers in NM mountain streams
Virginia Thompson, University of New Mexico

The impact of the invasive American Bullfrog on Woodhouse Toad demographics in the Rio Mora Wildlife Refuge in northeastern New Mexico
Alfonso Trujillo, New Mexico Highlands University

POSTER SESSION AT A GLANCE

Poster submissions are sorted alphabetically by title.

The age of algae
Giovanni Echave, Santa Fe Community College

Algae growth monitoring in commercial photobioreactors (PBRs)
William Torres-Longo, Santa Fe Community College

Algal-based single-step, energy-efficient treatment of urban wastewaters
Shanka Henkanatte Gedara, New Mexico State University

Batch extractions of metals from bicarbonate and ascorbic acid solutions
Chris Hirani, Central New Mexico Community College

Chemical geothermometers applied to New Mexico groundwaters and springs
Tanner Grulke, University of New Mexico

Computational studies of electronic coupling involving σ-pathways in donor-bridge-acceptor systems
Ranjana Dangi, University of New Mexico

Conserving water for now, sustaining water for the future
Cameron Bayly, Santa Fe Community College

Cultivation of microalgae in dairy wastewater on an Algal Turf Scrubber®: Adaptation to a local environment
Brittney Dlouhy-Massengale, Eastern New Mexico University

Dual-stage cultivation of Ettlia sp. YC001
Felly Montelya, New Mexico State University

Effect of encapsulation on algal photosynthesis
Nadia Mabrouk Mujynya, Santa Fe Community College

Emergency water generator
Francisco Whitson-Brown, Santa Fe Community College

Energize New Mexico Teacher Institute
Selena Connealy, New Mexico EPSCoR

Evaluating hydrothermal and meteoric water mixing along the Embudo Fault system, northern NM
Valerie Blomgren, University of New Mexico

Evaluation of cost-effective harvesting technology to make algal systems economical
Chaitanya Kukutla, New Mexico State University

Fault networks of the Embudo Zone, northern New Mexico: Evaluating differential incision in the Rio Grande and implications for hydrothermal fluid pathways
Marisa Repasch, University of New Mexico

Fluid flow and groundwater mixing along the Nacimiento Fault, San Ysidro, NM
Chris McGibbon, University of New Mexico

Hot springs of New Mexico: Summarizing occurrence and history for outreach and education
Lauren Rust, University of New Mexico

Hydrothermal liquefaction oil and hydrotreated product from pine feedstock characterized by ultrahigh resolution FT-ICR mass spectrometry and heteronuclear 2D NMR spectroscopy
Nilusha Sudasinghe, New Mexico State University

Impacts of conventional uranium mining on groundwater in the San Juan Basin
Katie Zemlick, University of New Mexico

Increasing productivity of algae culture to supply bio-crude oil production
Tim Torres II, University of New Mexico

Integrated environmental and economic assessment of using dairy waste for algae bio-energy production in New Mexico
Janak Joshi, University of New Mexico

Migration of low-level uranium contamination in the TseTah Wash, Red Mesa, AZ
Susan Little, New Mexico Tech

New Mexico geothermal resources: A database compilation for New Mexico EPSCoR
Alexandra Minitrez, University of New Mexico

Nitrogen removal from wastewaters: Biological processes vs. algal-based system and modeling
Nitharsan Kanapathippillai, New Mexico State University

Photons to Formate: Solar driven conversion of CO_2 to solar fuels
Devin Bruce, New Mexico Highlands University

Photons to Formate: Solar driven conversion of CO_2 to solar fuels
Claudia Petr, University of New Mexico—Valencia

Preferences on energy sources, trade-offs, and how they vary across New Mexico
Kara Walter, University of New Mexico

Preliminary Study of CO_2 efflux across the Nacimiento Fault, San Ysidro, New Mexico
Hyunwoo Lee, New Mexico State University

Separation and analysis of produced water for osmotic power development
Elizabeth Jackson, Eastern New Mexico University

Unpaired electrons as reporters of excited state interactions
Benjamin Stein, University of New Mexico

What is inside an invasive frog? Bullfrog diet of the Mora River
Steven Salinas, New Mexico Highlands University

Bioalgal energy development

A review on treating dairy manure effluents using microalgae cultivated on an Algal Turf Scrubber®

Juchao Yan, Eastern New Mexico University

Treatment of dairy manure effluents often relies on the physical, chemical and biological processes in lagoon systems. These systems are not intended for high-quality treatment, but rather limit runoff into surface and ground waters. For aged lagoons or lagoons in stormiest areas, surface and groundwater contamination, especially by nitrates, occurs. Cultivating microalgae on nitrogen and phosphorus in dairy manure effluents has real potential in purifying the wastewaters while producing a biomass suitable for biofuel production. Algal turf scrubber® (ATS®) flows pulsed wastewaters over a slopping surface with attached and naturally seeded filamentous microalgae. ATS® has been utilized to treat surface water runoff, and agricultural and municipal effluents through microalgae cultivation. In this talk, I will review the latest literature of using ATS® for the dual purposes of dairy wastewater treatment and sustainable biofuel production. In particular, I will focus on the recovery of nitrogen, phosphorus, and trace metals, and on the assessment of the environmental and cost impacts. Because of its modular and flexible design, ATS® can be easily installed on-farm for dairy wastewater treatment and biofuel production. Although not quite economically viable at present, ATS®seems to be the most ideal solution for treating dairy manure effluents if such a treatment is to be mandated in the future.

Hydrothermal liquefaction with algae biofuel

Julian Bojorquez, New Mexico Tech

The search for an alternative efficient energy resource has had many developments. Many of which are not as efficient as we wish them to be. We are constantly looking for an energy source that will be efficient and be good for the environment as well as ourselves. This research will be addressing renewable resources and the creation of biofuel from algae. Algae biofuel can be created through the method of Hydrothermal Liquefaction (HTL). HTL is a process in which the algae are put through high pressure and high temperatures in order to extract biocrude oil. This process has been around since the 1980s and finally used commercially in 1996. In a week of experimentation, the algae strand Chlorella was tested in temperatures from 180˚C up to 300˚C. The pressure reactor that contained the algae was filled with Nitrogen air in order to have little to no reaction with air particles. After our reaction, we added a solvent with the biochar produced. The solvent consisted of dichloromethane which served as a way to separate water and the biocrude oil. al this was done through a filter paper which does not let the biochar through in order to separate any solids left. In the end we are left with the crude oil, water with nutrients and biochar.

Recovery and reuse of nutrients released by hydrothermal liquefaction of algal biomass

Thinesh Selvaratnam, New Mexico State University

Hydrothermal liquefaction (HTL) is emerging as one of the promising options for extracting the energy content of algal biomass in the form of biocrude. HTL eliminates the need to dry biomass for downstream processing. This study evaluated the feasibility of recycling the aqueous byproduct of HTL, that is rich in organic carbon (200-21500 mg L-1) and nutrients (830-3900 mg L-1 ammoniacal nitrogen and 20-250 mg L-1 Phosphates), to the cultivation step to boost biomass productivity. Since the composition of this aqueous product (AP) depends on the temperature at which HTL is done, heterotrophic growth of *Galdieria sulphuraria* cultivated in the AP of HTL conducted over a range of temperatures (180 to 3000C) and dilutions (1%, 2%, 4% and 8%) was evaluated in this study. Results showed that biomass productivity with recycled AP was greater than that with the standard growth medium. Based on the range of parameters tested, maximal biomass productivity was attained using the aqueous fraction from an HTL temperature of 1800C and dilution of 8%. Estimates of net energy yields over this range of temperatures also used to reaffirm the optimal HTL temperature for *Galdieria sulphuraria*.

Increasing productivity of algae culture to supply bio-crude oil production

Tim Torres II, University of New Mexico

Bio-crude oil has the potential to be part of the solution to global warming as algae derived crude oil can offset carbon dioxide (CO_2) emissions via its metabolic cycle. Algae fission consumes (CO_2) which in turn creates oxygen gas and ethanol as by-products. Algae can then be processed into crude oil and supplemented into current oil refinery production, offsetting their future (CO_2) emissions. Scaling up algae cultivation is difficult due to water and sunlight exposure requirements, as well as the production area needed. We chose to analyze the growth rates and resource utilization of *Galdieria Sulphuraria* (red algae) at 10cm and 20cm depths. Our setup included (2) separate 3m x 1.5m bio-reactor bags with a paddle wheel and moat system designed to mix growth media and algae. The bags are fed 2L/min of CO_2/air mixture in the same light/temperature environments. We observed self-shading and decreased temperatures in the 20cm bag reducing growth rates by 36%. The rate decrease, by doubling the volume, still produced 2g/m^2/day more biomass. It has been documented that biomass can be grown at higher aerial productivity by increasing the depth of bioreactors, however, the point of diminishing returns has yet to be reached. More work needs to be done at variable water depths and other sunlight exposure to further reduce the growth footprint, making algal biomass a viable feedstock for the production of bio-crude oil.

Solar energy development

Computational studies of electronic coupling involving σ-pathways in donor-bridge-acceptor systems

Ranjana Dangi, University of New Mexico

Aviram and Ratner first suggested that a donor-bridge-acceptor (D-B-A) molecule could function as a rectifier when used in a molecular device. This has spurred numerous experimental and theoretical research efforts directed toward understanding specific interactions that allow for electronic coupling in D-B-A and related systems. We have utilized both computational and spectroscopic methods to understand exchange and electronic coupling in D-B-A biradical systems. These studies have primarily focused on electronic and magnetic coupling mediated by the delocalized π-orbitals of the bridge (B). However, studies directed toward understanding the nature of D-B-A biradical interactions mediated by σ-pathways have not been explored to date. We will present our latest research in this area that details the nature of bridge mediated σ-orbital pathways in various D-B-A systems that do not possess π conjugation. Electronic structure calculations utilizing a broken-symmetry approach indicate that magnetic exchange interactions via these localized σ-pathways are only ~1% as strong as the exchange interactions mediated by delocalized π systems. We will discuss differences between hole- and electron-transfer mechanisms for super-exchange as they relate to these systems and provide an orbital-based understanding of magnetic and electronic communication in these D-B-A biradical constructs.

Photons to formate: Utilizing earth-abundant materials for mitigating CO and generating solar fuels

Michael Heagy, New Mexico Tech

One potential approach to reducing atmospheric CO_2 linked to global climate change is the trapping and subsequent photoinduced conversion to a value-added product without the use of additional CO2 generating power sources. This approach, referred to as "chemical carbon mitigation" can lead to methanol as an end product; a potentially useful and important bulk chemical. The "methanol economy" has been highlighted as an alternative to the "hydrogen economy" and championed by Chemistry Nobel laureate George Olah as a renewable and readily transportable fuel compared to hydrogen. Homogenous photosensitizer systems with metal cocatalysts and semi-conductor colloids have been observed to produce only CO and formic acid. The observation that the incomplete reduction of CO_2 to methanol reaches an electrochemical endpoint at formate or formaldehyde is predicted by thermodynamics. Our recent contribution and progress in this area involved the comparison of ZnS micron size and nanoparticulate photocatalysts. This study examined the photocatalytic features of wurtzite ZnS compared

sphalerite ZnS and these results will be presented. One serious drawback to be solved in the present reaction system; ultraviolet light [280 nm] can only be utilized to photoexcite the ZnS microcrystals. In an effort toward improving the optical absorption of this system, new photosensitizer systems will be discussed and recent results presented as our research efforts move forward in developing such systems.

Making the most of the sun, part II

JT Goodart, Grants High School

It is a well-known fact that the demand for an efficient renewable energy source is on the rise. Currently, one of the many options being looked at is solar power. However, it is seen as being unreliable, and restricted to its ability to harness power. It should, however, be looked at much more in depth. Last year, the experimenter built solar oven-style devices that were able to enhance the electrical output of the solar panel. This year, the designs were improved and tested. The main questions being asked in this experiment are: 1) which surface for the reflectors (shiny aluminum, dull aluminum, or white) will produce the highest level of voltage, amperage, and wattage; 2) which one of these surfaces will then be able to power a fan the quickest, as well as provide the longest lasting power after sunlight is cut off from the panel; 3) which surface will be able to charge a battery the best in intervals of 1, 5, and 10 minutes that can then power a light bulb for the longest amount of time; 4) which surface will be the most efficient, using the average and maximum voltage in the efficiency formula; and 5) which device will be the most cost efficient? The hypothesis for all five questions of the experiment is that the shiny aluminum reflectors will work the overall best, based off of the results from the experiment performed last year, as well as the reflective properties of shiny aluminum foil. In order to test all of the questions, multiple things were tested. First, the voltage and amperage were measured. These can then be used to calculate the wattage. Once the wattage is calculated, the wattage can be used in all other calculations, such as cost efficiency. Then, the times of the various trials that involve the solar panels powering devices must be recorded. Finally, various weather events (such as temperature, wind, etc.) should be recorded in order to see if there is any correlation between them and the output of the solar panel. The final results supported the hypothesis, with shiny foil reflectors being the most overall efficient in the five areas tested. Also, there were no major correlations between weather phenomena and the output of the solar panel. Overall, solar power could be successfully improved through increasing the amount of sunlight that reaches the solar panel with the use of external solar oven-style devices.

A molecular breakwater-like tetrapod for organic solar cells

Jianzhong Yang, University of New Mexico

Most small conjugated molecules applied in solar cells have linear structures containing multiple aromatic groups connected in series. However, unfavorable film forming ability and grain boundaries both originated from high crystallinity of linear small molecules are detrimental to device performances. As a result, significant attention has been paid to small molecules having conjugation extended in three dimensions. Among the many 3-D structures, breakwater-like tetrapods are especially interesting owing to their unique ability to mutually interlock, which prevents dislodging and provides high structural stabilities. Herein, we synthesize and characterize a tetrapodal breakwater-like small molecule, **SO**, containing a tetraphenylsilane core and four cyanoester functionalized terthiophene arms. **SO** possesses a deep lying HOMO energy level of -5.2 eV and a narrow bandgap of 1.9 eV. Absorption, X-ray scattering and differential scanning calorimetry experiments indicate crystalline nature of this compound but slow crystallization kinetics. Solar cells employing **SO** and phenyl-C61-butyric acid methyl ester (PCBM) were fabricated and evaluated. Relatively low performance was obtained mainly due to the lack of any phase separation, which was caused by molecularly mixed blends with PCBM. Addition of poly(thienylene vinylene) (PTV), a low bandgap highly crystalline conjugated polymer, into the **SO**/PCBM blend was found to induce appreciable phase separation. Such ternary blend devices showed cooperatively improved performances over binary devices employing

either **SO** or PTV alone. Our findings can give useful insight on the structure-property relationships of such 3-D small molecules and their applications in multi-component organic solar cells.

Engineering and Energy

Energy, water and New Mexico: Challenges and constraints

Bruce Thomson, University of New Mexico

New Mexico has large reserves of energy resources including fossil fuels (coal, oil, and gas), uranium, and hydropower as well as renewable energy sources (solar, wind, and biofuels). The areas of the state with large amounts of traditional resources are the San Juan Basin in northwestern NM with important reserves of fossil fuels and uranium, and the Permian Basin of southeastern NM with large resources of oil and gas. When considering these resources it is important to note that most are closely associated with scarce and increasingly valuable water resources. This association includes reserves that are located in or near important aquifers such as uranium, or energy resources in which large volumes of water are required for their development of the resource. It is becoming evident that impacts on water resources, both their quantity and quality, may constrain future energy development projects. This paper will summarize the portfolio of traditional energy resources in New Mexico and their relationship to surface and groundwater resources. It will discuss the impact that development of these resources has on regional water resources. The focus will be on development of gas resources using hydrofracturing methods, produced water from oil and gas development, and ground water impacts from possible future uranium mining.

Sustainable energy for sustainable water: Solar heat-driven desalinating system for providing clean and safe water for rural areas

Vladislav Sevostianov, Las Cruces High School

This work presents the concept of solar heat-driven membrane water desalinator and its experimental validation. In the present research, the desalinator is designed, built, and experimentally tested. The designed and constructed desalinating system consists of a desalinating reactor, water pump, β-type Stirling cycle engine and parabolic solar heater. As a key element of the design, a desalinating reactor cell using the Direct Contact Membrane Distillation process is built. Three types of membrane materials donated by Fluorotechniques Membrane Products Inc. are tested— M-C8520, M-8A2000, and M-A8515. The tests were negative in contrast with the manufacturer's claim. To explain the problem, (1) microstructure of membranes was studied using SEM and confocal microscopy, and Image-J software; and (2) hydrophobicity of the membranes was estimated using an optical tensiometer. Results show that the used membrane materials cannot work properly since pore size is too large, and hydrophobicity is insufficient. At the same time, solar energy is sufficient to rich operating temperature of Stirling engine, 1200°-1500° F, which is sufficient for the mechanical part of the system to work properly. The proposed desalinating system is economically affordable, technologically simple, and leads to a new approach for water management in rural areas; however, the membrane material should be changed.

Water runoff energy collection

Samuel Pearson, Santa Fe Community College

Huge amounts of energy go to waste by way of water runoff and pumping water through infrastructure. The modification and use of old technology can potentially be used to both collect energy from all water runoff, and offset the amount of energy used to move water through pipes. Hydraulic ram pumps date back to the 19th century. Using only gravitational energy, they amplify hydraulic pressure to pump water uphill. These pumps could be installed in many different configurations and situations, and could either aid in pumping water around, or be modified to collect energy that is untapped from all water runoff, with an extremely low impact. These simple

machines are not the most efficient, but their energy input is one that is normally completely untapped and wasted. If installed in the right configuration they could conserve and/or collect massive amounts of energy that is literally flushed down the toilet. Because hydraulic ram pumps are simple and affordable to build, there is potential in the future to use them in any water drainage or runoff system, including parking lots and storm drains, water treatment facilities, sewage systems, streams and rivers, and just about anywhere else that water flows downhill. With some thoughtful modification and engineering, these could be a major part of a global energy solution.

Osmotic power development

Cassandra Sanchez and Kelsy Wagamman, New Mexico Tech

The Osmotic Power Development team is working to harness the osmotic pressure created from the salinity gradient between high salinity and low salinity produced water streams to generate electricity. Produced water is the waste stream generated by oil production. Through Pressure Retarded Osmosis technology, energy can be recovered from produced water, which would otherwise remain a substantial waste stream. Pressure Retarded Osmosis is a form of osmosis in which pressure is applied to retard the forward osmosis process and produce a pressurized stream. The pressurized stream drives a turbine to generate electricity. Current barriers include limitations of membrane technology and membrane fouling. Bench scale tests will be conducted in the lab utilizing a model Pressure Retarded Osmosis system. The impact of membrane fouling on water flux and osmotic pressure will be evaluated. Energy usage and final energy output will be calculated from osmotic pressure and water flux measurements. The model system will provide data regarding the barriers and strengths attributed to a commercially functioning pilot scale Pressure Retarded Osmosis plant that utilizes high salinity produced water.

CONCURRENT SESSIONS (B) ABSTRACTS

Water and Energy

Positive impacts on groundwater resources subsequent to wildfire in the Lincoln National Forest in New Mexico

Marco Wikstrom, University of New Mexico & John Shomaker & Associates

National Forests in the southwestern United States have become increasingly susceptible to wildfires as a result of various processes, including long-term drought, destruction of trees by bark beetles, and overgrown forests. The 2012 Little Bear Wildfire in the Lincoln National Forest in New Mexico burned more than 44,300 acres of which about 35,300 acres were National Forest Lands. The fire impacted numerous watersheds, including nearly 99 percent of the North Fork Eagle Creek Watershed. More than 51 percent of the North Fork Eagle Creek watershed was classified as having moderate- to high-burn severity. Reduced vegetation and reduction in woody debris on the forest floor appear to have resulted in an increase in groundwater recharge to both the shallow-alluvial and deep-volcanic aquifer systems based on monitoring well and precipitation data. The data suggest that a more active vegetation management strategy within our National Forests could provide more reliable water supplies.

The occurrence and mobility of uranium and co-occurring constituents in soil at an abandoned mine waste site in northeastern Arizona

Johanna Blake, University of New Mexico

We assessed the occurrence and release of metals from an abandoned uranium mine waste site located in the Navajo Nation in northeastern Arizona. Community members at this site have had concerns about water sources in the proximity of abandoned mine wastes as they and their livestock drank from these sources over the years. The aqueous uranium (U) concentration from a seep located in the vicinity of these abandoned mine wastes is 4.5 times the EPA maximum contaminant level (MCL) of 30 µg/L and concentration of arsenic (As) in this seep is almost at the MCL of 10 µg/L. Therefore, assessment of the occurrence and mobility potential of uranium and

co-constituents in nearby soils are important questions to address. Total acid extractable concentrations of As and U in soils are 20-40 mg/kg and 1,000 to 2,000 mg/kg respectively. Solid sample analyses performed by XRF resulted in concentrations of 0.66% U, 0.43% V, and 0.35% mg/kg Fe. The presence of Fe(II), Fe(III), As(III, I, 0), and the predominance of U(VI) and V(V) in the top 5 nm of abandoned mine waste solids suggest complex redox interactions between these metals. We ran batch and sequential extraction experiments with the solid samples, which revealed mobility of As and U with 10mM bicarbonate (both As and U), deionized water (U), and $MgCl_2$ (As), each of which release the more weakly bonded elements from solids. This study has important implications related to the fate and mobility of these metals in communities located close to AUM wastes.

Community-based student research experience projects

Nader Vadiee, Southwestern Polytechnic Institute

Southwestern Indian Polytechnic Institute (SIPI) seeks to meet the STEM (Science, Math, Engineering, and Technology) educational needs of American Indian college students. In an effort to fulfill this mission, SIPI employs paid student internships not only to retain students majoring in the STEM fields, but also to encourage students in developmental courses to stay in college and pursue STEM careers. Students are linked to each other and to graduate students, instructors, and industry professionals via the Vertically Integrated Pyramid (VIP) Model that SIPI's Department of Advanced Technical Education has crafted to build the relationships and sense of community that are important to Native students. For their paid work on engineering-related projects, SIPI student interns are usually under the direction of graduate or post-doctoral students who also serve as mentors. Increasingly, the graduate students are SIPI alumni who are enrolled at nearby universities. Student research projects offered during the fall 2013 trimester illustrate the nature and diversity of SIPI's engineering programs: mobile robot development, wind tunnel test-bed, bioengineering systems modeling and simulation, solar power plant and geothermal resources studies and community outreach, and design and environmental monitoring systems. Through its vertically integrated approach, SIPI is working to prepare Native students to be productive life-long learners as tribal members in an ever-changing global environment. As a land grant institution, SIPI partners with tribes, employers, and other organizations with a stake in Indian education. An enduring commitment to student success is the hallmark of SIPI's operations.

Method development of speciation and characterization techniques for uranium in water

Samantha Saville, New Mexico Tech

Uranium transport has been studied extensively over the years, but because of its sensitivity to its surroundings i.e. ionic strength, pH, etc., uranium speciation is easily changed. Literature has shown that uranium binding can be very strong with several different ligands in multiple scenarios but there seems to be no uniformed opinion on uranium speciation. My thesis will hopefully give light to some more general trends of uranium in natural water conditions. For my uranium speciation experiments I will be using varying concentrations of uranium, humic acid, and carbonate. Using a size exclusion (SEC) high performance liquid chromatographer (HPLC) in line with an inductively coupled mass spectrometer (ICPMS) I will be able to analyze both humic acid shifts and uranium concentration to determine the binding capacity of uranium in natural waters. Using the modeling software Titrator and an ion chromatograph (IC) in line with the ICPMS I will be able to look at uranium carbonate speciation characteristics similar to the humic acid characterization. Once these trends are determined I will be looking at the calcium and magnesium competition factors for both carbonate and humic acid binding scenarios. This will give some insight to uranium binding in natural water behavior with common ground water elements and substances.

Solar Chemistry

High intra-chain order improves doping efficiency in J-aggregate poly(3-hexylthiophene) aggregate nanofibers

Martin Kirk, University of New Mexico

We explore the effect of intrachain order and packing arrangements of poly(3-hexylthiophene) (P3HT) chains within self-assembled nanofiber aggregates on charge transfer doping efficiency. We fabricate nanofibers displaying the limiting H- and J-aggregate signatures in their optical spectra and study their doping characteristics by adding varying amounts of the charge transfer dopant, 2,3,5,6-tetrafluoro-7,7,8,8-tetracyanoquinodimethane (F4-TCNQ). Doping efficiency is assessed using a combination of optical, Raman and EPR spectroscopies. We then correlate these behaviors to structural changes incurred upon doping with Raman spectroscopy and TEM imaging. Comparing doping efficiencies of H- and J-aggregate P3HT nanofibers reveals significantly different behavior where the latter exhibit the maximum amount of free charges at ca. 25% (w/w) F4-TCNQ loading and the former display their maximum efficiency at ~7% loading. Both F4-TCNQ-:P3HT+/F4-TCNQ absorption ratios and integrated EPR signals decrease in H-type nanofibers after the maximum dopant loading level is reached, which is consistent with the formation of bound charge transfer complexes. J-type nanofibers show increasing F4-TCNQ-:P3HT+/ F4-TCNQ absorption ratios for all dopant loadings whereas EPR signals decrease after ~25% loading. We attribute the loss of EPR signal to antiferromagnetic coupling between mobile hole polarons delocalized along the highly ordered J-type P3HT chains. H-type NFs show decreases in EPR signal at much lower F4-TCNQ loading (~5%) which is consistent with previous observations of charge mobility of doped P3HT thin films. These findings demonstrate that by accurately controlling the ordering and electronic coupling of π-stacked P3HT aggregates doping efficiencies can be greatly improved.

Unpaired electrons as reporters of excited state interactions

Benjamin Stein, University of New Mexico

Spin is an intrinsic property of electrons and it is responsible for the vast majority of magnetic behavior in matter. Furthermore, the interaction between *unpaired* electron spins can lead to many interesting and useful molecular systems. When a molecule absorbs a photon of light, two unpaired electrons are typically formed and it is the interactions between these two electrons, and with their molecular environment, that are the dominant force in controlling excited state behaviors. Careful control of excited state behaviors is crucial to fields as diverse as solar energy and molecular electronics, and this work demonstrates one part of the toolbox that we are developing to understand these complex phenomena. In particular, this work focuses on how to use the interaction between the photogenerated, unpaired electrons and additional *pendant radicals* to understand the short lived excited states which are formed upon the absorption of light. Specifically, our work involves the development of ways to modify molecules in a way that does not change their basic properties, but allows for the use of more advanced techniques to better understand key relationships between molecular structure and their electronic behavior. This, in turn, will enable the construction of a complete molecular toolbox for the construction of new and useful molecules. These modifications allow for the use of advanced high-field magnetic techniques, and we will discuss how these are being used to understand the complex interactions between ground and excited states as the pertain to magnetic exchange interactions.

The role of differential covalency in the excited state lifetimes of platinum donor-acceptor complexes

Logan Giles, University of New Mexico

A series of diimineplatinum(II) dichalcogenolenes have been studied using sulfur K-edge X-ray absorption spectroscopy. Previously, we reported that these complexes possess charge-separated dichalcogenolene→diimine charge transfer excited state lifetimes with a nonperiodic lifetime dependence on the heteroatoms of the

dichalcogenolene ligand. In order to understand this nonperiodic dependence, we have suggested that the lifetimes are a function singlet-triplet energy gaps, ligand and metal dependent spin-orbit coupling, and anisotropic covalency contributions to the Pt-E (E = O, S, or Se) bonding scheme. Here we use sulfur K-edge X-ray absorption spectroscopy to directly measure the degree of Pt-S covalency. The S K-edge X-ray absorption spectroscopic data have been evaluated in the context of density functional theory based calculations that address the nature of the anisotropic covalency differences between the diiminеplatinum(II) dichalcogenolene complexes.

The influence of structure-directing cations on fluorescent MOFs

Carlos Ordoñez, New Mexico Highlands University

Metal-Organic Frameworks are among the most versatile, and promising materials that have emerged in the past 20 years; due to their incredible ability to form intricate nanoscale networks with large voids and large surface areas. Metal-Organic Frameworks have been primarily utilized to handle tasks such as gas storage and gas separation. However these compounds have also been implemented as drug delivery agents, and in the past decade, research on the luminescent properties of these materials has increased. Our group is interested in the fluorescent ability of Metal-Organic Frameworks, more specifically as to whether this fluorescence can be tuned and controlled. Thirteen anionic Metal-Organic Frameworks based on zinc, benzenetricarboxylic acid, and various structure directing cations such as ammonium based or imidazole were synthesized via the solvothermal technique. Utilizing single crystal X-ray diffraction it was observed that the dimensionality of the framework was altered by the amount of hydrogen bonding the cation was capable of achieving within the framework. For example the ammonium ion with four possible hydrogen bonding sites produced a 1-Dimensional framework, while two or less hydrogen bonding sites produced a 3-Dimensional framework. Moreover, the fluorescence of each framework was effectively tuned according to the type of dimensionality, the size of the cation within the framework, and the type of metal clusters formed within the framework. Therefore it was concluded that the fluorescence of anionic zinc, benzenetricarboxylic acid based Metal-Organic Frameworks can indeed be tuned to a desired wavelength by carefully choosing the cation to achieve the wavelength.

Spectroscopic studies of donor-accepted excited state lifetimes

Jing Yang, University of New Mexico

We have synthesized a series of square-planar (dichalcogenolene)Pt(diimine), LPtL′, complexes and studied their excited state properties using a combination of transient absorption and emission spectroscopies. These studies reveal charge-separated dichalcogenolene→diimine charge-transfer excited state lifetimes that do not display a periodic dependence on the heteroatoms, E, of the dichalcogenolene ligand. We explain these results in terms of metal and ligand spin-orbit coupling, E-dependent singlet–triplet (S–T) energy gaps, and anisotropic covalency contributions to the M–E (E = O, S, Se) bonding scheme. For the dioxolene complex, 1-O,O, we find that E(T2) > E(S1) and this leads to rapid nonradiative decay between S1 and S0. In marked contrast, for the heavy atom congeners E(T2) ≤ E(S1) providing a mechanism for rapid inter-system crossing. Subsequent internal conversion to T1 produces a long-lived, emissive triplet. The three LPtL⊠ complexes with mixed chalcogen donors and 6-Se,Se display excited state lifetimes that are intermediate between those of 1-O,O and 4-S,S.

Ecosystems

The impact of invasive Bullfrogs on the demographics of Northern Leopard Frogs in northern NM

Robert Ortega, New Mexico Highlands University

Invasive species alter the dynamics of the trophic levels of an ecosystem and have no natural controls. They displace native species in the food web, and prey on species with no adaptive defenses. The Rio Mora National Wildlife Refuge has both invasive Bullfrogs and native Northern Leopard Frogs. The purpose of this study is to investigate

the effects of the presence of the invasive Bullfrog on the demographics of the native Northern Leopard Frog in northern New Mexico. The Mora River was divided into two 2400-meter long section, a control site containing Bullfrogs and an experimental site, where Bullfrogs were eradicated. Call, visual, and radio telemetry surveys were utilized to sample the population. Fifty-one Leopard Frogs were captured, pit tagged, and processed for demographic data. Six frogs were fitted with radio transmitters. Control and experimental regions did not differ in the relative abundance of Leopard Frogs. We did not find a significant difference in the mass of frogs from the two regions. However, preliminary data does show lower average mass and greater abundance in the experimental region suggesting an increase in recruitment of metamorphosis frog into the population. Telemetry data for four frogs in the control region produced a mean home range size of 531.7 square meters. The Telemetry data shows a large range of sizes in their home range area. Further study of the home range will be conducted to determine if there is a difference in home range between the control and experimental areas.

Metapopulation structure of two sympatric garter snake species (*Thamnophis elegans* and *Thamnophis cyrtopsis*) in the Mora River watershed

Lisa McBride, New Mexico Highlands University

Much of New Mexico's riparian habitat is vulnerable to increasing drought and agricultural practices. These modifications to the riparian habitat provide a working model of larger scale changes occurring throughout the Southern Rocky Mountains. In a new study, we will use microsatellite markers to examine the population structures of two sympatric garter snake species, *Thamnophis elegans* and *Thamnophis cyrtopsis*, to determine if particular land use is associated with common patterns of gene flow in the Mora watershed. It is hypothesized that population genetic analyses will reveal similar source/sink dynamics for both species based on shared habitat across a fragmented landscape. In our first sampling season, 45 individuals were collected from three sites in close proximity to riparian habitat along the Mora and Sapello rivers. Micro-satellite genotypes will be scored and analyzed using GENEPOP (v. 4.2), Arlequin (v. 3), and STRUCTURE (v. 2.3.4) to determine population structure, allelic diversity, and gene flow among the three locations. Thamnophis population patterns will help to identify corridors important for many riparian species and pinpoint critical sites needed for restoration. The results from this investigation will help increase habitat connectivity, thus improving the future outlook for these two species of garter snakes and potentially, other members of riparian ecosystems in this area of the Southern Rockies.

Effects of forest fire on submerged aquatic macrophytes: Ecosystem engineers in NM mountain streams

Virginia Thompson, University of New Mexico

Surface water systems are increasingly critical for human water supply, and submerged aquatic macrophytes (SAMs) can strongly influence these ecosystems. High elevation headwater areas, such as the East Fork Jemez River (EFJR) in the Jemez Mountains of northern New Mexico, are a key component of these surface water networks. The EFJR, in the Valles Caldera National Preserve (VCNP), is a low gradient grassland stream with very high primary productivity driven throughout the growing season by four main aquatic plant species: *Elodea canadensis*, *Ranunculus aquatilis*, *Potamogeton richardsonii*, and *Stuckenia pectinata*. The Las Conchas fire, which burned over 157,000 acres of forest and grassland in June and July of 2011 including 36% of the East Fork Jemez watershed, created an excellent opportunity to study the effects of a catastrophic forest fire on SAMs both as individual species and as a dominant community for primary production. SAMs extract nutrients from both the water column and the sediment. Fire increases both dissolved nutrients and the transport of nutrient-rich particles to streams. Plant tissue samples collected before and after the Las Conchas fire are being analyzed for percent carbon (C), percent nitrogen (N) and percent phosphorous (P) to see if the elemental stoichiometry of the tissues in the SAMs has responded to the nutrient enrichment. Understanding the effects of catastrophic forest fires on the growth and composition of SAMs will provide valuable new information on the recovery of these key components of aquatic primary production in mountain headwater streams throughout New Mexico.

The impact of the invasive American Bullfrog on Woodhouse Toad demographics in the Rio Mora Wildlife Refuge in northeastern New Mexico

Alfonso Trujillo, New Mexico Highlands University

The introduction of bullfrogs (*Lithobates catesbeianus*) has a negative impact on native species by out competing them for food and habitat. Woodhouse toads (*Anaxyrus woodhousii*) are among the native species to the Rio Mora National Wildlife Refuge (RMNWR) that co-exists with Bullfrogs. Early on bullfrogs were eradicated from a 2,600 meter section of the Mora River to evaluate the impact of their eradication on the local fauna while a control site of the river was left untouched where bullfrog density did not change. A parallel study on the diet of the euthanized bullfrogs found the presence of Woodhouse toads in their diet. The goal of this project is to investigate the impact of bullfrogs on Woodhouse toads by using three methods to determine differences between the control and experimental sites: (1) Determine abundance via two methods: a mark-recapture study demographic parameters (rate of increase, survival, capture rate) and a distance sampling using random or systematic transects in the study area; (2) comparison of demographic structure using the animals caught in both sites; and (3) radio telemetry to explore habitat use and mobility of the Woodhouse toad as well as how it is affected by the presence of Bullfrogs.

POSTER SESSION ABSTRACTS

Poster submissions are sorted alphabetically by title.

The age of algae

Giovanni Echave, Santa Fe Community College

Many global communities are currently under great stress with three major factors health wise; being overweight, under-nourished and suffering from immune deficiencies. Spirulina is a cheap, cost effective way to address these critical issues of society. Spirulina can be eaten and thus provide enough nutrition to ensure that eating too much 'junk' food or nutrient-sparse food is not an issue. It has also been known to give the immune system the strength to fight off a cold or flu and has shown promising results in the ability to abate cancer. Also Spirulina is really cheap when produced in mass and you don't need to eat much to become full. It's economically helpful, health increasing, and possibly the answer to ending hunger in America and other parts of the world. It can grow in effluent water with the existing nutrients and produce polished water for downstream uses. The growing of it in the said example also allows the evaporated water to go back into the river as clean water. Spirulina is up to 65% protein which is much higher than meat and it can be cultivated at a much larger scale, more cheaply, effectively with a lower cost on resources. One example is water: it takes 2,400 gallons of water to produce one pound of animal protein verses 100 gallons to produce one pound of Spirulina protein a week. Spirulina micro farming is a rapidly growing practice in Africa, India and Asia.

Algae growth monitoring in commercial photobioreactors (PBRs)

William Torres-Longo, Santa Fe Community College *Luke Spangenburg, Santa Fe Community College*
Steve Gomez, Santa Fe Community College

Microalgae have many applications such as the production of high value compounds (polyunsaturated fatty acids, pigmentation, beta carotene, chlorophyll and astaxanthin), energy production (biofuel, methane) or in environmental remediation (especially in oil well produced and back flow water). Monitoring and controlling the chemical and biochemical processes in the reactor is vital for optimal use of resources. Real time data collection helps to maximize the efficient use of resources. SFCC is using commercial sensor array probes obtained with funds from an EPSCoR seed grant to monitor the commercial scale photobioreactors in the SFCC Biofuels laboratory. Operating temperatures, pH, chlorophyll content and other parameters can be monitored and controlled in real time to ensure the maximum algae production and biomass densities. Parameters for growing both monoculture and polyculture can be rapidly collected to determine the optimal conditions of each strain. This poster is an in-progress EPSCoR research work where the principal objective is to define the parameters to increase biomass and estimate micro-alga production

in a photobioreactor. The capture of data in real time under continuous operation helps to highlight the performance of the photobioreactors and in the optimization of long term microalgal biomass productivity. This poster is a presentation of the preliminary data of the EPSCoR experiments.

Algal-based single-step, energy-efficient treatment of urban wastewaters

Shamka Henkanatte-Gedera, New Mexico State University *Peter Lammers, New Mexico State University*
Thinesh Selvaratnam, New Mexico State University *Wayne Van Voorhies, New Mexico State University*
Nirmala Khandan, New Mexico State University

Current urban wastewater (UWW) treatment plants have been designed solely for the purpose of meeting the mandatory discharge regulations to protect receiving waters and public health. These technologies dissipate valuable carbon and nutrient content of wastewater to the environment and consume substantial amounts of energy. Since algal biomass carbon to nitrogen ratio is closer to that of UWW than a traditional heterotrophic bacteria based system, algal system could be engineered to remove Biochemical Oxygen Demand (BOD) and nutrients in a single step. Objectives of this study are (i) to demonstrate BOD and nutrient removal by *Galdieria sulphuraria* in primary effluent and (ii) analyze biomass productivity in UWW comparison to synthetic growth medium (MCM). The test culture was cultivated in borosilicate glass tubes (culture volume = 6 mL) placed in a CO_2-enriched incubator at 40°C. The volumetric removals of BOD5, ammoniacal nitrogen and phosphates over the first three days were 18.57 mgL-1day-1, 15.5 mgL-1day-1, and 3.6 mgL-1day-1 respectively. Productivity analysis showed a similar growth in raw primary effluent compared to MCM prepared with primary effluent and higher than MCM prepared with deionized water. The results demonstrate that *G. sulphuraria* can be cultivated in primary effluent of UWW with the potential for removal of BOD and nutrients at rates comparable to traditional unit operations. Moreover, higher biomass yields with *G. sulphuraria* growing in raw wastewater compared to MCM supports the rationale behind energy positive and cost effective wastewater treatment when coupled with energy recovery via hydrothermal liquefaction.

Batch extractions of metals from bicarbonate and ascorbic acid solutions

Chris Hirani, Central New Mexico Community College

Northeastern Arizona is home to an abandoned uranium mine which is the source of contamination from metals in soil. Inductively Coupled Plasma was used to analyze batch extractions from 10mM sodium bicarbonate (NaHCO3-) and 10mM ascorbic acid (C6H8O6) solutions. U and As are more readily released from the Claim #28 soil sample when introduced to the C6H8O6 solution than with the NaHCO3- solution. The data collected from these extractions strongly suggest the correlation of U and V release into solution, confirming the detection of carnotite [(K2(UO2)2(VO4)2·3H2O] from electron microscopy analyses. Based on preliminary spectroscopy observations, we hypothesize the presence of arsenopyrite (AsFeS). A correlation between the release of arsenic and iron was observed for ascorbic acid extractions after 2 hours of reaction. These findings have important implications to better understand the fate and transport of U and As in abandoned mine waste sites.

Chemical geothermometers applied to New Mexico groundwaters and springs

Tanner Grulke, University of New Mexico *Laura Crossey, University of New Mexico*

Chemical geothermometers are a useful tool in assessing geothermal potential. The geothermometers take advantage of temperature-dependent, water-rock reactions that change the chemistry of circulating fluids to estimate the temperature of subsurface reservoirs. Some of the common chemical constituents used in geothermometry include dissolved silica, Na, K, Ca, Mg, Cl, and bicarbonate. Trace elements such as lithium and fluoride are also useful indicators of geothermal systems. The purpose of this work is to apply these tools to assessment of potential New Mexico field areas. The composition of geothermal fluids depends on several conditions: whether the system is in chemical equilibrium, mixing with other ground waters, dissolution/precipitation and ion exchange with surrounding geologic materials, and residence time in the reservoir. These processes can limit the application of geothermometers.

We take the approach of calculating a range of possible reservoir temperatures depending on several assumptions and compared to measured temperature. We examine the applicability of several well-known geothermometers to existing data from the EPSCoR Data Portal and several other sources to New Mexico geothermal areas. Computations are performed using excel. Where possible, multiple geothermometers have been applied and examined for consistency. Future plans include applying a suite of chemical geothermometers to geothermal waters obtained by the NM EPSCoR geothermal team.

Computational studies of electronic coupling involving σ-pathways in donor-bridge-acceptor systems

Ranjana Dangi, University of New Mexico *David Shultz, North Carolina State University*
Benjamin Stein, University of New Mexico *Martin Kirk, University of New Mexico*
Logan Giles, University of New Mexico

Aviram and Ratner first suggested that a donor-bridge-acceptor (D-B-A) molecule could function as a rectifier when used in a molecular device. This has spurred numerous experimental and theoretical research efforts directed toward understanding specific interactions that allow for electronic coupling in D-B-A and related systems. We have utilized both computational and spectroscopic methods to understand exchange and electronic coupling in D-B-A biradical systems. These studies have primarily focused on electronic and magnetic coupling mediated by the delocalized π-orbitals of the bridge (B). However, studies directed toward understanding the nature of D-B-A biradical interactions mediated by σ-pathways have not been explored to date. We will present our latest research in this area that details the nature of bridge mediated σ-orbital pathways in various D-B-A systems that do not possess π conjugation. Electronic structure calculations utilizing a broken-symmetry approach indicate that magnetic exchange interactions via these localized σ-pathways are only ~1% as strong as the exchange interactions mediated by delocalized π systems. We will discuss differences between hole- and electron-transfer mechanisms for super-exchange as they relate to these systems and provide an orbital-based understanding of magnetic and electronic communication in these D-B-A biradical constructs.

Conserving water for now, sustaining water for the future

Cameron Bayly, Santa Fe Community College *Luke Spangenburg, Santa Fe Community College*

Water, in its liquid state, is one of the most if not the most vital component to carbon-based life. Humans cannot simply find water from anywhere because there are a variety of things that can make water unsafe to drink, so humans have to treat water. Drinking quality water is becoming scarce across the world caused by the majority of currently employed water management techniques. A few large corporations have realized the importance of water and are seeking to restrict water resources to only those that can pay their price. A solution to the problems of poor water management and increasing monopoly is to promote water sustainability literacy and develop subsystems designed for water reuse and conservation, and water sequestration that are adaptable across a small range of environments; such an initiative is best undertaken between a collaboration of the public and private sector. The best scale to solve both problems is at the small to medium community scale, where a significant number of people as well as the "organizing and leadership body" of the community can be made aware of these problems and solutions available (hopefully even in the context of their own lives) and take steps toward water sustainability. The "organizing and leadership body" can then reiterate the importance of best water practices to its community and can then get an optimized water budget best suited to their environment, purchasing subsystems accordingly. These subsystems working in concert with water budgets will make communities water sustainable.

Cultivation of microalgae in dairy wastewater on an Algal Turf Scrubber®: Adaptation to local environment

Brittney Dlouhy-Massengale, Eastern New Mexico University *Juchao Yan, Eastern New Mexico University*
Roger Grano, Eastern New Mexico University

Relying primarily on anaerobic lagoons for the wastewater management, New Mexico dairy farmers are challenged

with an effective way to minimize the surface and ground water contaminations (especially by nitrates). The use of microalgae to treat wastewater while providing a source of biomass for biofuel production was first developed in 1957. The technique, however, has not been implemented on the east side of New Mexico, where 77.5% of the milk in the state is produced. The goal of this study is to adapt the technique to local conditions and maximize the bio-mass production, specifically dry weight and lipid content. A pilot-scale Algal Turf Scrubber (ATS®) was constructed near the main campus of Eastern New Mexico University. Effluents collected from a local dairy provide nutrients to the system. Four times per week we collect water samples and analyze the concentrations of nitrate, nitrite, ammonia and phosphorus. During September 2014 we harvested the microalgae approximately once per week. At the time of harvest, the concentrations of nitrate, nitrite, ammonia and phosphorus ranged from 0.0-0.5 mg/L, 0.000-0.009 mg/L, 0.04-0.10 mg/L, and 0.00-0.10 mg/L, respectively. We are in the process of extracting the lipids. We will use Gas Chromatography-Mass Spectrometry to analyze the lipid content, and determine whether there is a correlation between the levels of nutrients at the time of harvest and the lipid content of the microalgae. Successful adaptation of the technique could provide local dairy farmers a solution to treat wastewater while creating a sustainable biofuel source.

Dual-stage cultivation of Ettlia sp. YC001

Felly Montelya, New Mexico State University
Nirmala Khandan, New Mexico State University
Peter Lammers, New Mexico State University
W. Farooq, Korea Advanced Institute of Science and Technology
M.S. Park, Korea Advanced Institute of Science and Technology
J.W. Yang, Korea Advanced Institute of Science and Technology

Algal biofuels are recognized as one of the preferred alternatives to fossil fuels. However, algal biofuels are not yet economically viable due to the high costs of cultivation and downstream processing to yield the finished product. A major barrier in the algal biofuel pathway is the harvesting step. Harvesting microalgae is challenging due to the nature of microalgal cells and the concentration of biomass in culture systems, which is generally low (0.2-10 gDW * L -1). Most solid-liquid separation techniques used for microalgae are still very energy intensive, a single centrifugation step widely used for harvesting consumes 8 kWh/m3 of energy. The bioflocculation of oleaginous microalgal strains for biofuel production with autoflocculating microalgae would not require additional use of chemical flocculants, which would the re-use of the medium without the need for additional treatment. This study evaluated a dual-stage cultivation process looking at autoflocculation and lipid production of Ettlia sp. YC001 under nutrient deprived and saline conditions during the second-stage process. Maximum lipid content of almost 80% was seen within the culture under nitrogen-depleted conditions and autoflocculation was observed under all stress conditions with in 48 hours. Moreover, it is the first time anyone has demonstrated the cultivation of fresh water alga under saline conditions.

Effect of encapsulation on algal photosynthesis

Nadia Mabrouk Mujynya, Santa Fe Community College
David Hanson, University of New Mexico
John Roesgen, University of New Mexico

Prior research suggests that encapsulated algae cells divert cellular resources away from cell division and toward cell metabolic processes. Consequently, encapsulation may lead to an enhancement of photosynthesis. If true, this could generate new clues in the regulation of photosynthesis and ways to increase productivity. To test the effect of encapsulation on photosynthesis, we used non-invasive, rapid measures of photosynthetic efficiency via variable chlorophyll fluorescence from microalgae encapsulated in gels that differed in thickness and inorganic carbon supply. We found that microalgae in thick gels are more limited by light or carbon supply than those in thin gels or liquid culture. In future work, we will improve the control of environmental conditions in the gel and determine if the light and carbon limitations in thin gels can be overcome.

Emergency water generator

Francisco Whitson-Brown, Santa Fe Community College Stephen Gomez, Santa Fe Community College

Natural disasters can result in major infrastructure damage and utility service disruptions. Water deliveries to homes and businesses could cease or be severely limited due to loss of power to pump water or damage to the water distribution system itself. It is usually impossible to know how long water service will be impacted, but it is likely that it could take several days (in some cases, months) to have the water and utility systems repaired to routine operating conditions. A portable containerized atmospheric water generator can provide emergency potable water in disaster situations by pulling moisture out of the air though various filters and condensing it. The container holds a self-sufficient system which does not rely on damaged local utilities and can produce up to 1700 gallons per day of potable water. The system is powered by a 100 kWh pyrolytic generator set and fueled by disaster debris (such as 2x4 wood framing, asphalt shingles or even newspaper) or virtually any combustible material. The gasifier genset and atmospheric water generator, along with a water quality testing laboratory, are stored inside a shipping container for easy transportation and deployment. Once on scene, a large foldable storage bladder can be opened and filled next to the container while a separate indoor tank can hold hot water produced by the unit. These units, projected to cost approximately $450,000 to produce, could be stored in disaster-prone regions for quick deployment when needed.

Energize New Mexico Teacher Institute

Rachael Cutrufello, Nat'l Museum of Nuclear Science & History
Selena Connealy, New Mexico EPSCoR
Tish Morris, New Mexico Museum of Natural History & Science
Marcia Barton, NM Public Education Dept.
Deb Novak, New Mexico Museum of Natural History & Science
Eric Meyer, ¡Explora!

As part of the New Mexico Informal Science Education Network (NM ISE Net), NM EPSCoR and three Albuquerque area science museums, with support from NM Public Education Department, collaborated to develop and implement a week-long Teacher Institute in June 2014. The Institute focused on New Mexico-relevant energy projects to address Common Core, the New Mexico Science Standards and recommendations from the National Research Council's Framework for K-12 Science Education. Twenty-six upper-elementary school teachers learned strategies for integrating literacy, math and science, and increased their knowledge of energy as a crosscutting concept. Institute instructors are providing continued support of program outcomes throughout the school year.

Evaluating hydrothermal and meteoric water mixing along the Embudo Fault System, northern NM

Valerie Blomgren, University of New Mexico
Karl Karlstrom, University of New Mexico
Laura Crossey, University of New Mexico
Marisa Repasch, University of New Mexico

The Embudo fault zone is a neotectonically active transfer zone in the Rio Grande rift that lies along the Jemez Lineament south of the Taos Plateau in Northern New Mexico. Ponce de Leon and other springs and wells along the Embudo fault may be chemically influenced by both geothermal as well as meteoric sources. The purpose of this study is to use hydrochemistry of the regional fluids in order to assess the process of hydrothermal waters flowing to the surface and mixing with shallow meteoric water by identifying shallow recharge aquifers, mapping faults and measuring water chemistry. Our methods include the use of several chemical and isotopic parameters to test for mixing of meteoric and hydrothermal water. The major ions most abundant in hydrothermal waters are Ca, Mg, HCO_3, SO_4, Cl, and SiO_2. These major ions will be graphically presented on a Piper diagram to chart potential mixing of diverse waters. Other tracers providing further evidence of deep and shallow mixing include comparing variations in δ2H, 13C, and Ca/Sr vs. 87Sr/86Sr. We will also compare our spring water samples to the Taos Plateau meteoric water to determine if our spring samples have been enriched or depleted in δ2H and δ18O. We will use gas analysis will look for the gases most typically found in hydrothermal water such as excess CO_2, H_2S and CH_4. The results of this project will be important for understanding the character of mixing of geothermal fluids with near-surface hydrologic systems and potential groundwater quality degradation.

Evaluation of cost-effective harvesting technology to make algal systems economical

Chaitanya Kukutla; New Mexico State University *Peter Lammers; New Mexico State University*
Nirmala Khandan; New Mexico State University

Biodiesel from Microalgae is proven to be promising approach for sustainable biofuels. However, the economic viability of algal biomass-to-biofuel production is currently limited by the harvesting step due to high energy requirements. The efficiency of the harvesting step is severely limited by the microscopic size of algal cells, specific gravity, charge, morphology, and low concentration of biomass. The focus of this study is to evaluate the low energy harvesting technologies and compare the commercial feasibility. This study presents energy free harvesting approach to pre-concentrate microalgae which makes the process a lot easier and economical. Bio-flocculation using self-flocculating algae to concentrate non-flocculating algae is an energy free approach, and also cost efficient as there is no use of chemical flocculants and it does not require any further treatment of supernatant. Experimental results showed good harvesting efficiency of *Chlorella Sorokaniana* using a flocculating strain *Coelastrella* with a concentration factor of nearly 5 at seven hours of gravity settling under 80-20% ratio of *Chlorella* and *Coelastrella*. Increasing the ratio of flocculating strain resulted in higher concentration factor. Laboratory and field studies are being carried out at New Mexico State University to develop energy-efficient and cost-effective harvesting technologies for various strains. The work presented here has profound implications for future studies of harvesting microalgae and making the biofuel production available in commercial scale.

Fault networks of the Embudo Zone, northern New Mexico: Evaluating differential incision in the Rio Grande and implications for hydrothermal fluid pathways

Marisa Repasch, University of New Mexico *Laura Crossey, University of New Mexico*
Karl Karlstrom, University of New Mexico *Valerie Blomgren, University of New Mexico*

The Rio Grande rift has evolved into one of the largest drainage basins in North America, capturing waters from more than 675,000 km^2. Active tectonics continues to influence the geomorphology and spring discharge along the Rio Grande, as the river flows across zones of active faulting and unstable lithosphere. The purpose of this project is to evaluate different mechanisms that influence fluvial incision rates. Long-term incision rates have been estimated from 60-90 m/Ma over the last 2-4 Ma in northern New Mexico, but these rates have varied both temporally and spatially. One important method we will use is to quantitatively analyze stream profiles. Marked by a prominent convexity extending nearly 200 km, the profile of the Rio Grande river is atypical of major drainages whose profiles tend to be concave. The steepest section of the river profile crosses the Jemez volcanic lineament and terminates just south of the Embudo fault zone. Our hypotheses include mechanisms influenced by neotectonics such as differential incision, mantle-supported dynamic topography, and regional fault networks, as well as more local controls such as lithology, differential sediment supply, and headward erosion. Previous work has shown there is a strong connection between river knickpoint development and mantle-driven uplift beneath the Jemez lineament; however, several studies have also suggested that the knickzone was produced by drainage basin integration. We will evaluate the incision history of the Rio Grande across the Embudo fault zone and examine fault system geometries that may influence both river incision and discharge of geothermal waters.

Fluid flow and groundwater mixing along the Nacimiento Fault, San Ysidro, NM

Chris McGibbon, University of New Mexico *Karl Karlstrom, University of New Mexico*
Laura Crossey, University of New Mexico *Abdul-Mehdi Ali,University of New Mexico*

San Ysidro, NM, provides a location where fault-controlled deeply circulated geothermal fluids can be studied within highly saline, CO_2 rich, travertine depositing springs. Along the basin bounding Nacimiento fault, numerous springs occur and the presence of extensive travertine accumulation demonstrates the long-lived nature of the fault conduit. Springs associated with the Jemez geothermal system fifty kilometers northeast show elevated temperature

and mantle volatiles: the purpose of this study is to assess potential distal effects of the Jemez geothermal system on the San Ysidro area springs. The study methods include continuous monitoring of depth, temperature and specific conductance in six springs and multi-year (2012-2014) campaign water sampling (major ions, stable isotopes of water and carbon). Seasonal and diurnal variations are seen as well as systematic depth (discharge) changes. Monitoring data highlight connectivity of three springs along the fault, while a fourth shows potential anthropogenic influences. Major ion chemistry from water samples collected over a multi-year period shows similar hydrochemical facies for three springs west of the river while samples from the east and the Rio Salado show greater temporal variability. These geochemical data support previous geophysical experiments at the site showing circulation patterns of saline fluids in the fault zone. Similarities in stable isotopes and major ion chemistry support connections to the Jemez geothermal system. These combined data indicate that groundwater movement along faults is an important process that influences water quality in surface and aquifer waters and that understanding fault conduits is important for geothermal studies in New Mexico.

Hot springs of new Mexico: Summarizing occurrence and history for outreach and education

Lauren Rust, University of New Mexico *Laura Crossey, University of New Mexico*
Graham Thomas, University of New Mexico

This study compiles and summarizes the geologic and historical information about several hot springs throughout New Mexico. We include sites such as the Gila Hot Springs, the Truth or Consequences Hot Springs, Jemez Springs and Radium Springs which are of particular interest due to their geothermal activity and their historical, cultural and economic implications throughout southwestern human history. Our method is to extract geologic and historic information using literature, regional geologic maps and several geothermal databases to communicate information about the geothermal occurrences to a broad audience. By collaborating with the Cyberinfrastructure collective of Energize New Mexico, we intend to develop real and accessible data products that are open and readily available to the scientific community as well as to those interested in sustainable and alternative energy. To create this easily accessible information we will create a systematic data form for each hot spring giving information such as location, geologic setting, rock types, geologic layers and other viable information. Along with this data form there will also be satellite images and orthophotographs, geologic maps and geologic cross sections explaining clearly and concisely what is occurring in the area. This will provide a visual for the reader to fully understand and appreciate the impact and value the geothermal systems have had on the area. This information, collected along with the historical aspects of each spring (from recent to archeological time frames), will provide a better understanding of how important geothermal systems are to New Mexico's economy, environment and water resources.

Hydrothermal liquefaction oil and hydrotreated product from pine feedstock characterized by ultra-high resolution FT-ICR mass spectrometry and heteronuclear two-dimensional NMR spectroscopy

Nilusha Sudasinghe, New Mexico State University *Mariefel Olarte, Pacific Northwest National Laboratory*
John R. Cort, Pacific Northwest National Laboratory *Andrew Schmidt, Pacific Northwest National Laboratory*
Richard Hallen, Pacific Northwest National Laboratory *Tanner Schaub, New Mexico State University*

Hydrothermal liquefaction (HTL) crude oil and hydrotreated product from pine tree farm waste (forest product residual, FPR) have been analyzed by direct infusion electrospray ionization Fourier transform ion cyclotron resonance mass spectrometry (ESI FT-ICR MS) in both positive- and negative-ionization modes and high-resolution two-dimensional heteronuclear 1H-13C NMR spectroscopy. FT-ICR MS resolves thousands of compounds in complex oils and provides unparalleled compositional details for individual molecules for identification of compound class (heteroatom content), type (number of rings plus double bonds to carbon or double bond equivalents (DBE) and carbon number (degree of alkylation). Heteronuclear 1H-13C NMR spectroscopy provides one-bond and multiple-bond correlations between pairs of 1H and 13C chemical shifts that are characteristic of different organic functional groups. Taken together this information provides a picture of the chemical composition of these oils. Pyrolysis crude

oil product from pine wood was characterized for comparison. Generally, pyrolysis oil is comprised of a more diverse distribution of heteroatom classes with higher oxygen number relative to HTL oil as shown by both positive- and negative-ion ESI FT-ICR MS. A total of 300 N_1, 594 O_1 and 267 O_2 compounds were observed as products of hydrotreatment. The relative abundance of N_1O_1, N_1O_2, N_1O_3, N_2, N_2O_1, N_2O_2 and O_3 compounds are reduced to different degrees after hydrotreatment and other higher heteroatom containing species (O_4-O_{10}, N_1O_4, N_1O_5 and N_2O_3) are completely removed by hydrotreatment.

Impacts of conventional uranium mining on groundwater in the San Juan Basin

Katie Zemlick, University of New Mexico *Bruce Thomson, University of New Mexico*

With few exceptions, all conventional sources of electric power are associated with large volumes of water to produce the fuel and/or generate the electricity. Growing electric power demands thus result in increasing impacts on water resources, especially in the arid southwest. Electricity production from nuclear power provides 19% of total US energy demand, but more than 83% of the required uranium is currently imported. It is estimated that uranium reserves in the San Juan Basin in northwestern New Mexico contains nearly 600 million pounds of ore, primarily in the Morrison Formation, leading to renewed interest uranium mining in the basin. However, most of these reserves are located in high quality and productive aquifers consequently future underground development would have large impacts on an already limited resource. This paper describes a modeling study to explore the relationship between uranium development and water resources in the region. The basin was divided into nearly 300 interconnected cells to account for geologic and hydrologic variability and a spatial-compartmental (Roach & Tidwell, 2009) or mixing cell approach within a system dynamics framework was applied to model groundwater flow and the impacts of uranium mining on groundwater resources in the Morrison Formation. Results from the model simulations show storage loss in cells in the vicinity of potential mines, very large cones of depression and extraction of large volumes of water associated with mining. The model suggests that the impacts of uranium mining on groundwater vary largely as a function of sub-regional geology and groundwater hydrology.

Increasing productivity of algae culture to supply bio-crude oil production

Tim Torres II, University of New Mexico *Peter Lammers, New Mexico State University*
Nicholas Csaken, New Mexico State University

Bio-crude oil has the potential to be part of the solution to global warming as algae derived crude oil can offset carbon dioxide (CO_2) emissions via its metabolic cycle. Algae fission consumes (CO_2) which in turn creates oxygen gas and ethanol as by-products. Algae can then be processed into crude oil and supplemented into current oil refinery production, offsetting their future (CO_2) emissions. Scaling up algae cultivation is difficult due to water and sunlight exposure requirements, as well as the production area needed. We chose to analyze the growth rates and resource utilization of *Galdieria Sulphuraria* (red algae) at 10cm and 20cm depths. Our setup included (2) separate 3m x 1.5m bio-reactor bags with a paddle wheel and moat system designed to mix growth media and algae. The bags are fed 2L/min of CO_2/air mixture in the same light/temperature environments. We observed self-shading and decreased temperatures in the 20cm bag reducing growth rates by 36%. The rate decrease, by doubling the volume, still produced 2g/m^2/day more biomass. It has been documented that biomass can be grown at higher aerial productivity by increasing the depth of bioreactors, however, the point of diminishing returns has yet to be reached. More work needs to be done at variable water depths and other sunlight exposure to further reduce the growth footprint, making algal biomass a viable feedstock for the production of bio-crude oil.

Integrated environmental and economic assessment of using dairy waste for algae bio-energy production in New Mexico

Janak Joshi, University of New Mexico *Jingjing Wang, University of New Mexico*

The increasing population and expanding socio-economic activities have caused a drastic increase in the demand for

food and energy throughout the world. New Mexico is one of the leading producers of dairy products and fossil fuels in the United States. However, the expansion of dairy and fossil fuel based industries over the past few decades have raised various concerns in the state over the deterioration of environmental and public health. Improper management of animal waste from large dairy farms can lead to both water and air pollution, while the energy sector emits greenhouse gases which are the major cause of climate change. Optimal management of these negative externalities associated with the two industries is crucial for the sustainable development of the region. Given the characteristics of the dairy sector and the energy sector of New Mexico, we assess the environmental and economic benefits of utilizing dairy waste for bioenergy production. We employ an integrated life cycle analysis of using dairy waste for bioenergy production through anaerobic digestion, and bio-algae harvesting to evaluate the physical and economic feasibility of boosting green energy in New Mexico. We extend the analysis to compare different dairy waste management strategies such as direct land application and bioenergy production through anaerobic digestion coupled with bio-algae harvesting. This approach enables to identify that among the alternative dairy waste management practices, integrating bio-algae cultivation with anaerobic digestion process is the most cost-effective and sustainable approach.

Migration of low-level uranium contamination in the TseTah Wash, Red Mesa, AZ

Susan F.B. Little, New Mexico Tech *Daniel Cadol, New Mexico Tech*
Shaina Willie, Western New Mexico University *Perry Charley, Diné College*
Bonnie Frey, NM Bureau of Geology and Mineral Resources

The mesas surrounding Red Mesa, AZ hosted numerous small-scale uranium mining operations during the 1960's and 70's. While all of these mines have been sealed, waste rock is still visible on the mesa flanks downslope from the mine entrances. The TseTah Wash, our study site, is located in this environment, with mines visible on either side of the ~1km-wide valley. The visibility of the mines in this area prompted the hypothesis that low-level uranium contamination could be spread by runoff from the mine sites into the wash and ponding areas on the valley floor. The uranium levels in the wash were of particular interest due to the fact that gravel from these locations has been used by local residents in the production of concrete for homes. In this study, nine locations were sampled: four in the wash itself, and five in ponding areas. These soil samples were then digested and analyzed for total uranium content using inductively coupled plasma mass spectrometry. The two location types were found to be distinct in their uranium content, with samples from the wash having an average of 3.90ppb, and 17.5ppb for those taken from the ponding areas. Additionally, radiation levels as much as twice background exist in ponding areas, while the levels in the wash are less than or equal to background. Although the reasons for this discrepancy are unclear, it is apparent from the analyses that uranium contamination from the mines is migrating down the mesa slopes and into the valley below.

New Mexico geothermal resources: A database compilation for NM EPSCoR

Alexandra Minitrez, University of New Mexico *Laura Crossey, University of New Mexico*
Joliviette Sloan, University of New Mexico

The overall objective of the NM EPSCoR geothermal component is to obtain a deeper understanding of geothermal systems in New Mexico. New Mexico has undeveloped and undiscovered potential that could expand geothermal production and offer sustainability. This purpose of this project is to compile existing geothermal water chemistry data from diverse sources and help incorporate data generated by the team into the data portal using methods shown in this presentation. The main purpose of this work is compiling existing geothermal data within New Mexico. Over the past several decades, there have been investigations of several areas, including the Jemez geothermal system in the north-central part of New Mexico, the Truth or Consequences area, south of Socorro, and the Gila Mountains in the southwestern part of the state. By incorporating the existing information about water chemistry, temperature and discharge into a database, we will make the task of comparing different systems and selecting sites for further study more manageable. Specifically our methods will be to combine various data sets using Excel, apply quality

control measures to the data, and work with the cyberinfrastructure team to develop metadata standards and upload information to the portal. The results to date include compiling data from several existing sources for New Mexico, making hundreds of geothermal water chemistries accessible through the EPSCoR data portal.

Nitrogen removal from wastewaters: Biological processes vs. algal-based system and modeling

Nitharsan Kanapthippillai, New Mexico State University *Nirmala Khandan, New Mexico State University*
Thinesh Selvaratnam, New Mexico State University

Publicly owned treatment works (POTWs) originally designed for organic carbon removals are now being required to remove nutrients such as nitrogen from wastewater to meet the discharge standards. Even though many POTWs have adopted biological nutrient removal (BNR) processes for doing so, they are energy-intensive. Ongoing research at NMSU is developing algal systems as energy-positive alternatives to traditional and emerging BNR processes. In this study, the algal approach is compared against emerging BNR processes such as ANNAMOX, CANON, Aerobic Deammonification, and DEAMOX, and the traditional Nitrification-denitrification process on the basis of net energy per unit mass of nitrogen removed. The comparison result shows that the algal approach has the potential to yield higher positive energy of about 15 kWh per kg of N removed in contrast to traditional and emerging biological nitrogen removal technologies. This energy-based analysis shows that the algal approach is more sustainable than the other alternatives for nutrient removal from urban wastewaters. Further, a mathematical model is being developed which is capable of predicting growth of microalgae on, and removal of nitrogen from urban wastewaters as a function of time. The model is validated with experimental data on *Galdieria Sulphuraria* species of microalgae cultivated in standard growth medium.

Photons to Formate: Solar driven conversion of CO_2 to solar fuels

Devin Bruce, New Mexico Highlands University *Dan Leonard, New Mexico Tech*
Claudia Petr, University of New Mexico—Valencia *Michael Heagy, New Mexico Tech*

We have seen many problems with CO_2 greenhouse emissions. One result of large CO_2 emissions is climate change with temperatures rising on our surface and oceans. To solve this, we need to use other forms of energy besides fossil fuels such as solar or wind to reduce the amount of CO_2 emissions. My research was focused on transferring excited electrons through a series of catalysts in order to convert CO_2 to Formate and then to Methanol. This process wasn't easy because the molecules we wanted to use were not easily soluble and other methods had to be used in order to get results. Results and further research will be discussed at the conference.

Photons to Formate: Solar driven conversion of CO_2 to solar fuels

Claudia Petr, University of New Mexico—Valencia *Victoria Risley, New Mexico Tech*
Michael Heagy, New Mexico Tech *Devin Bruce, New Mexico Highlands University*
Daniel Leonard, New Mexico Tech

Greenhouse gas emissions have increased in correlation with increasing global temperatures. The US alone generates over 0.5 gigatons of carbon per year in the transportation sector, which only accounts for 28% of the total greenhouse gas emissions. In efforts to mitigate greenhouse gas emissions, current research is focused on using the sun's energy in unconventional way. We could use the sun and the carbon that is being produced to convert carbon dioxide to formate then to methanol. By combining carbon dioxide (CO_2) with water (H_2O) and with the sun activating a catalyst this will help to generate formate and then methanol. Methanol is the simplest form of alcohol and is in liquid form, so it's very dense energy that can be easily stored. The research that I contributed to focused on finding a photocatalyst that would effectively reduce carbon dioxide to formate. We tested Zinc and Cobalt Phthalocyanine as possible photosensitizers in the catalytic pathway. Both were chosen because they have a similar structure to Porphyrin, which has been shown to have an increase in absorbance in wavelength so that more of the sun's energy can be used. The challenges we faced was that neither the Zinc nor the Cobalt solutions possessed the required

energy levels needed to activate the ZnS semiconductor material. For future research, we could continue making a solution that would be best for this photocatalytic or research other alternatives.

Preferences on energy sources, tradeoffs, and how they vary across New Mexico

Kara Walter, University of New Mexico *Jennifer Thacher, University of New Mexico*
Janie Chermak, University of New Mexico *Janak Joshi, University of New Mexico*

There are many different technologies that have been or are being developed that can be used for energy production and New Mexico has the potential to extract and produce many of them. While New Mexico consistently ranks in the top 15 for energy production and has large reserves, little is known about how New Mexicans feel about various options and the tradeoffs between them. If the public is unwilling to switch or if they do not believe that technologies will help the economy, their community, or environment, then technologies are unlikely to gain traction. Some of these are currently economically viable, meaning that they are cost effective and can be used on a large scale, such as coal or solar while others are still being developed, such as bioalgal. To address these questions, we are conducting a statewide survey that will allow us to see how opinions across the state vary. This poster presents the research questions underlying the survey, our hypotheses, and maps specific survey questions to the hypotheses and research questions. Such questions include the perceived threat to the environment and water supply based on current production and potential. Questions about extraction and production energy on public lands are also included. We expect preferences to vary across the state, where distance to technologies and resources, beliefs about the environment, and state of their local community are important determinants.

Preliminary study of CO2 efflux across the Nacimiento Fault, San Ysidro, NM

Hyunwoo Lee, University of New Mexico *Laura Crossey, University of New Mexico*
Christopher McGibbon, University of New Mexico *Karl Karlstrom, University of New Mexico*
Valerie Blomgren, University of New Mexico *Tobias Fischer, University of New Mexico*

The Nacimiento fault in northern New Mexico forms the boundary between the Nacimiento Mountains and the San Juan basin. A series of travertine-depositing CO2-rich springs is associated with the structure, implying a long history of significant CO_2 efflux. Previous work has shown 3He/4He ratios of 0.17-0.20 RA indicating the presence of mantle-derived 3He. Carbon isotope values range from 0 to -8.1%. Many studies have reported diffuse CO_2 emissions at volcanic areas and some fault zones (e.g. San Andreas Fault and Anatolian Fault). This preliminary study is the first campaign to measure diffuse CO_2 fluxes in the Rio Grande rift in order to understand how much CO_2 is emitted from the San Ysidro area. On September 22, 2014, CO_2 flux variations across the fault were measured by EGM-4 (PP systems) with a gas accumulation chamber. A t-shaped connector with a needle was used for gas sampling into evacuated glass vials with a rubber septum. The CO_2 flux rates at fault zones of 11.5 g/m2d to 282.5 g/m2d are higher than measured background values of 3.4 g/m2d to 7.9 g/m2d. These results imply that the Nacimiento fault is a major pathway for CO_2 migration. Gas samples will be analyzed for CO2 concentration, overall gas composition, and additional carbon isotope compositions in order to further constrain endogenic gas flux and CO_2 sources. The results are important for understanding the broader Jemez geothermal system and mantle degassing in continental interiors.

Separation and analysis of produced water for osmotic power development (#24)

Elizabeth Jackson, Eastern New Mexico University

Produced water is a term used in the oil industry to describe water that is produced as a byproduct along with oil and gas. Most produced water contains: dissolved inorganic salts, dispersed oil droplets, dissolved organic compounds (dissolved oil), treatment and work over chemicals, dissolved gases (hydrogen sulfide and carbon dioxide), bacteria and other living organisms, and dispersed solid particles. Due to the high concentrations of ions this type of water is a viable option for the production of osmotic power. The high concentrations produce a flux across a semi-permeable

membrane producing well over 3x the power density of regular New Mexico water. In order to test this theory the produced water must be separated into a polar species and an organic layer using a separatory funnel and a non-polar organic solvent. The organic layer will proceed to be removed and a drying agent will be administered for the removal of any excess water. After the completion of the drying agent the species will undergo thin layer chromatography (TLC) for the analysis of molecules present, as indicated by single black dots on the plate. The use of TLC will also aid and give insight into the amount of ions present in the sample. For future analysis, GC-MS will be used as a technique in determining the exact amount of ions present in the sample and Ion Chromatography will be used in determining the exact concentrations of those said ions.

Unpaired electrons as reporters of excited state interactions

Benjamin W. Stein, University of New Mexico
David A. Shultz, North Carolina State University
Christopher R. Tichnell, North Carolina State University
Martin L. Kirk, University of New Mexico

Spin is an intrinsic property of electrons and it is responsible for the vast majority of magnetic behavior in matter. Furthermore, the interaction between unpaired electron spins can lead to many interesting and useful molecular systems. When a molecule absorbs a photon of light, two unpaired electrons are typically formed and it is the interactions between these two electrons, and with their molecular environment, that are the dominant force in controlling excited state behaviors. Careful control of excited state behaviors is crucial to fields as diverse as solar energy and molecular electronics, and this work demonstrates one part of the toolbox that we are developing to understand these complex phenomena. In particular, this work focuses on how to use the interaction between the photogenerated, unpaired electrons and additional pendant radicals to understand the short lived excited states which are formed upon the absorption of light. Specifically, our work involves the development of ways to modify molecules in a way that does not change their basic properties, but allows for the use of more advanced techniques to better understand key relationships between molecular structure and their electronic behavior. This, in turn, will enable the construction of a complete molecular toolbox for the construction of new and useful molecules. These modifications allow for the use of advanced high–field magnetic techniques, and we will discuss how these are being used to understand the complex interactions between ground and excited states as the pertain to magnetic exchange interactions.

What is inside an invasive frog? Bullfrog diet of the Mora River

Steven Salinas, New Mexico Highlands University
Robert E. Ortega, New Mexico Highlands University
Micah Daboub, New Mexico Highlands University
Adrian Carter, New Mexico Highlands University
Justin Saíz, New Mexico Highlands University
Jesús Rivas, New Mexico Highlands University

Invasive species are the single worst conservation problem at the species level worldwide. Invaders can negatively affect the diversity of native species via predation or competition for resources. American Bullfrogs was introduced in Northern New Mexico since the 1940s and because the introduction was so long ago there have been no quantification on the impact bullfrogs cause on the native aquatic fauna. In this study I analyzed 400+ stomach contents of bullfrogs in the Mora River. Most of the stomachs contained northern crayfish (Orconectes virilis) followed by whatever insect was abundant at the time. We found often some unidentified white slime that we believe may be from eggs masses of other amphibians or fishes. Surprisingly, we did not find any leopard frogs in the diet of bullfrogs. The fact that leopard frogs are not present in the diet of bullfrogs, yet they are locally common, suggest that there may have experienced a micro evolutionary process that allows them to coexist with the invasive predator. We believe that this population may be used to restock other sites where leopard frogs have been driven extinct by bullfrogs.

POSTER SESSION AWARDS

Presentations at the afternoon Poster Session were reviewed by an independent panel of judges who scored each poster for content and presentation. Awards for the best undergraduate and graduate posters were presented at the conclusion of the Symposium.

Undergraduate Posters

First Place

Chris Hirani, Central New Mexico Community College
Batch extractions of metals from bicarbonate and ascorbic acid solutions

Second Place

Alexandra Minitrez, University of New Mexico
New Mexico geothermal resources: A database compilation for New Mexico EPSCoR

Third Place (Tie)

Nadia Maqbrouk Mujyna, Santa Fe Community College
Effect of encapsulation on algal photosynthesis

Francisco Whitson-Brown, Santa Fe Community College
Emergency water generator

Graduate Posters

First Place

Chaitanya Kukutla, New Mexico State University
Evaluation of cost-effective harvesting technology to make algal systems

Second Place

Brittney Dlouhy-Massengale, Eastern New Mexico University
Cultivation of microalgae in dairy wastewater on an Algal Turf Scrubber: Adaptation to a local environment

Third Place

Marisa Repasch, University of New Mexico
Fault networks of the Embudo Zone, northern New Mexico: Evaluating differential incision in the Rio Grande and implications for hydrothermal fluid pathways

THE NEW MEXICO ACADEMY OF SCIENCE AWARDS FOR OUTSTANDING SCIENCE TEACHING 2014

Each year the New Mexico Academy of Science presents two Awards for Outstanding Science Teaching. Nominations for these awards come from school superintendents, principals, other teachers, parents, and students. An NMAS Awards Committee reviews the nomination materials. Traditionally one award is made to a high school teacher and a second to a middle school teacher although, on occasion, the latter group is extended to include an elementary school teacher. The awards are presented at the Annual Meeting of the Academy which coincides with the Annual Research Symposium.

The recipients of the 2014 Awards for Outstanding Science Teaching are:

Lindsay Henson

Public Academy for Performing Arts, Albuquerque, NM

Lindsay Henson is a science teacher for grades 9-12 at the Public Academy for Performing Arts in Albuquerque. As a science teacher, Ms Henson believes that her students should feel as though the only limits to what they can do and what they can learn is what they limit themselves to, not what others say they can or cannot do. Many of the science projects she creates for students are cross-curricular. She started the National Honor Society chapter at the school. She has had four students accepted in the NASA WISH Program (Women in STEM High School Scholars Program). During the 2013-2014 school year, Ms Henson had students participating in the ExploraVision National Science Competition sponsored by Toshiba and NSTA.

Colleen Ruiz

Annunciation Catholic School, Albuquerque, NM

Colleen Ruiz is a science teacher for grades 3-6 at Annunciation Catholic School in Albuquerque in a hands-on lab setting. Her 6th grade students participate in the Future City competition and last year her students placed 2nd and 3rd at the state competition and won the best essay award. Her third through sixth graders have won many awards in the Destination ImagiNation competitions. She has been a board member of the New Mexico Science Teachers Association for several years and helps coordinate the annual conference. She was awarded the NM Science Teacher of the year in 2013 and the Catholic Award for Teachers from the Catholic Foundation. She has been nominated for the Presidential Award for Excellence in Science Teaching.

Additional information about these Awards, and the procedures for submitting nominations can be found on the Academy's web page at http://www.nmas.org.

STUDENT PAPERS

CHARACTERIZATION OF CARROTS IN MAKINGFRUIT/VEGETABLE JUICES: WILL CARROTS DESTROY ASCORBIC ACID?

Lilly Chiou

ABSTRACT

Ascorbic acid oxidase (AAO) catalyzes the reaction: 2L-ascorbate + O_2 -> 2 dehydroascorbate + $2H_2O$ and has been found in fruits and vegetables such as orange, broccoli, squash and cucumber. In this project, carrots and zucchini were tested to see if they have the ability to oxidize ascorbic acid. Different forms of carrot samples: shredded, juice, residue, and blended were added to 0.05% ascorbic acid solution. All of them caused a decrease in ascorbic acid concentration compared to the control sets without carrot added. For example, after 15 minutes, 10g shredded carrots decreased ascorbic acid by 28% and blended carrots by 50%. As for zucchini, 10g shredded zucchini decreased ascorbic acid by 40% and blended zucchini up to 97% after 15 minutes. Carrots and zucchini were further tested by blending with red bell pepper juice which is rich in ascorbic acid and resulted in 55% and 75% decrease in 15 min, respectively. For the same weight, zucchini caused a higher percentage of ascorbic acid loss than carrots, suggesting that AAO activity or the amount of the enzyme is higher in zucchini. Different temperature treatments were also applied to test their effect on AAO activity. The results show that the heat treatment (steaming and boiling) is more effective in inactivating AAO than the cold treatment (freezing). For example, after 15 min, 10g frozen shredded carrots still reduced ascorbic acid by 24% (compare to 28% of untreated carrot), but 10g boiled carrots only decreased ascorbic acid by 5%. Blended 1g frozen zucchini decreased ascorbic acid by 45% after 15 minutes (compare to 81% of untreated zucchini), but 1g boiled zucchini caused no deduction of ascorbic acid. This suggests that AAO can be denatured by heat more easily than cold and is more sensitive to extreme temperature in zucchini than in Carrots. Further tests also show that this enzyme is water soluble. This characterization of AAO activity toward reducing ascorbic acid is very useful when making selections for a healthy fruit and vegetable juice in order to avoid losing ascorbic acid in the process.

Vitamin C has two major forms: L-ascorbic acid, the dominant reduced form in our diet, and dehydroascorbic acid (DHAA), the oxidized form (Figure 1). These two forms are absorbed by separate transporters in the intestine[1]. Ascorbic acid is absorbed through the Na^+-dependent transporters SVCT1 and SVCT2 and then diffused into the bloodstream directly; DHAA is absorbed by the GLUT glucose family transporters, and then rapidly reduced back to ascorbic acid by DHAA reductase before diffusing into the bloodstream. It is more efficient to have ascorbic acid than DHAA in our diet as a vitamin C source because the uptake of DHAA by the GLUT transporters can be blocked by dietary sugars when they saturate the transporters[2, 3].

Lilly Chiou, student at Carlsbad High School, 3000 West Church Street, Carlsbad, NM 88220. chiou.lilly@gmail.com

Ascorbic acid oxidase (AAO), first found in cabbage [4], is able to oxidize ascorbic acid to DHAA in plant tissues. AAO was later found in many other fruits and vegetables like orange, broccoli, carrot, cucumber, and zucchini[5, 6, 7, 8]. Unlike the previous researchers' focus on identifying the function of AAO in plant development, my focus here is the effect of AAO on ascorbic acid level in our diet, like in fruit and vegetable juices, and how to avoid the oxidation of ascorbic acid to DHAA by AAO.

Carrots were tested first since they are a popular choice in making fruit/vegetable juice and also contain AAO. Different forms of carrots were mixed for different time periods with ascorbic acid rich solutions including daikon (like white radish) and red bell pepper juices. The ascorbic acid levels were measured by iodine titration and then compared to the control sets without carrots. Zucchini is the second subject tested. Different temperature treatments like freezing and boiling were also applied to carrot and zucchini to mimic the cooking and storage methods toward the effect on AAO activity.

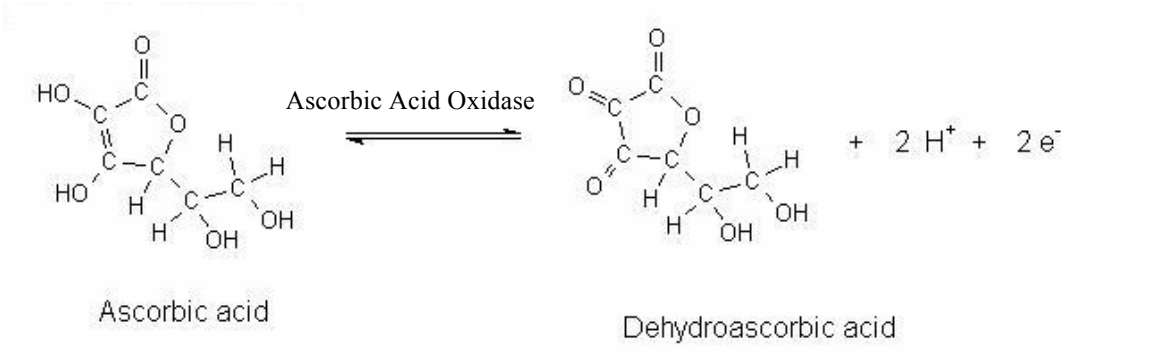

Figure 1. Chemical structures for the reduced form (ascorbic acid) and the oxidized form (dehydroascorbic acid) of Vitamin C[9].

METHODS

Ascorbic acid sources:

Ascorbic acid sources were: 0.05% ascorbic acid solution, daikon and red bell pepper juices. Blend 1200g daikon with 1000ml water or 3 bell peppers (~600g) with 700ml water for 2 minutes in 2 portions. Remove residues by sieve.

Test setting:

For each test, four different time periods were selected between 5 minutes to 2 hours and six 250ml beakers were used each time period. Three were ascorbic acid sources with carrots/zucchini, two were controls with ascorbic acid only, and one was carrots/zucchini in water as the control for the contribution of ascorbic acid from added carrots/zucchini. After each time period, iodine tincture was used to titrate the ascorbic acid content, represented by the drops used. The percent decrease of ascorbic acid is calculated as follows:

[Average I_2 drops used in control set without carrots – (average I_2 drops used in carrots/ascorbic acid- I_2 drops used in carrots/water)] / Average I_2 drops used in control without carrots

Prepare carrot juice and residues:

Carrot juice and residues were collected using a Black & Decker juice extractor(10g carrot per test beaker). The juice was then poured through a sieve.

Prepare blended carrots/zucchini:

Carrots/zucchini were blended with proper amounts of solution (10g/40ml) for 2 minutes. Adjust the control solution to the same volume as the blended ones. Carrots/zucchini were also blended in water (10g/40ml). Timing started at the end of blending.

Temperature treatment on carrots/zucchini:

Shredded carrots (10g) were put in a) sealed Petri dishes andfrozen for 3 days, b) 250ml beakers covered by plastic wrap and steamed for 30 minutes, c) a folded aluminum foil and boiled in water for 30 minutes. Carrot juice was put in screw-capped tubes then frozen for 3 days or boiled in water for 10 minutes. Zucchini was sliced to small pieces then frozen for 1 day or boiled in water for 30 minutes.

Prepare zucchini-soaked water:

Soak 100g shredded zucchini in 420ml water overnight and filter by Whatman #40. Add 1ml 2% ascorbic acid solution to 40ml filtered water. The concentration of zucchini was 9.5g/40ml water.

RESULTS

Shredded carrots caused a significant decrease in ascorbic acid content when compared to the control sets without carrots (Table 1 and Figure 2). After15 minutes of mixing, the ascorbic acid content decreased by 20-28%. After 1 hour, it decreased further to 33%. By 2 hours, 40-46% ascorbic acid was lost.

Table 1. The Percent Decrease of Ascorbic Acid in Different Solutions after Mixing with 10g Shredded Carrots for Different Time Periods.

		5 min.	15 min.	30 min.	1 hr.	1.5 hr.	2 hr.
40 ml 0.05% Ascorbic Acid	Set 1	21.7	24.7	27.3			
	Set 2	20.2	31.8	33.3			
	Set 3			31.1	30.4	40.0	43.2
	Set 4			35.4	36.0	35.4	46.0
	Average	21.0	28.3	31.8	33.2	37.7	44.6
50 ml daikon juice	Set 1		26.2	33.3		36.2	41.0
	Set 2		28.6	34.9		38.1	39.7
	Average		27.4	34.1		37.2	40.4
40 ml red bell pepper juice	Set 1		22.3	24.1	32.7	36.9	39.3
	Set 2		19.4	29.4	33.7	38.0	43.4
	Average		20.9	26.8	33.2	37.5	41.4

Figure 2. Data Corresponding to Table 1 with Samples Mixing with 10g Shredded Carrots.

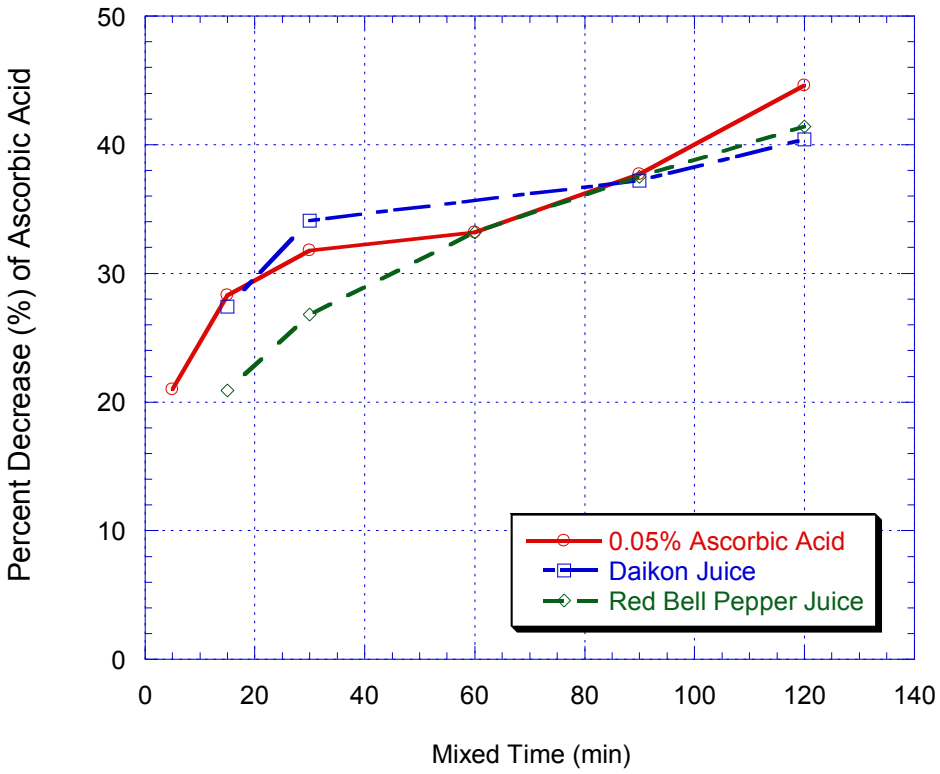

Pure carrot juice, carrot residues, and blended carrots all had the ability to decrease ascorbic acid as shredded carrots did (Figures 3, 4 and 5). Blending carrots directly had the most effect as half of ascorbic acid was lost in only 15 minutes after blending. Mixing with carrot juice was much less effective, resulting in only an 11-16% loss after 30 minutes but the decrease can go up to 22-31% in 2 hours. The residue was slightly more effective than the juice. At 30 minutes an 18-26% loss was observed, and the decrease went up to 25-33% in 1.5 hours.

Figure 3. The Percent Decrease of Ascorbic Acid after Mixing with 5.6ml* Carrot Juice.

*juice extracted from 10g carrots.

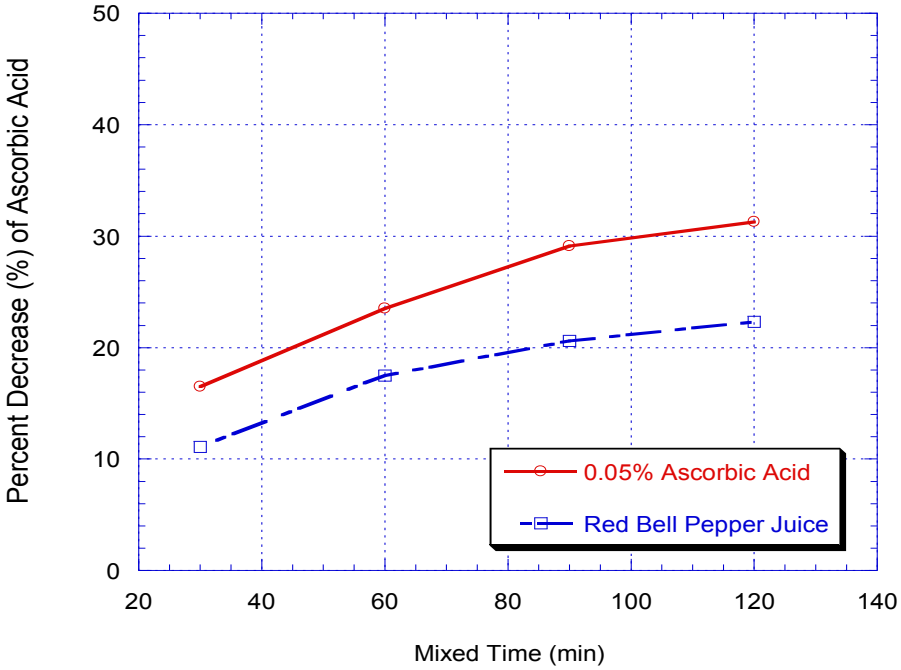

Figure 4. The Percent Decrease of Ascorbic Acid after Mixing with Carrot Residues*.

*Residue added is equivalent to extractions from 10g carrots.

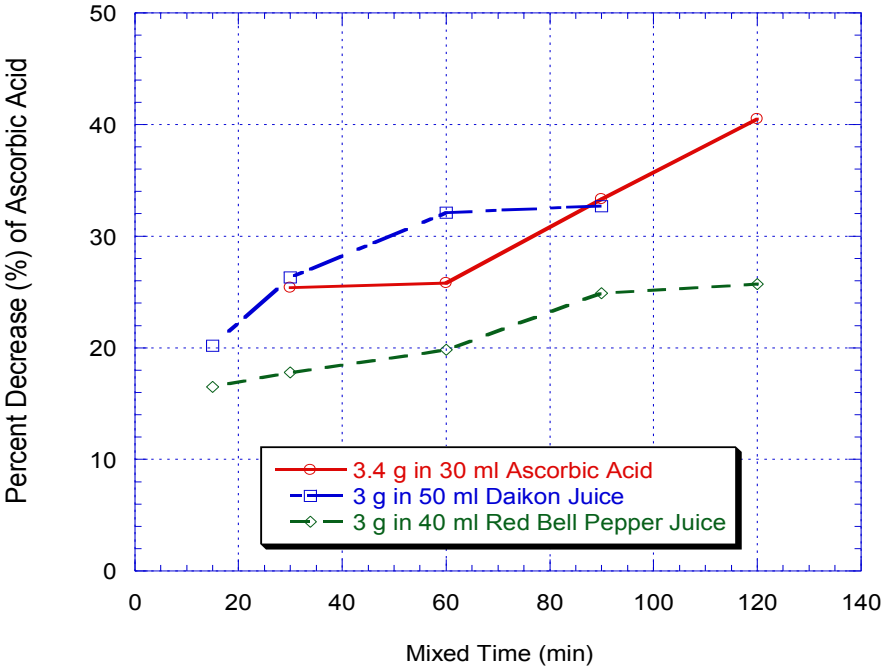

Figure 5. The Percent Decrease of Ascorbic Acid after Blending with 10g Carrots.

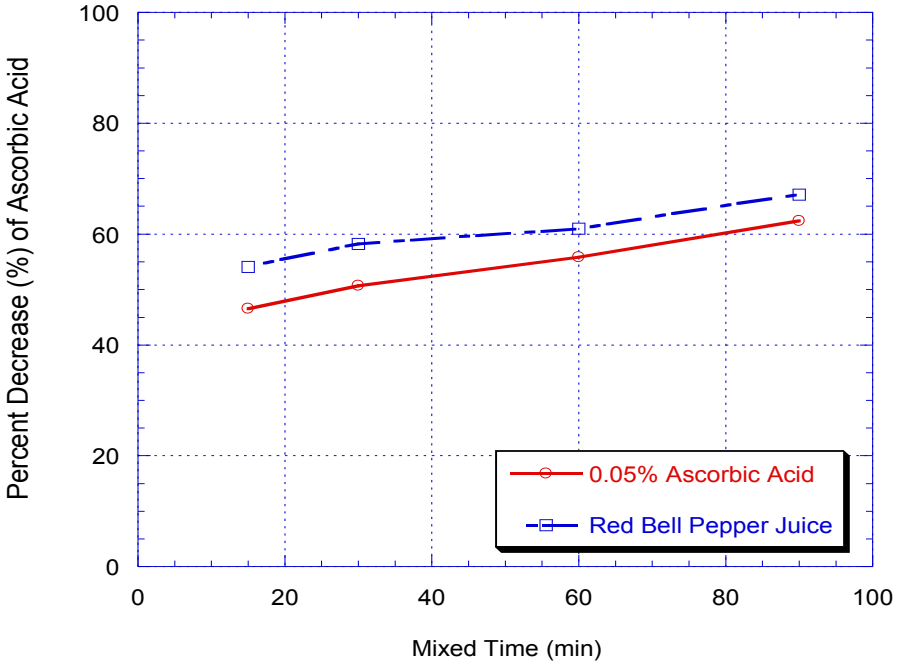

Blending carrots caused the most decrease in ascorbic acid (Table 2 and Figure 6). When comparing 10g shredded carrots to 10g carrots blended, the latter caused a decrease of 51% but the former only 32%. The blending process cuts carrots into many more tiny pieces than shredding does, so it provides larger surface areas to release AAO and hence causes more decrease of ascorbic acid. Because the carrot juice and residues originated together from 10g carrots, their combined effect was similar to that of 10g blended carrots.

Table 2. The Percent Decrease of Ascorbic Acid in 40 ml0.05% Ascorbic Acid Solution mixed with Different Carrot Samples*

*All carrots samples are from 10g carrots.

	30 min.	1 hr.	1.5 hr.
10 g shredded Carrot	31.8	33.2	37.7
5.6 ml Carrot Juice	16.5	23.5	29.1
3.4 g Carrot Residue	25.4	25.8	33.3
Carrot Juice + Residue	41.9	49.3	62.4
10 g Blended Carrot	50.7	55.8	62.4

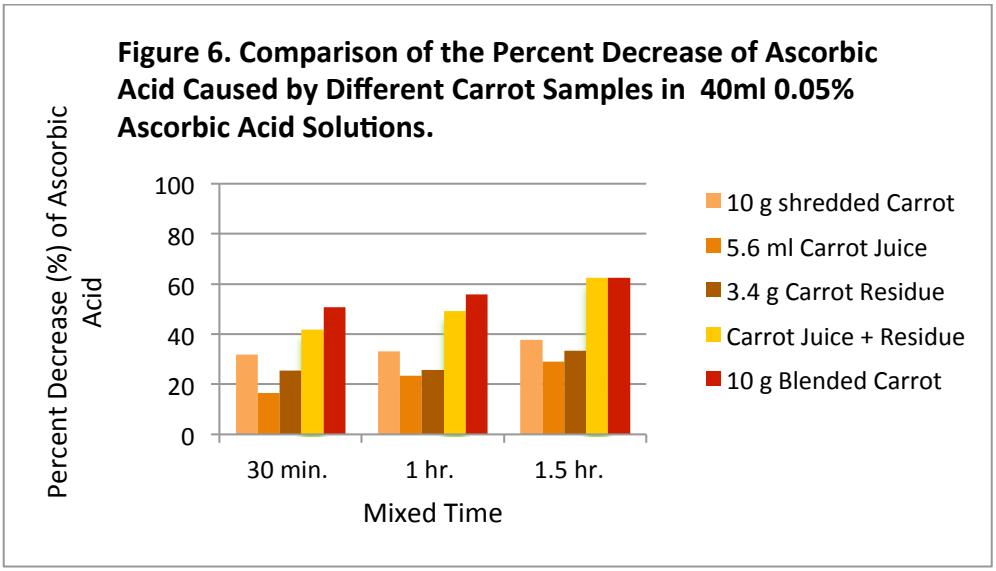

The ability to decrease ascorbic acid was also observed in zucchini (Table 3). When 10g shredded zucchini was added, the ascorbic acid content decreased by 40% after 15 minutes and up to 50% in 1 hour. The same effectiveness of blending over shredding was also observed, 97% decrease compared to 40% after 15 minutes. The strength or abundance of AAO in zucchini seems much higher than in carrots as only 1g zucchini reduced ascorbic acid by 80% in only 5 minutes after blending.

Table 3. The Percent Decrease of Ascorbic Acid in Different Solutions after Mixing or Blending with Zucchini.

	5 min.	10 min.	15 min.	30 min.	45 min.	1 hr.	1.5 hr.
10g shredded with 40 ml 0.05% ascorbic acid			39.2	42.6		49.8	57.3
10g unpeeled blended with 40ml ascorbic acid			97.4	97.4	97.5	97.4	
10g peeled blended with 40 ml ascorbic acid	79.8	97.3	97.3	97.3			
1g unpeeled blended with 40ml ascorbic acid	79.8	80.8	81.4	83.7		91.3	
1g unpeeled blended with 40ml red bell pepper juice	71.1	74.2	73.9	74.3		74.1	

The freezing treatment of carrots had only a slight effect on AAO (Figure 7). After 15 minutes, ascorbic acid was decreased by 23.7%, similar to the 28.3% decrease caused by untreated carrots. However the heat treatment, both steaming and boiling, had a more pronounced effect as ascorbic acid decreased only by 5-7%.

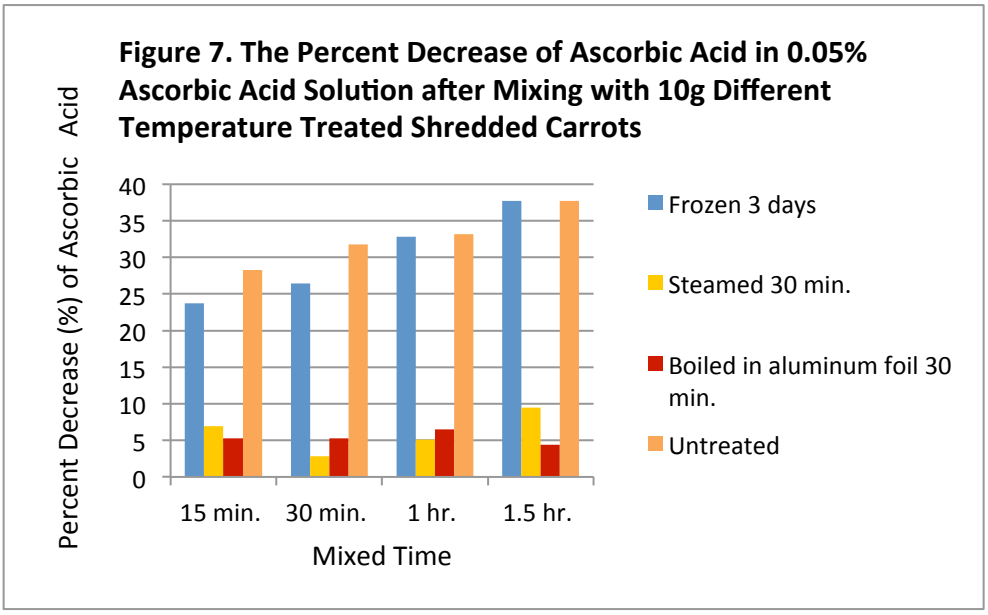

A similar pattern was also observed in carrot juice (Figure 8). Freezing treatment hadonly a slight effect, as ascorbic acid was reduced to 12% at 15 minutes, similar to 14.4% of the untreated carrot. On the contrary, only less than 5% of ascorbic acid was lost up to 1.5 hours if carrot juice was boiled first.

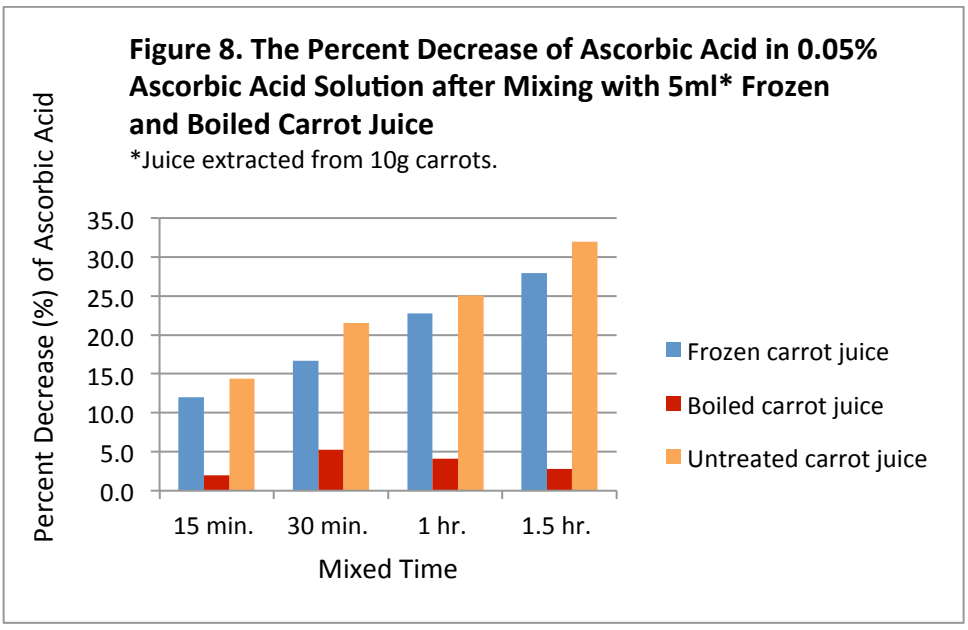

A similar temperature effect was also shown in zucchini (Figure 9). No ascorbic acid decrease was observed if the zucchini was previously boiled for 30 minutes. However, the frozen zucchini still decreased ascorbic acid by 40-60% in a time period of 1 hour.
The differences between the frozen and untreated zucchinis (Figure 9) were much larger than what was observed between frozen and untreated carrots (Figures 7 and 8), suggesting AAO in zucchini was more vulnerable to cold temperatures. These various responses toward temperature treatments may relate to the character of the heat shock proteins in carrots and zucchini.

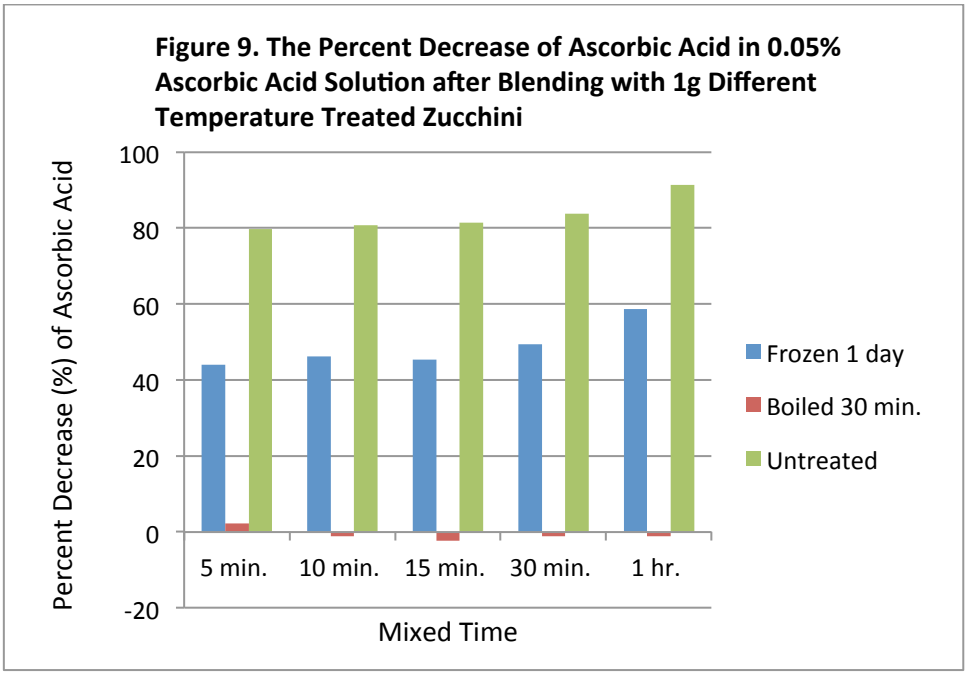

Filtered carrot juice still carried the ability to decrease ascorbic acid (Table 4 and Figure10). Since all the solid residues were filtered out, the decrease is caused by the enzyme existing in the liquid; that is, AAO is soluble in water. This is further supported by the fact that the zucchini-soaked water can cause ascorbic acid decrease (Table 4 and Figure 11), similar to the effect caused by shredded zucchini.

Table 4. The Percent Decrease of Vitamin C in 40ml 0.05% Ascorbic Acid Solution after Soaked Zucchini Water* and Filtered Pure Carrot Juice** are Added.
*equivalent to 9.5g shredded zucchini **extracted from 10g carrots

	15 min.	30 min.	1 hr.	1.5 hr.	2 hr.
Soaked zucchini water*	33.3	41.3	57.4	63.8	
10g shredded zucchini	39.2	42.6	49.8	57.3	
5ml carrot juice**, filtered by Whatman #40 filter paper		6.7	7.9	14.1	18.9
5.6ml carrot juice**, unfiltered		16.5	23.5	29.1	31.3

Figure 10. The Percent Decrease of Ascorbic Acid in 40ml 0.05% Ascorbic Acid Solution after Adding Differently Filtered Pure Carrot Juice.

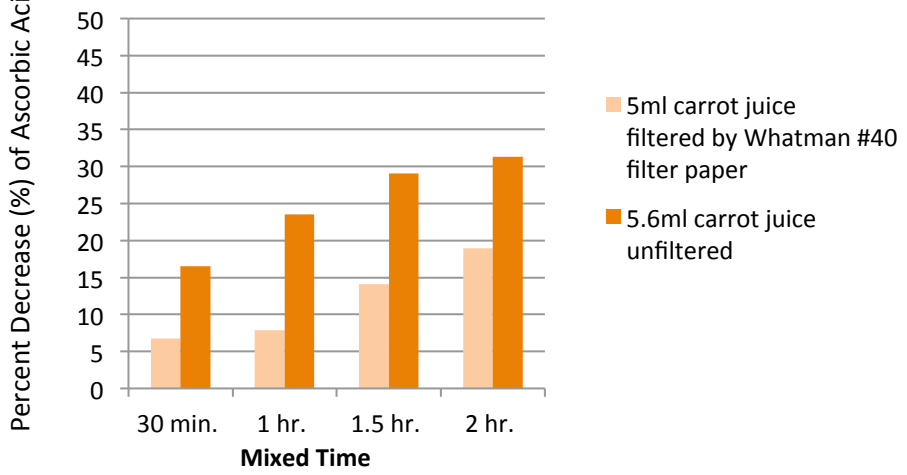

Figure 11. A Comparison of the Percent Decrease of Ascorbic Acid in 40ml 0.05% Ascorbic Acid Solution after Adding Zucchini Soaked Water and Shredded Zucchini.

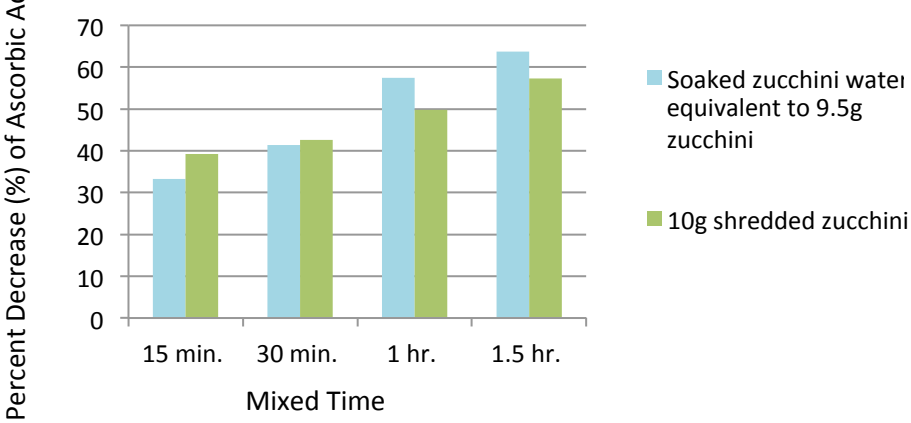

Zucchini is more effective at decreasing ascorbic acid than carrot. For the same weight, adding zucchini always resulted in higher loss than adding carrot, in both shredded and blended forms (Table 5 and Figure 12). This suggests that either the strength of AAO in zucchini is higher than in carrot, or the abundance of the enzyme in zucchini is much higher than in carrot.

Table 5. A Comparison of the Percent Decrease of Ascorbic Acid Caused by Carrots and Zucchini in 40ml 0.05% Ascorbic Acid Solution under the Same Conditions.

	15 min.	30 min.	1hr.
10g shredded carrot*	28.3	31.8	33.2
10g shredded zucchini	39.2	42.6	49.8
10g carrot blended with ascorbic acid	46.5	50.7	55.8
10g zucchini blended with ascorbic acid	97.4	97.4	97.4

*Average from Table 1.

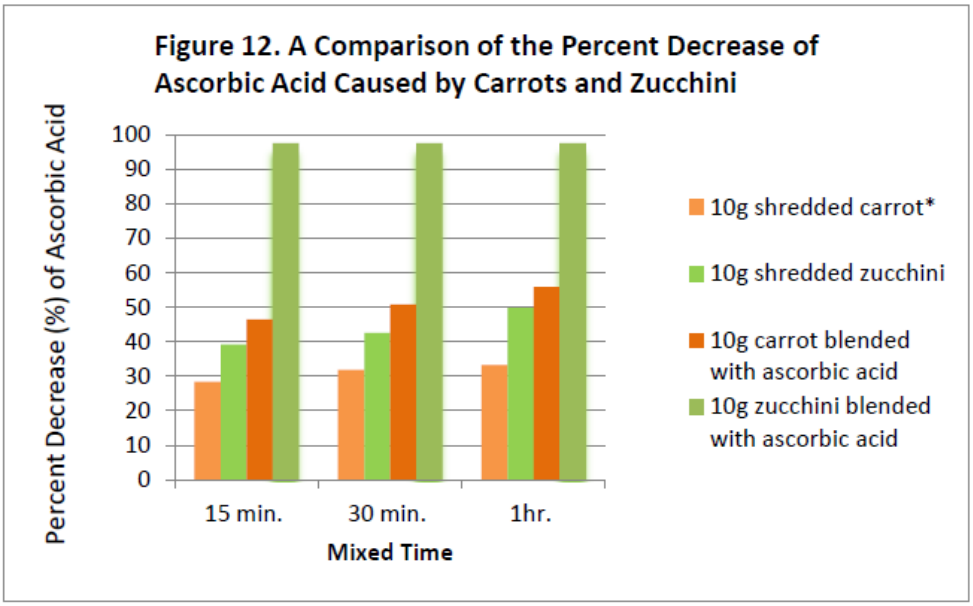

DISCUSSION

The effect of AAO on reducing ascorbic acid in our diet has not been addressed before. Results from this project show that both carrot and zucchini can reduce the ascorbic acid content when mixed with other vegetable juices. Two factors play an important role regarding the extent of ascorbic acid loss: the method and the duration of mixing. The larger contact surface and the longer duration cause higher decrease. This could be due to the water soluble character of this enzyme. As a result, blending carrots/zucchini directly with the ascorbic acid source causes the greatest loss.

The effect of thermal treatment on AAO activity is consistent with the ones previously reported in broccoli[10] and carrot[11]; high temperatures, like boiling and steaming, will inactivate/denature the enzyme. It has been reported that in general freezing will slow down, but does not destroy enzymes in fruits and vegetables[12], explaining why the freezing treatment shows much less effect compared to the thermal treatment.

The plants in the family of Cucurbitaceae such as cucumber and squash are the most abundant sources of AAO[7]. This could explain the higher decrease of ascorbic acid caused by zucchini than carrot. The Cucurbitaceae family also includes watermelon and other melons. Melons, cucumber and carrot are common choices when making fruit/vegetable juices. If the AAO activity in them is high, the ascorbic acid level in the juices would be considerably reduced. Therefore, by studying their AAO activity, we can make better selections when preparing fruit/vegetable juice to avoid the loss of ascorbic acid. The lesson learned here is never blend carrot and zucchini together with other fruits/vegetables!

REFERENCES

1. Gropper S, Smith J (2012) Advanced Nutrition and Human Metabolism (6th edition). Cengage Learning .
2. Liang WJ *et al* (2001) Vitamin C transport systems of mammalian cells. MolMembr Biol. 18(1): 87-95
3. Corpe CP *et al* (2013) Intestinal dehydroascorbic acid (DHA) transport mediated by the facilitative sugar transporters GLUT2 and GLUT8. J BiolChem 288: 9092-9101
4. Szent-Gyorgyi A (1931) The function of hexuronic acid in the respiration of the cabbage leaf. J Biol Chem. 90: 385-393
5. Meiklejohn GT *et al*. (1941) Ascorbic acid oxidase from cucumber. Biochem. 35(7): 755-760
6. Vines MH *et al*. (1963) Citrus fruit enzymes, ascorbic acid oxidase in orange. Plant Physiol. 38(3):333-337
7. Lin L, Varner JE (1991) Expressionof ascorbic acid oxidase in zucchini squash (*cucurbitapepo* L.). Plant Physiiol. 96: 159-165
8. Shimada Y, Ko S (2008) Ascorbic acid and ascorbic acid oxidase in vegetables. Chugokugakuen J. 7: 7-10
9. Dr. Koni Stone (2002) Chem 1112 Vitamin C, Department of Chemistry, California State University Stanislaus
10. Munyaka A *et al* (2010) Thermal stability of L-ascorbic acid and ascorbic acid oxidase in broccoli (*Brassica oleraces var. italica*). J Food Sci. 75(4): 336-340
11. Leong SY, Oey I (2012) Effect of endogenous ascorbic acid oxidase activity and stability on vitamin C in carrots (*Daucascarota subsp. Sativus*) during thermal treatment. Food Chem. 134(4): 2075-2085
12. Willenberg BJ (2003) Quality for Keeps: Freezing Basics. University of Missouri Extension, GH1501

ACKNOWLEDGMENTS

I would like to thank Mr. Robert Cope, the science teacher in my high school, for letting me use the electronic balance and beakers in the chemistry lab. I also want to thank my parents for proofreading and helpful discussions about this paper.

CHASING COMETS; FINDING THE ORBITS OF COMETS USING GAUSS'S METHOD

Chloe Madsen Keilers[1]

ABSTRACT

This project's purpose is to determine orbital parameters for three comets from the Fall 2013 sky. The three comets chosen were ISON (C/2012 S1) – discovered in September 2012; LINEAR (C/2012 X1) – discovered in December 2012; and Brewington (154P) – discovered in August 1992. The method uses more than three dozens angular coordinates (right ascension and declination) taken daily over a 38 to 60 day period from the website: http://www.theskylive.com. The basic Gauss method takes three sets of angular coordinates at three different times and determines the position vector to the comet at the central time, $\vec{r}_2$. The result will be up to three roots, each corresponding to one possible set of the six orbital elements. Each root was further investigated by an "improved Gauss" routine that starts with the basic Gauss results and iterates the procedure to improve the results. For each set of elements, a score was generated to determine which set gave the best fit to all the data. The score is the statistically combined variances of the errors. The best calculated orbital elements were close to those by the Jet Propulsion Laboratory. Most elements are in good agreement with two exceptions: Brewington's eccentricity is off by eight percent and its date of closest approach to the sun is off by one day. ISON's elements were the hardest to find as the eccentricity was the closest to one and slightly hyperbolic (e = 1.0002), but the results are very close to the actual orbit. LINEAR's elements were easier to calculate since it had a lower eccentricity (e = 0.989), but it was still more difficult to find than Brewington's (e = 0.67). This outcome is very good given that these comets have eccentricities close to 1 (i.e., parabolic), which is computationally difficult.

COMETS AND THE CLASSICAL ORBITAL ELEMENTS

Comets are a few kilometers in size, have highly eccentric orbits, and emit spectacular tails of gas and dust as they approach the sun. While collisions during the Earth's early years may have brought the elements for life to Earth, prior collisions may also have caused mass extinctions of species, and new collisions would have devastating consequences. Increasing space traffic, both satellites and planetary missions, also present more objects at risk. Therefore, it is important to study the orbits of comets and other orbiting projectiles.

The primary purpose of this project is to use angular sky coordinates to determine the orbital elements of three comets that were visible in the Fall 2013 sky: ISON (C/2012 S1), Brewington (154P), and LINEAR (C/2012 X1); once found, the orbital elements can be used to predict the past and future positions of the comets. The six classical orbital elements are: q – periapsis – closest approach distance to the Sun; e – eccentricity; Ω – longitude of the ascending node; ω – argument of periapsis; i – inclination – the tilt from the earth's orbital plane (the ecliptic); T – time of periapsis passage, which is related to the current location angle, called the true anomaly, θ.

1. Corresponding author: chloeklrs@gmail.com. Institution: Los Alamos High School, Los Alamos, NM.

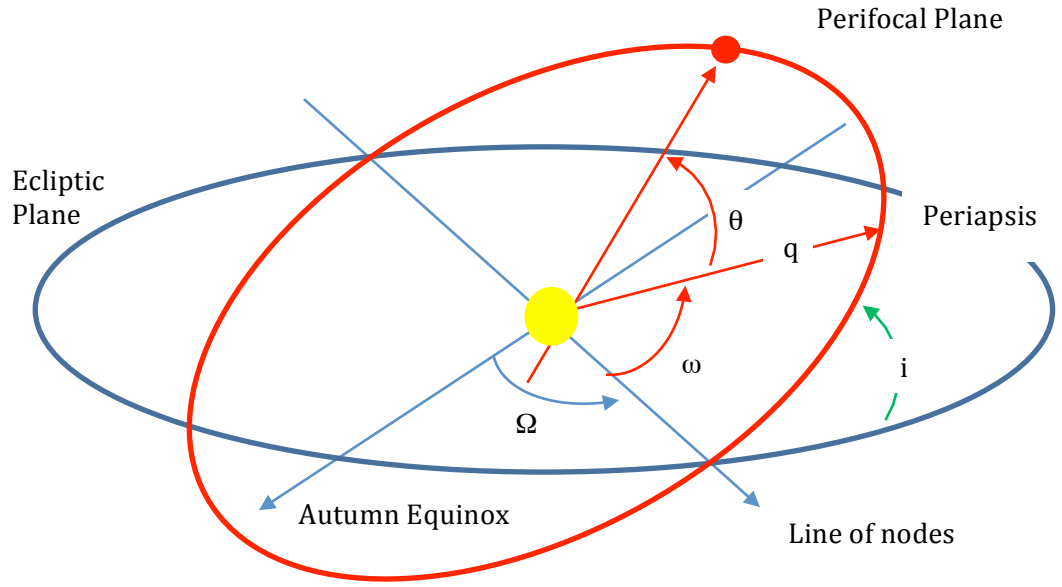

Figure 1: Classical orbital elements

Kepler's laws are key to finding orbital elements. The first law is that comet orbits are conics (i.e., ellipses, hyperbolas, or parabolas) with the Sun at a focus. The second law states that the line connecting a comet to the Sun sweeps out equal area in equal time.

The two common methods for orbit determination are Gauss's method and Laplace's method. Both methods rely on line-of-sight vectors from the earth to the comet at three different times. Both have the same level of complexity. Laplace's method finds an equation to approximate how the line-of-sight vector changes with time and then takes the time derivatives of that equation. Gauss's method takes advantage of the fact that a comet's orbit is in a plane and uses approximations for the areas of two adjoining triangles made by three observations. In addition, once an initial estimate for the comet position is found, the Gauss method can be modified to improve the accuracy of the estimate. For these reasons, this project uses Gauss's method.

A secondary purpose of this project is to determine sensitivity of the estimated elements to the difference in times between the three angular observations. The analysis was repeated several hundred times using sets of angular coordinates spaced 1, 3, 5, 7 or more days apart. For each set of elements found, a score was calculated to determine which set gave the best fit for all the data for each comet. Determining the orbital elements becomes more challenging if the eccentricity approaches one, due to loss of computational accuracy.

METHOD

Finding the orbits requires angular sky coordinates – right ascension and declination – at three or more different times (Figure 2). For this study, 38 days of data were used for Brewington and LINEAR and 60 days of data were used for ISON. The angular coordinates were taken daily from theskylive.com, which interpolates data from the NASA Jet Propulsion Laboratory (JPL) (Figure 3). Table 1 shows typical input data; all the input data is plotted in Figures 4 and 5. Since comets with right ascension within 15 degrees of the sun would be obscured by sunlight at dusk or dawn, data in that range was not used.

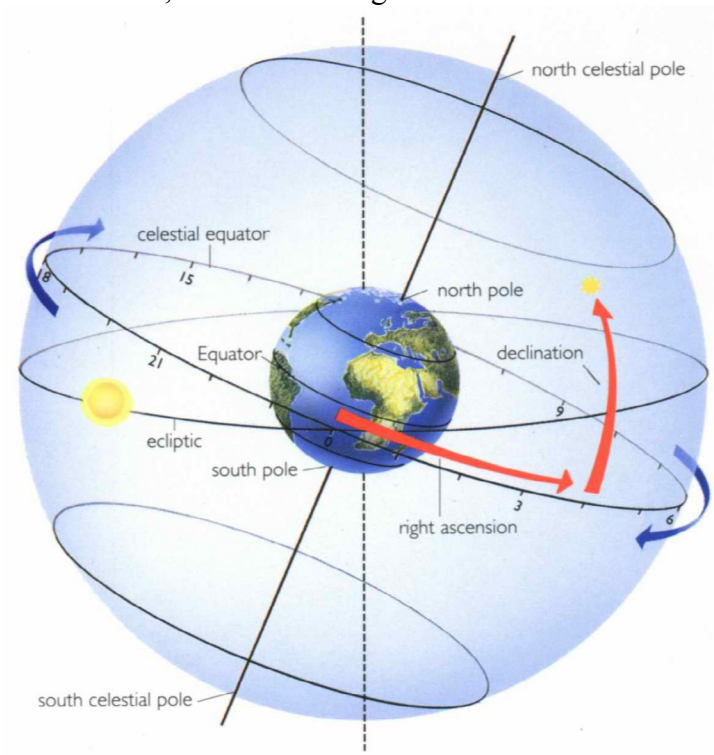

Figure 2: Equatorial coordinate system – showing the right ascension and declination angles and the ecliptic and equatorial planes (source: http://crab0.astr.nthu.edu.tw/~hchang/ga1/f0202-equatorial.JPG)

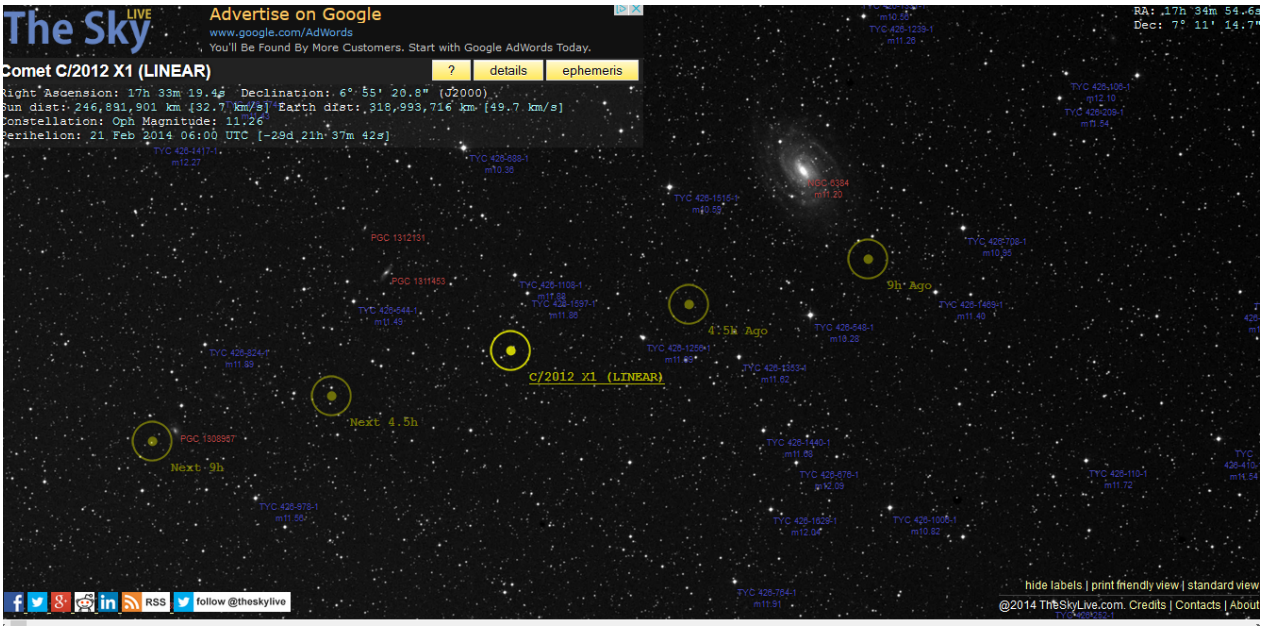

Figure 3: Representative data from theskylive.com

Object	Magnitude	Right Ascension	Declination	Constellation	
Sun	-26.78	20h 17m 09s	-19° 42’ 20”	Capricornus	tracker
Venus	-4.00	19h 02m 54s	-15° 51’ 35”	Sagittarius	tracker
Jupiter	-2.66	▼ 06h 57m 01s	+22° 57’ 45”	Gemini	tracker
…					
Comet 154P/Brewington	9.98	▼ 00h 42m 24s	+24° 30’ 28”	Andromeda	tracker
…					
Comet C/2012 X1 (LINEAR)	11.26	▲ 17h 33m 19s	+06° 55’ 20”	Ophiucus	tracker

Table 1: Representative data from theskylive.com

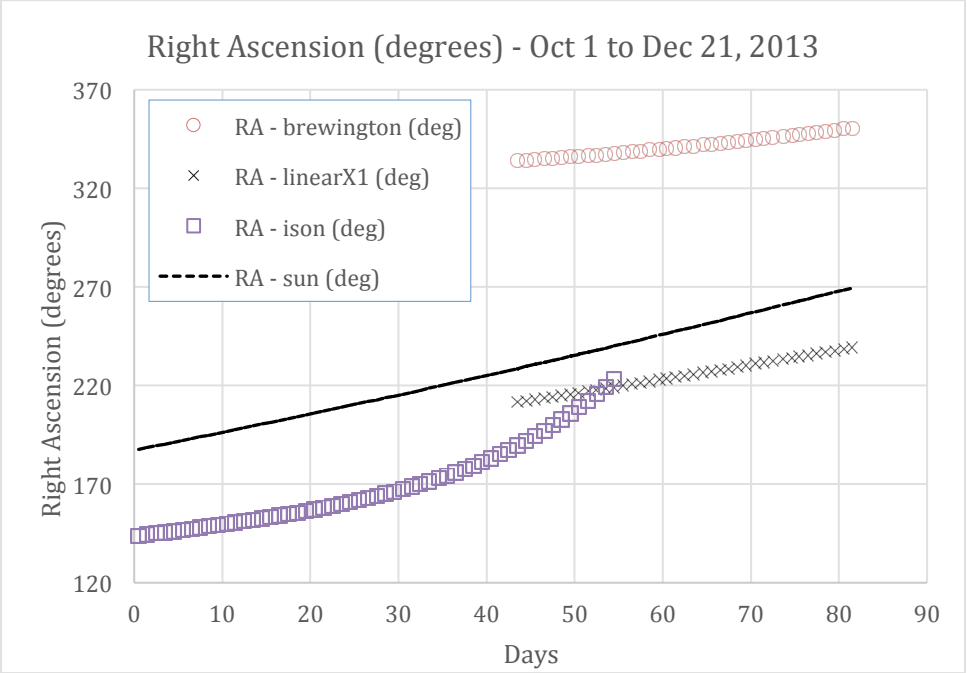

Figure 4: Right ascension input data

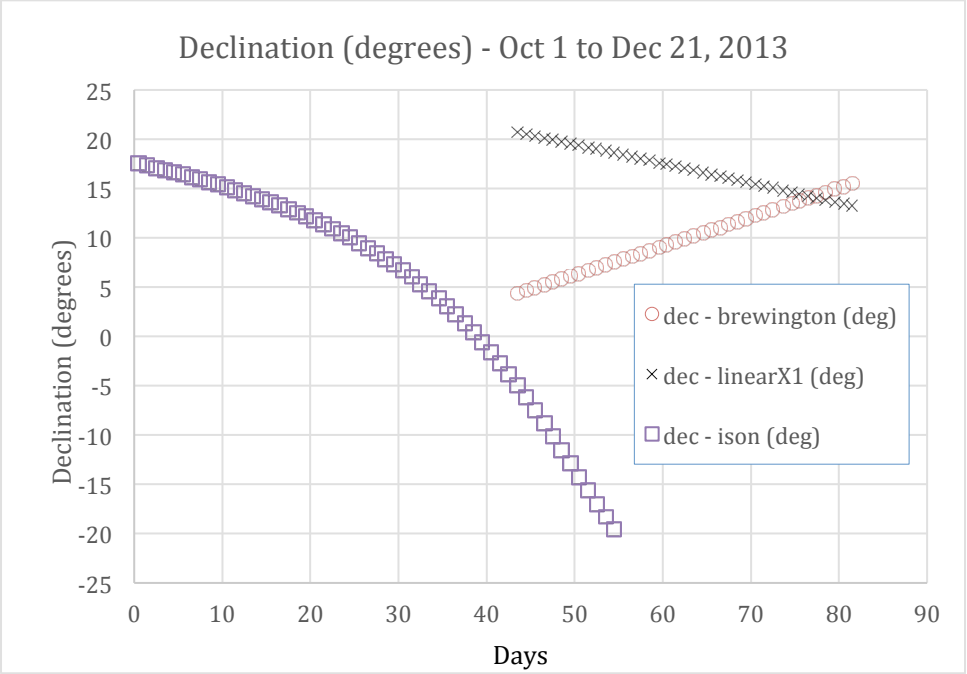

Figure 5: Declination input data

Gauss method was implemented using the computer language, Freemat [Freemat]; the step-by-step method is in Appendix A. At each observational time, the Earth's position vector and the comet's line-of-site vector were found. These values provided coefficients for an eighth-order characteristic equation for the distance (r_2) from the comet to the Sun at the central time, t_2. There are at most three real roots (roots are possible distances) to this equation, leading to three possible sets of orbital elements (the roots are circled in the Figure 6 example).

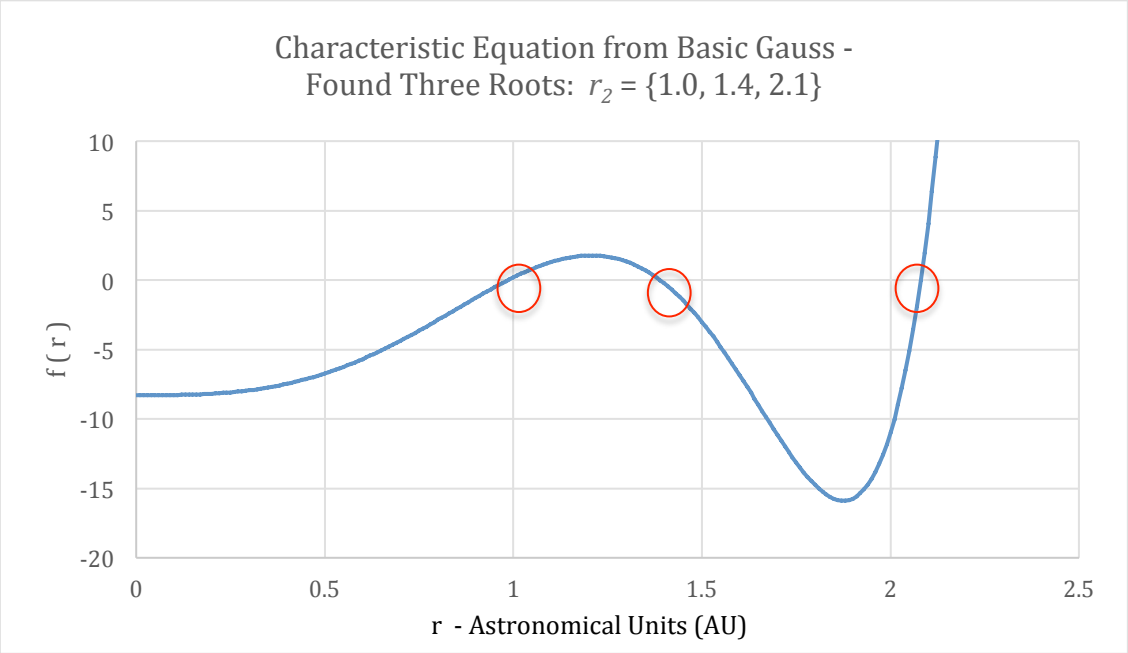

Figure 6: Plot of a representative characteristic equation

Each of these sets of elements was improved upon by an "Improved Gauss" routine. This program uses the initial estimated position of the comet to improve the estimated ratio of the areas of the triangles, leading to an improved estimate of the comet's position at the central time (Figure 7).

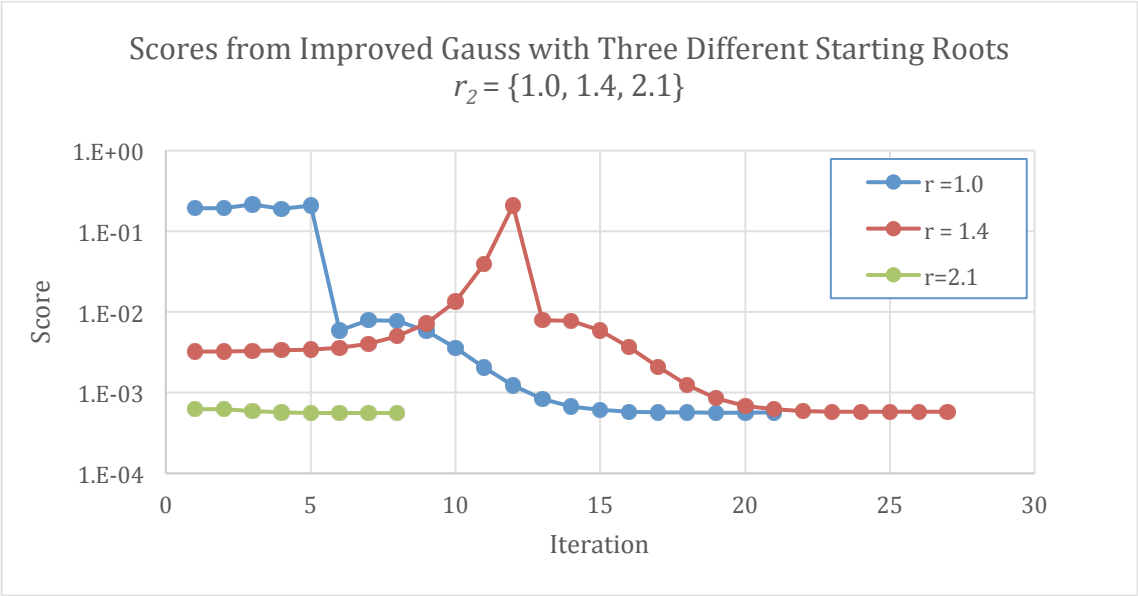

Figure 7: Representative example of iteration with the Improved Gauss routine

A score was determined for each calculated set of elements and is a metric for how well the corresponding angular coordinates agree with those reported by theskylive.com. The score (units of radians) was found using the errors (observation – calculated) of the right ascension ($\Delta\alpha_j$) and declination ($\Delta\delta_j$), at each time t_j, and then taking the combined variances of the errors [Meyer].

$$score^2 = \left\{\frac{1}{n}\sum(\Delta\alpha_j)^2 - \left(\frac{1}{n}\sum\Delta\alpha_j\right)^2\right\} + \left\{\frac{1}{n}\sum(\Delta\delta_j)^2 - \left(\frac{1}{n}\sum\Delta\delta_j\right)^2\right\} \qquad (1)$$

A lower score – or higher inverse score – means better agreement with theskylive.com for all the daily data for a particular comet. Figure 7 shows the best root is r = 2.1 AU.

RESULTS

The orbital elements and scores from the hundreds of runs made for each comet are shown in Figures 8, 9, and 10. For Brewington, many runs indicated a similar best set of elements. ISON had only a few runs (close to the time of periapsis passage) with higher inverse scores that identify the best set of elements; without a systematic data set (e.g., daily measurements), it would have been difficult to precisely find the ISON elements. Finding the best set for LINEAR was slightly harder than Brewington but easier than ISON.

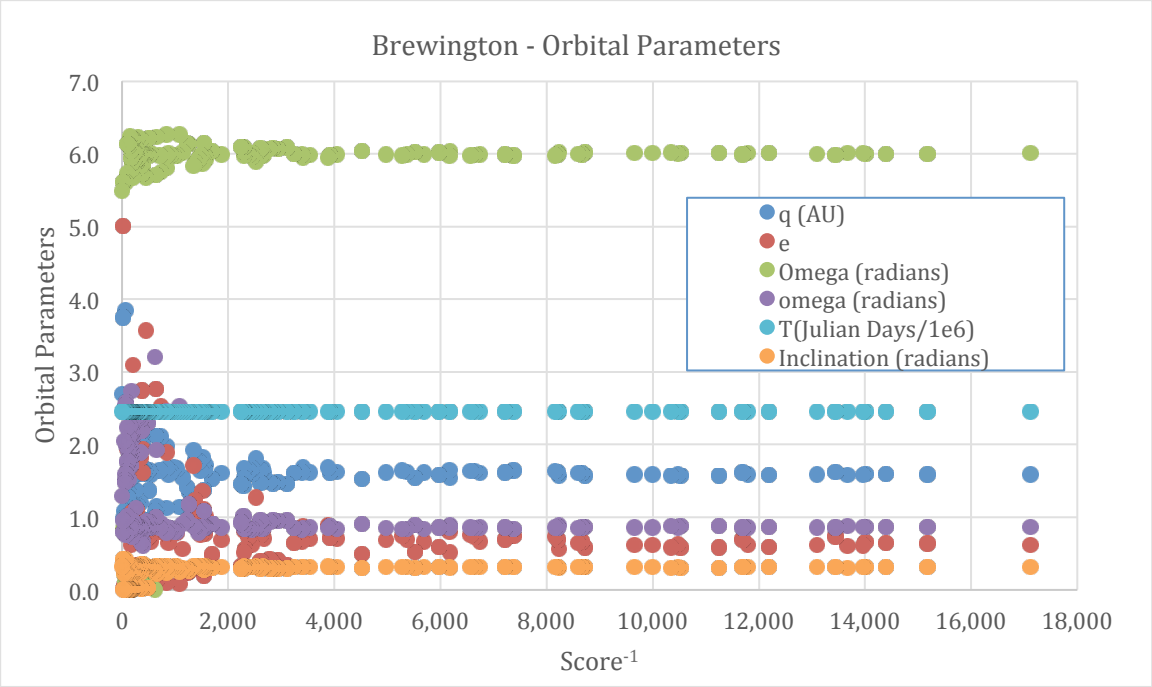

Figure 8: Brewington orbital elements vs. the inverse score

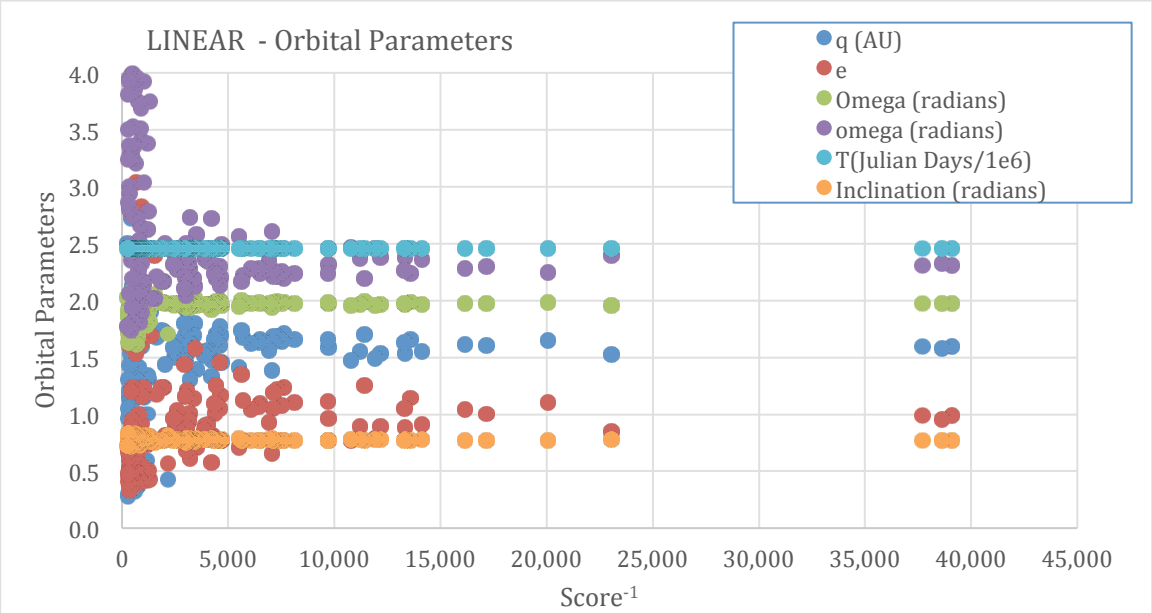

Figure 9: LINEAR orbital elements vs. inverse score

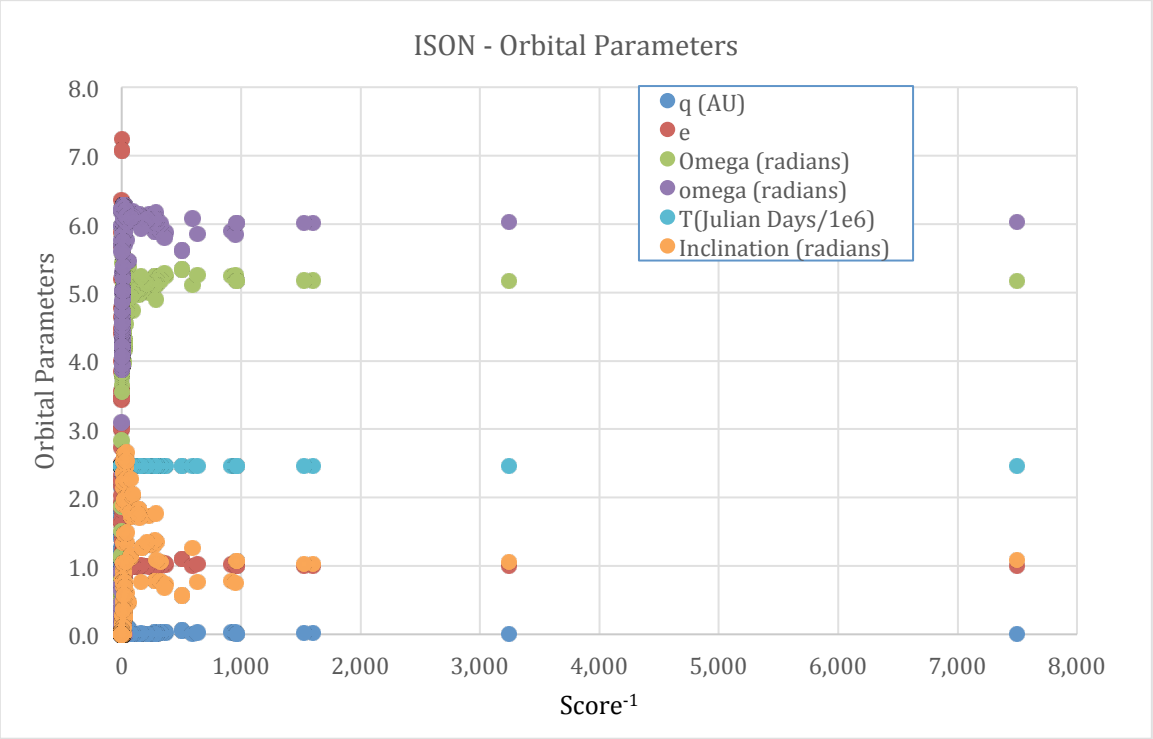

Figure 10: ISON orbital elements vs. inverse score

Brewington							
	q(AU)	e	Ω (deg)	ω (deg)	i (deg)	Periapsis Year Month	Periapsis Day
el1	1.585840	0.617809	344.179625	49.675614	17.711406	2013 Dec	13.6638
JPL	1.607906	0.670554	343.495373	49.032611	17.832175	2013 Dec	12.5011
ratio	0.986276	0.921342	1.001992	1.013114	0.993228	difference (days)	1.1628
LINEAR							
	q(AU)	e	Ω (deg)	ω (deg)	i (deg)	Periapsis Year Month	Periapsis Day
el1	1.595838	0.987091	113.144856	132.103821	44.365343	2014 Feb	21.9148
JPL	1.599336	0.989469	113.082175	132.334189	44.351880	2014 Feb	21.6533
ratio	0.997813	0.997596	1.000554	0.998259	1.000304	difference (days)	0.2615
ISON							
	q(AU)	e	Ω (deg)	ω (deg)	i (deg)	Periapsis Year Month	Periapsis Day
el1	0.012512	1.000099	295.712757	345.508314	62.030969	2013 Nov	28.8026
JPL	0.012453	1.000201	295.652032	345.531241	62.403978	2013 Nov	28.7787
ratio	1.004732	0.999898	1.000205	0.999934	0.994023	difference (days)	0.0239

Table 2: Lowest-score orbital elements (el1) and a comparison to JPL values at http://ssd.jpl.nasa.gov/horizons.cgi

Table 2 compares the best element sets (el1) to those from the NASA's Jet Propulsion Laboratory (JPL) website. Most elements are in good agreement with two exceptions: Brewington's eccentricity is off by 8% and its date of periapsis passage is off by one day.

Figures 11 and 12 show the daily errors between calculated angular coordinates using the best elements and those from theskylive.com. The angular errors are about 0.02 degrees or less.

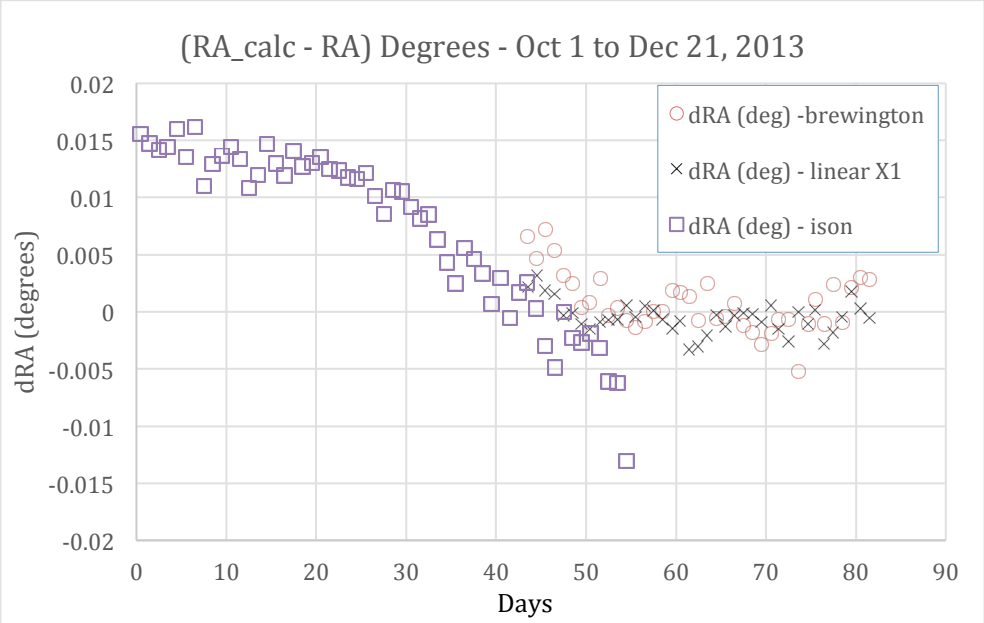

Figure 11: Error in daily right ascension using best sets of elements

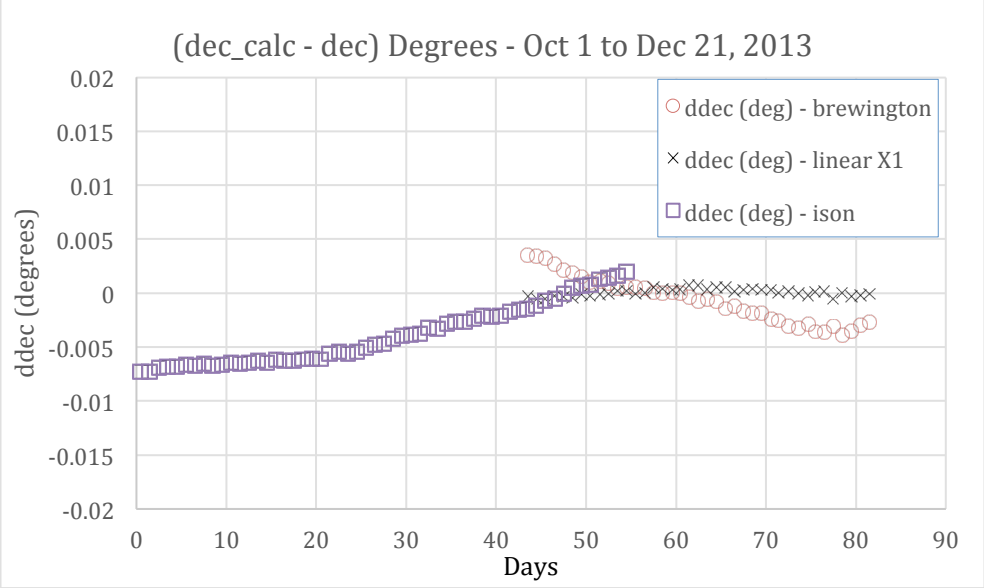

Figure 12: Error in daily declination using best sets of elements

For Brewington and LINEAR, Figures 13 and 14 show the sensitivity to time differences, true anomaly differences, and angular differences in observations. The best scores tend to take place between five to eight days separation and three to five degrees separation in the sky.

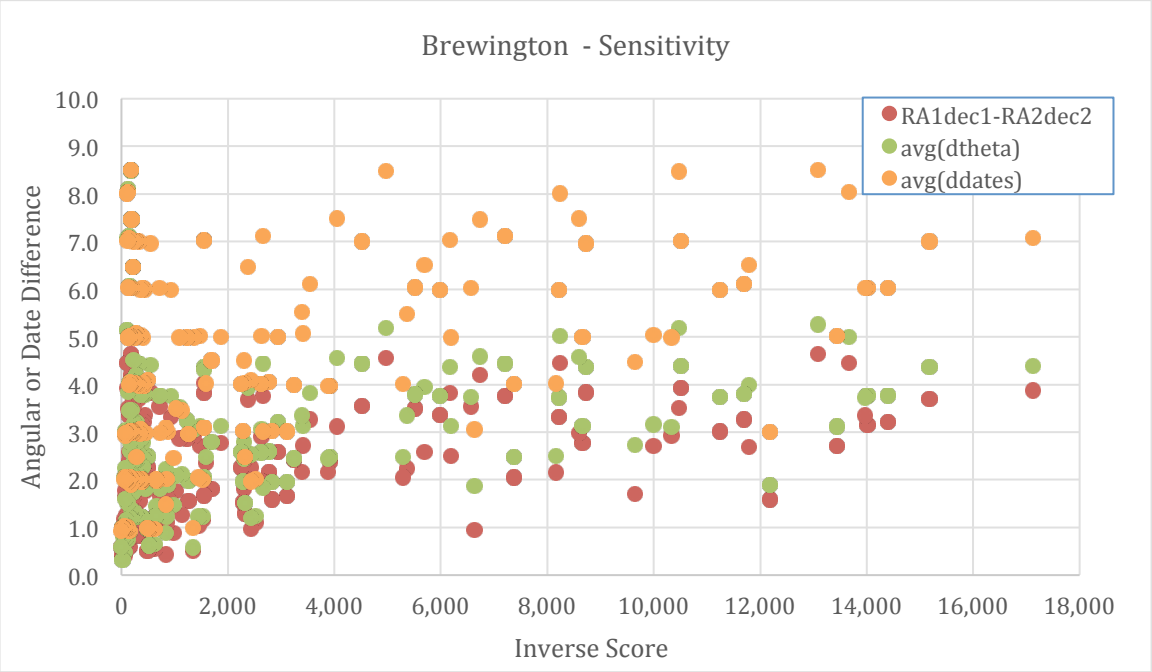

Figure 13: Sensitivity of Brewington orbital elements to date and angular spacing

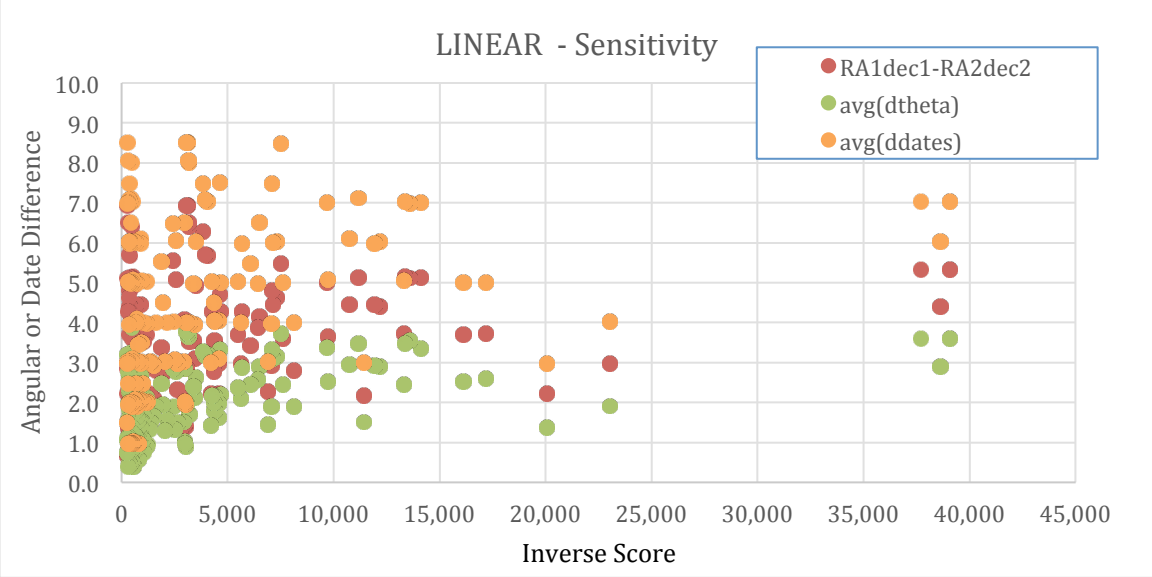

Figure 14: Sensitivity of LINEAR orbital elements to date and angular spacing

The next three graphs show the calculated true anomalies, distances from the Sun, and speeds of each of the three comets (Figures 15, 16, and 17). These graphs tell the story of the comets. LINEAR and Brewington stay outside of the Earth's orbit. ISON is heading straight toward the Sun and gathering speed as it get closer. ISON did not survive intact its closest approach to the Sun (i.e., periapsis).

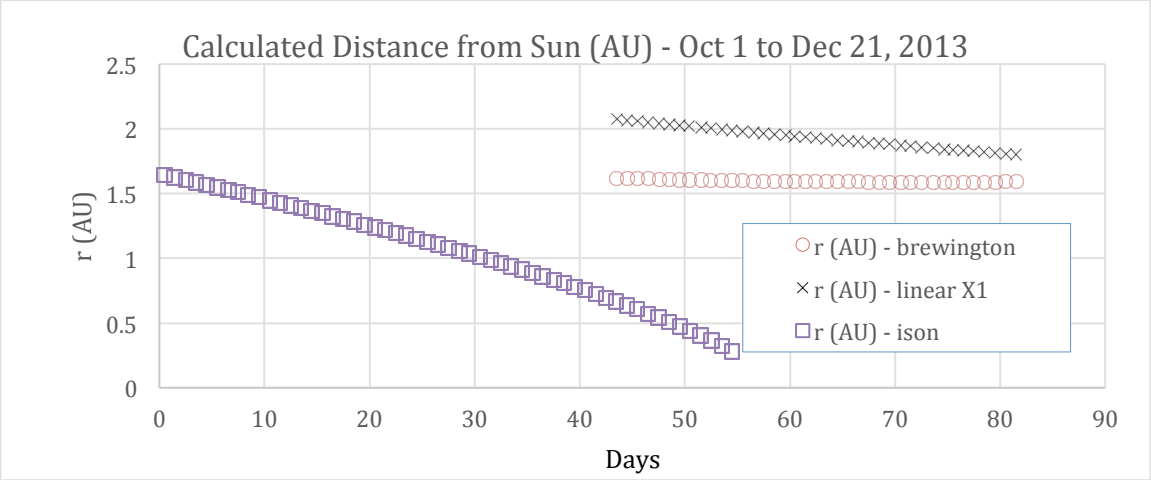

Figure 15: Calculated distance from Sun, using the lowest-score orbital elements

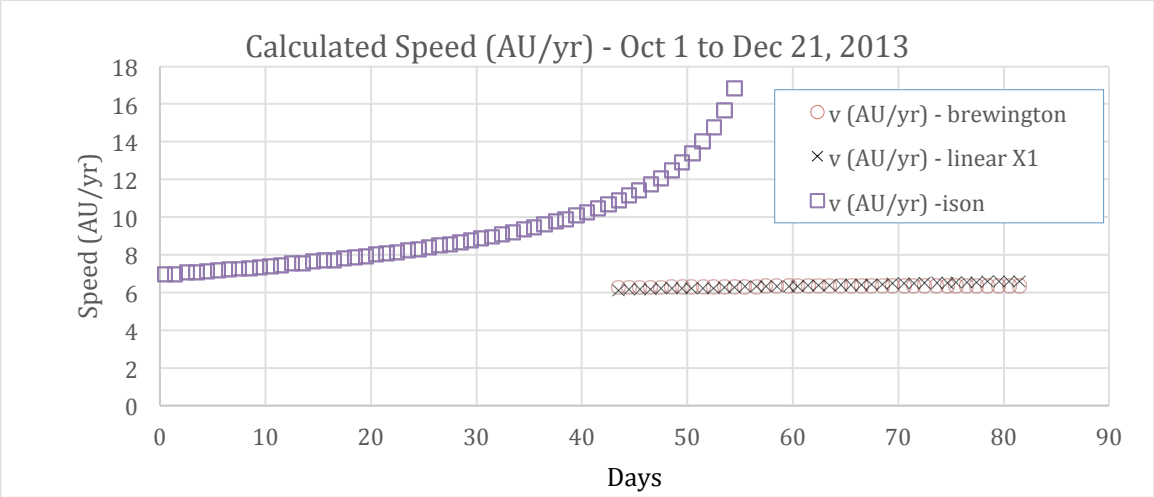

Figure 16: Calculated speed using the lowest-score orbital elements

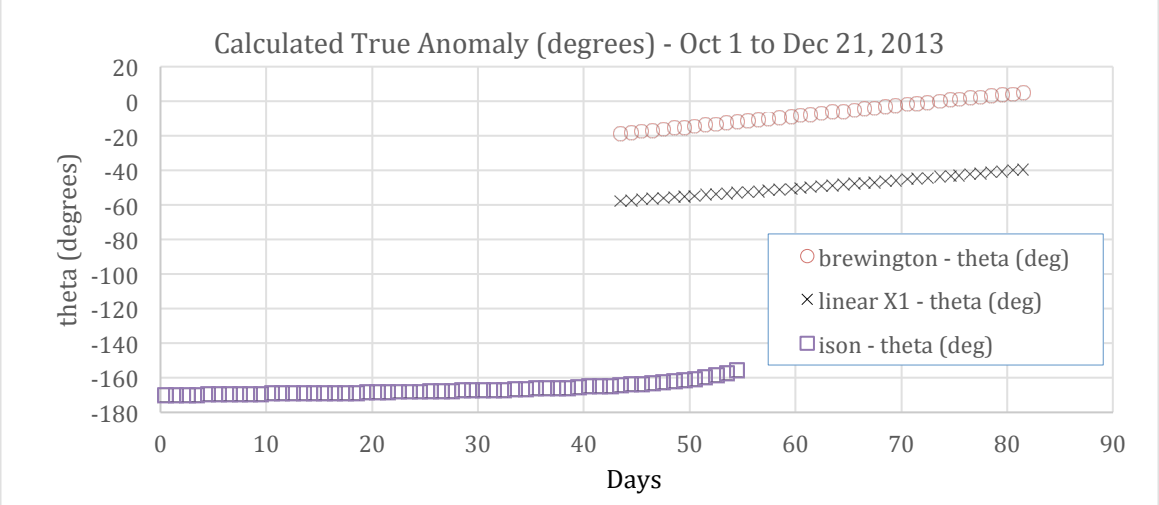

Figure 17: Calculated true anomaly using the lowest-score orbital elements

ISON's sun-grazing dive is best illuminated in the 3-dimensional plot of its orbit (Figure 18). LINEAR's plot shows it stays outside the Earth's orbit (Figure 19). Brewington's plot shows two lines (Figure 20). The dotted line is the orbit as predicted by JPL's orbital parameters, and the solid line is the orbit as predicted by this project. The visible difference between the two lines is due to the eccentricity being off by 8% and the periapsis passage being off by a day.

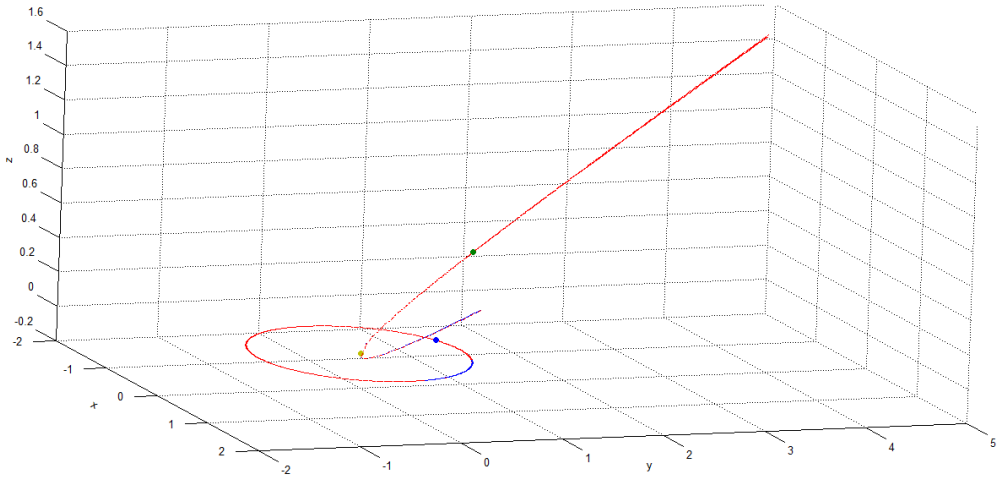

Figure 18: ISON calculated position, relative to Sun and Earth, on January 11, 2014 and its trajectory from October 1, 2013 to October 1, 2014

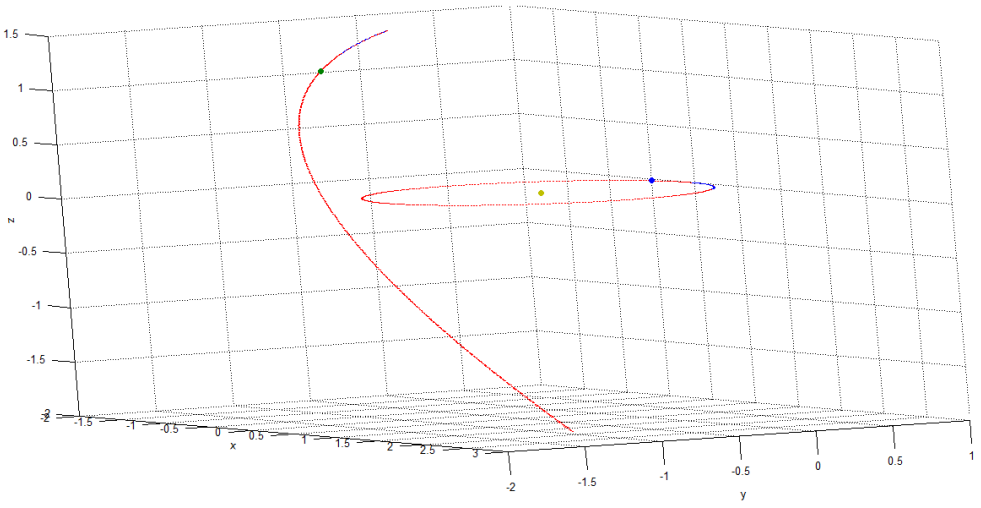

Figure 19: LINEAR position on January 11, 2014 and its trajectory from October 1, 2013 to October 1, 2014

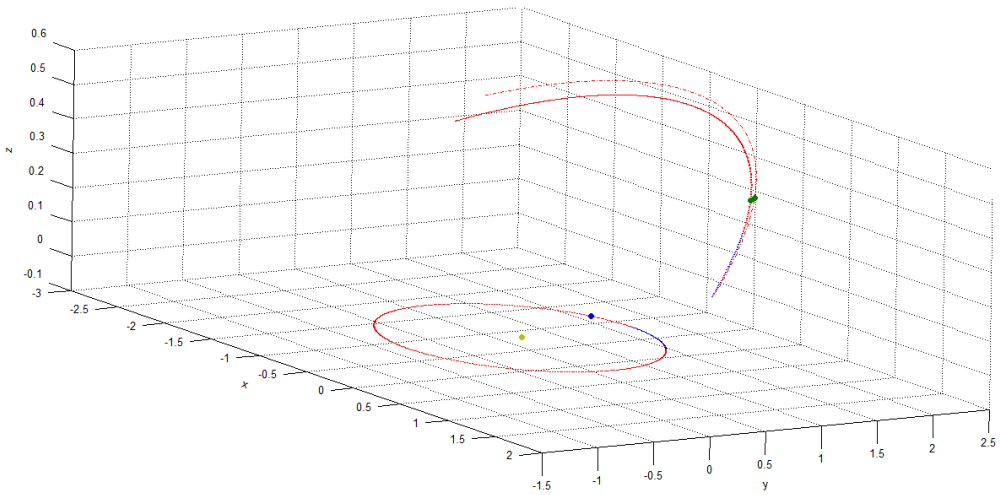

Figure 20: Brewington position on January 11, 2014 and its trajectory from October 1, 2013 to October 1, 2014

CONCLUSIONS

The best sets of orbital elements for all three comets closely agree with NASA's elements. ISON's elements were the hardest to find because the eccentricity was close to one and slightly hyperbolic ($e = 1.0002$). LINEAR's elements were easier to calculate since it had a lower eccentricity ($e = 0.989$), but it was still more difficult to find than Brewington's ($e = 0.67$). Brewington's eccentricity and periapsis passage were not as accurate as the other two comets; this may be because more care was spent on the other two comets as they were expected to be harder due to their eccentricities being closer to one.

While these elements may be in good agreement with theskylive.com data, the predicted orbits may never be 100% perfect. Other factors can have a hand in the orbits of comets. One factor is the gravity of other planets. Another factor is a rocket effect on the comets as they approach the Sun. When comets heat up, they release gases that can act as thrusters and push the comet in one direction or another.

Brewington and LINEAR's results indicate that time differences can have an effect on the accuracy of the orbital elements, where five to eight days separation appear to give the best results. A better conclusion will require more study.

Continued study of comet orbits is important. The methods used here could be applied to any object in orbit about the Sun to find its angular position in the sky and determine if it is on a collision orbit with Earth.

ACKNOWLEDGMENT

I would like to thank my family for their endless support, and my father and teachers for explaining the difficult concepts, preparing me to write my own programs, and helping me to write my own programs, and helping me understand the physics behind the equations.

REFERENCES

Bate, Mueller, and White, *Fundamentals of Astrodynamics,* Dover Publications, 1971.

Duffett-Smith, *Practical Astronomy with Your Calculator,* 3rd Edition, Cambridge Press, 1988.

Freemat, http://freemat.sourceforge.net/.

McCuskey, *Introduction to Celestial Mechanics*, Addison-Wesley, 1963.

Meyer, *Data Analysis for Scientist and Engineers*, John Wiley and Sons, 1975.

Schaeperkoetter, *A Comprehensive Comparison Between Angles-Only Initial Orbit Determination Techniques*, MS Thesis, Texas A&M University, 2011.

TheSkyLive.com, theskylive.com. A website that provides accurate location data for comets, planets, and even a few spacecraft in the sky. It receives funding from the U.S. Government, National Geographic, and several different observatories and groups of different nationalities.

CORRESPONDENCE SHOULD BE ADDRESSED TO:
Chloe Madsen Keilers
Los Alamos High School
chloeklrs@gmail.com

Appendix A: Step-by-Step Method

The Classical Orbital Elements

This project uses measurements of right ascension (RA) and declination to determine the six classical orbital elements for the chosen comets. Those elements are shown in Figure A.1.

From Kepler's first law, planet and comet orbits are conics with the sun at one focus. This means that the orbits occur in a plane, called the perifocal plane. Depending on the eccentricity (e), the orbits are ellipses ($0 \leq e < 1$), parabolas ($e = 1$), or hyperbolas ($e > 1$).

The perifocal coordinates are shown in Figure A.1:

- r – the position
- θ – the angle, called the **true anomaly**

The conic's properties are:

- e – the eccentricity
- a – the semi-major axis or, alternately
- q – the periapsis distance, where $q = a\ (1\text{-}e)$ for an ellipse

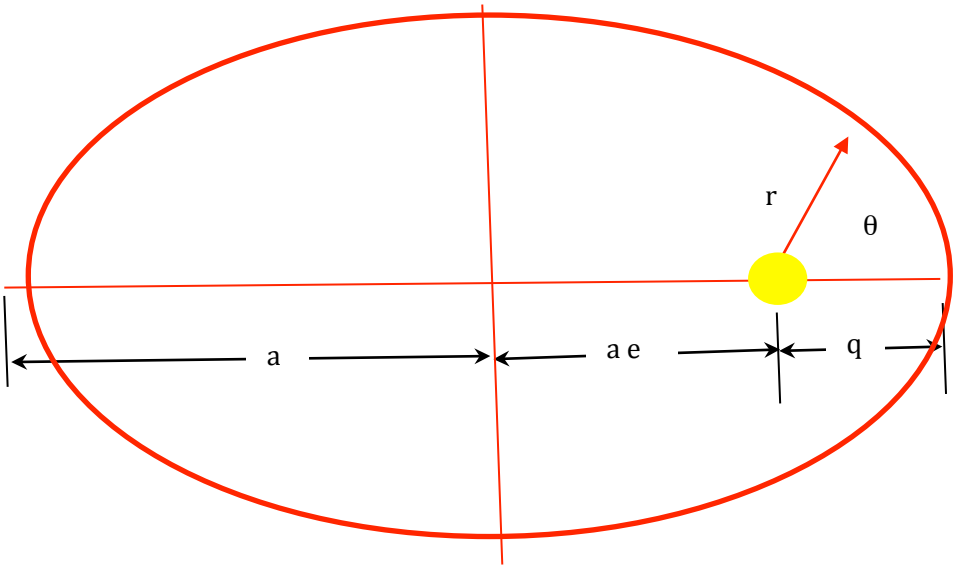

Figure A.1: Perifocal coordinates and the conic properties.

Kepler's equation (A.27) relates the true motion and **true anomaly** (θ) on the conic orbit to the **mean motion** (n) and an auxiliary angle (E, F, or w) on an axillary circle. The auxiliary angle is called the **eccentric anomaly**. The equation for all three types of conics is:

$$r = \frac{a(1-e^2)}{1+e\ \cos\theta} \qquad \text{A.1}$$

The Fundamental Equation of Astrodynamics (Newton's Law of Gravitation) also applies:

$$\ddot{\vec{r}} = \mu\left(\frac{\vec{r}}{r^3}\right) \qquad \text{A.2}$$

Where μ is the **gravitational constant** for the sun, $4\pi^2$ (AU^3/yr^2).

Comet orbits can have eccentricity, *e*, near 1, which is a parabolic orbit. As *e* approaches 1, the denominator for the true anomaly equation approach zero (A.28); this becomes numerically challenging to solve. For this reason, the comet problem can be more difficult to solve than it is for planets and asteroids that have near-circular orbits (i.e., eccentricities close to zero).

Gauss's Method

In 1802, Carl Friedrich Gauss calculated the orbit of the asteroid Ceres, using three sets of RA and declination measurements made by Giuseppe Piazzi. His method is now commonly used for orbit determination.

Given 3 line-of-sight vectors , $\vec{L}_j$, and 3 earth's position vectors, $\vec{R}_j$, at 3 different times (t_j), Gauss's method finds the comet's position at the central time, $\vec{r}_2$ and , $\vec{v}_2$; the 6 orbital elements can then be found from the position. Since there are 6 elements to find, it requires, at least, 2 angular measurements – right ascension and declination – at 3 different times.

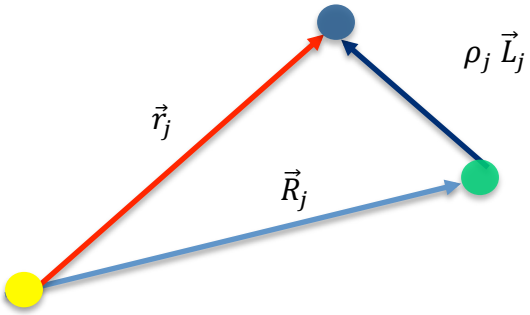

Figure A.2: Line of sight vector and Earth and Comet position vectors at time t_j .

Gauss's method can be derived using Kepler's first and second laws:

- The orbit is a conic, with the sun at a focus – i.e., the motion occurs in a plane.
- The line joining the body to the sun sweeps out equal areas in equal time.

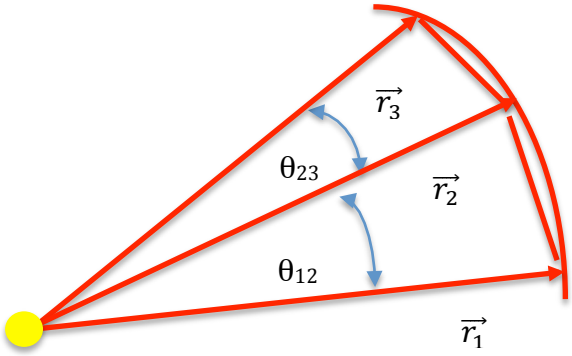

Figure A.3: Comet position vectors at 3 times

Define (r_1,r_2) as the area swept between two vectors, $\vec{r}_1$ and $\vec{r}_2$ (Figure A.3), then Kepler's second law relates the ratios of the areas swept to the ratios of the time differences, t_{31}, t_{21} and t_{32} (McCuskey):

$$\frac{(r_2,r_1)}{(r_3,r_1)} = \frac{t_{21}}{t_{31}}$$
$$\frac{(r_3,r_2)}{(r_3,r_1)} = \frac{t_{32}}{t_{31}} \qquad \text{(A.3)}$$

Define $[r_1,r_2]$ as the area of the triangle between the two vectors, $\vec{r}_1$ and $\vec{r}_2$, then the following approximations hold:

$$c_1 \overset{\text{def}}{=} \frac{[r_2,r_3]}{[r_3,r_1]} \cong \frac{(r_2,r_3)}{(r_3,r_1)} = \frac{t_{32}}{t_{31}}$$
$$c_3 \overset{\text{def}}{=} \frac{[r_1,r_2]}{[r_3,r_1]} \cong \frac{(r_1,r_2)}{(r_3,r_1)} = \frac{t_{21}}{t_{31}} \qquad \text{(A.4)}$$

This can be refined. Because the velocity $\vec{v}_2$, and the position vectors $\vec{r}_1$, $\vec{r}_2$, and $\vec{r}_3$ are all in the same plane, any of the vectors can be expressed as a combination of two of the vectors.

$$\begin{aligned} \overrightarrow{r_2} &= c_1\overrightarrow{r_1} + c_3\overrightarrow{r_3} \\ \overrightarrow{r_1} &= f_1\overrightarrow{r_2} + g_1\overrightarrow{v_2} \\ \overrightarrow{r_3} &= f_3\overrightarrow{r_2} + g_3\overrightarrow{v_2} \end{aligned} \qquad \text{(A.5)}$$

In these relations, f_1, g_1, f_3 , and g_3 are called Lagrange Coordinates (Bate 230). Relations for c_1 and c_3 can be found by taking cross products of these equations with individual vectors and realizing that the cross product of a vector with itself (i.e., two parallel vectors) is zero.

$$c_1 = \frac{(\vec{r}_2\times\vec{r}_3)(\vec{r}_1\times\vec{r}_3)}{|\vec{r}_1\times\vec{r}_3|^2} = \frac{g_3}{(f_1g_3 - f_3g_1)}$$
$$c_3 = \frac{(\vec{r}_1\times\vec{r}_2)(\vec{r}_1\times\vec{r}_3)}{|\vec{r}_1\times\vec{r}_3|^2} = \frac{-g_1}{(f_1g_3 - f_3g_1)} \qquad \text{(A.6)}$$

These relations between ratios of areas to ratios of time differences are the key to the Gauss Method.

The Basic Gauss Method

The Gauss Method was implemented using Freemat (Freemat). The steps are as follows:

1. The position of comets and planets in the sky are defined by two angles. In the earth's equatorial frame, the two angles are the right ascension and the declination. For this project, the RA and declinations were taken on a daily basis from the website http://theskylive.com.
2. To use the data, the RA and declination are rotated into the ecliptic frame through the obliquity angle (ε). The **longitude** (λ) and **latitude** (β) in the ecliptic frame can be found

from the right ascension (a) and declination (δ) for each measurement (Duffett-Smith #28: 42).

$$\lambda = \tan^{-1}\left\{\frac{\sin\alpha\cos\varepsilon + \tan\delta\sin\varepsilon}{\cos a}\right\}$$
$$\beta = \sin^{-1}\{\sin\delta\cos\varepsilon - \cos\delta\sin\varepsilon\sin a\} \quad \text{(A.7)}$$

3. The line-of-site vectors are determined: $\vec{L}j$ at time t_j (Bate, et al. 117).

$$\vec{L}j = \begin{bmatrix} L_{Ij} \\ L_{Jj} \\ L_{Kj} \end{bmatrix} = \begin{bmatrix} \cos\beta_j\cos\lambda_j \\ \cos\beta_j\sin\lambda_j \\ \sin\beta_j \end{bmatrix} \quad \text{(A.8)}$$

4. The earth's position vectors $\vec{R}j$ at time t_j are found using a method identical to that in the comet routine below (Duffett-Smith #54: 103). This involves solving Kepler's equation for an elliptical orbit and rotating the (r,θ) to the ecliptic (x,y,z) coordinates.
5. From the line-of-sight and earth position vectors at three times, t_1, t_2, and t_3, the coefficients of an eighth-order characteristic equation are found (C_0, C_3, C_6), using an approach described in Schaeperkoetter.
   a. Find the M matrix. $\boldsymbol{M} = \left[\vec{L}_1 \quad \vec{L}_2 \quad \vec{L}_3\right]^{-1} \cdot \left[\vec{R}_1 \quad \vec{R}_2 \quad \vec{R}_3\right]$ (A.9)
   b. Find the time differences: $t_{21} = (t_2 - t_1)$; $t_{32} = (t_3 - t_2)$; $t_{31} = (t_3 - t_1)$
   c. Define the following quantities:

$$a_1 = \frac{\tau_{32}}{\tau_{31}} \qquad a_3 = \frac{\tau_{21}}{\tau_{31}} \quad \text{(A.10)}$$
$$a_2 = \frac{a_1}{6}\left(\tau_{31}{}^2 - \tau_{32}{}^2\right) \qquad a_4 = \frac{a_3}{6}\left(\tau_{31}{}^2 - \tau_{21}{}^2\right)$$
$$a_5 = \left(\vec{R}_2 \cdot \vec{L}_2\right)$$
$$d_1 = M_{21}\ a_1 - M_{22} + M_{23}\ a_3$$
$$d_2 = M_{21}\ a_2 + M_{23}\ a_4$$

   $\mu = 4\pi^2$ (AU^3/yr^2) is the gravitational constant

   d. Then the coefficients of the characteristic equation are:

$$C_0 = -\mu^2 d_2^2$$
$$C_3 = -2\,\mu\,d_2 \quad \text{(A.11)}$$
$$C_6 = -(R_2 + d_1^2 + 2\,a_5\,d_1)$$

   e. The characteristic equation is:

$$f(r_2) = r_2^8 + C_6 r_2^6 + C_3 r_2^3 + C_0 \quad \text{(A.12)}$$

6. Solve for the roots, r_2, of the characteristic equation.
   a. First, an approximation for the roots is found by just plotting the function vs. r_2, as shown in the following example. This is the "coarse solve." This gives three roots as is shown in Figure 6 of this paper.
   b. Next, each root estimate for r_2 is refined by iteration using the Newton method. Repeatedly calculate r_{i+1} until dr is less than a tolerance (e.g., 1.0 x 10^{-9}).

$$r_{i+1} = r_i + dr \quad \text{(A.13)}$$

   Where:

$$dr = -(r_2^8 + C_6 r_2^6 + C_3 r_2^3 + C_0) \Big/ (8\,r_2^7 + 6\,C_6 r_2^5 + 3\,C_3 r_2^2)$$

7. Calculate the coefficients, c_1 and c_3 discussed above for the Gauss method.

$$c_1 = a_1 + a_2 \frac{\mu}{r_2^3} \qquad c_3 = a_3 + a_4 \frac{\mu}{r_2^3} \tag{A.14}$$

8. Find the distances, r_1, r_2, and r_3 along the line-of-sight vectors.

$$\begin{aligned} \rho_2 &= d_1 + d_2 \frac{\mu}{r_2^3} \\ \rho_1 &= (-M_{11}\ c_1 + M_{12} - M_{13}\ c_3\ )/c_1 \\ \rho_3 &= (-M_{31}\ c_1 + M_{32} - M_{33}\ c_3\ )/c_3 \end{aligned} \tag{A.15}$$

9. Find the position vectors, $\vec{r}_1$, $\vec{r}_2$, and $\vec{r}_3$ using $\vec{r}_i = \vec{R}_i + \rho_i \vec{L}_i$
10. Find the velocity vector, $\vec{v}_2$, at time t_2 using an approach described in Schaeperkoetter and attributed to Gibbs.

$$\begin{aligned} \vec{D} &= (\vec{r}_1 \times \vec{r}_2) + (\vec{r}_2 \times \vec{r}_3) + (\vec{r}_3 \times \vec{r}_{31}) \\ \vec{N} &= r_3(\vec{r}_1 \times \vec{r}_2) + r_1(\vec{r}_2 \times \vec{r}_3) + r_2(\vec{r}_3 \times \vec{r}_{31}) \\ \vec{S} &= \vec{r}_3(r_1 - r_2) + \vec{r}_1(r_2 - r_3) + \vec{r}_2(r_3 - r_1) \\ \vec{B} &= (\vec{D}_1 \times \vec{r}_2) \end{aligned} \tag{A.16}$$

$$\vec{v}_2 = \sqrt{\frac{\mu}{|\vec{N}||\vec{D}|}} \left(\vec{S} + \frac{1}{r_2}\ \vec{B} \right)$$

11. Find the orbital elements using, $\vec{r}_2$ and $\vec{v}_2$ (Bate, et al. 61-64). (A.17)
    a. The specific angular momentum vector: $\vec{h} = \vec{r} \times \vec{v}$
    b. The eccentricity vector points to periapsis: $\vec{e} = \left(\frac{1}{\mu}\right)\left(v^2 - \frac{\mu}{2}\right)\vec{r} - (\vec{r} \cdot \vec{v})\vec{v}$
    c. The $\vec{n}$ vector points to the ascending node: $\vec{n} = \hat{k} \times \vec{h}$
    d. The semi-latus rectum (p) is: $p \triangleq a(1 - e^2) = \frac{h^2}{\mu}$
    e. The eccentricity, e, is the magnitude of the eccentricity vector: $e = |\vec{e}|$
       The inclination, i, is always less than 180 degrees: $\cos i = \frac{h_k}{h}$
    f. The longitude of the ascending node, Ω: $\cos \Omega = \frac{n_I}{hn}$
       If $n_j < 0$, then Ω is negative.
    g. The argument of periapsis, ω: $\cos \omega = \frac{\vec{n} \cdot \vec{e}}{ne}$
       If $e_k < 0$, then ω is negative.
    h. The true anomaly, θ: $\cos \theta = \frac{\vec{e} \cdot \vec{r}}{er}$
       If $\vec{r} \cdot \vec{v} < 0$ then θ is negative.
    i. The time of periapsis passage T is then found using the true anomaly and solving Kepler's equation for the appropriate conic (see Comet routine).

The Improved Gauss Method

The basic Gauss method was derived using several approximations to estimate the ratios of the triangle areas, c_1 and c_3. Once estimates for r_1, r_2, and r_3 along the line-of-sight vectors are obtained, c_1 and c_3 can be refined by iterating the following steps. The steps are:

1. Follow the basic Gauss process above through step 5.b.
2. Correct the observation times for the speed of light, c (~ 173 AU/day).
$$t_j(new) = t_j - r_j/c \qquad \text{(A.18)}$$
3. Using the estimated orbital parameters, run the Comet routine, to find the true anomalies, θ_1, θ_2, and θ_3, and their differences, θ_{32} and θ_{21}.
4. Find the Lagrange coefficients, f_i and g_i, where i is 1 or 3 (Bate, et al. 218)
$$f_i = 1 - \frac{r_i}{q(1+e)}(1 - \cos(\theta_{i2})) \qquad g_i = \frac{r_i r_2}{h}(1 - \cos(\theta_{i2})) \qquad \text{(A.19)}$$
5. Find new estimates for c_1 and c_3, using:
$$c_1 = \frac{g_3}{(f_1 g_3 - f_3 g_1)} \qquad \text{(A.20)}$$
$$c_3 = \frac{-g_1}{(f_1 g_3 - f_3 g_1)}$$
6. Find new r_1, r_2, and r_3, similar to step 8 of the basic Gauss Method.
$$\rho_1 = (-M_{11}\ c_1 + M_{12} - M_{13}\ c_3)/c_1$$
$$\rho_2 = (\ M_{21}\ c_1 - M_{22} + M_{23}\ c_3) \qquad \text{(A.21)}$$
$$\rho_3 = (-M_{31}\ c_1 + M_{32} - M_{33}\ c_3)/c_3$$
7. Follow steps 9 – 11 of the basic Gauss method, to find the orbital elements. Test if the change to some parameter (such as ρ_2) is small enough for convergence or if the eccentricity, e, is diverging. Figure 7 of the paper shows an example of the iteration using 3 roots found during "coarse solve" (step 6 of the basic Gauss method).

The Comet Routine – Solving Kepler's Equation

Running the improved Gauss routine and finding the scores require calculating the comet position and velocity at a given time, with a set of orbital elements. This is done by solving Kepler's equation, (A.27) below. The following relationships hold. [Bate, et al. 182-188]

	Ellipse	Hyperbola	Parabola	Eqn
eccentricity e	$0 \le e < 1$	$1 < e$	$e = 1$	A.22
semi-major axis (a)	a = q/(1-e)	a = q/(e-1)	a is infinite	A.23
mean motion (n)	$n = \sqrt{\mu(1-e)^3/q^3}$	$n = \sqrt{\mu(e-1)^3/q^3}$	$n = \sqrt{\mu/2q^3}$	A.24
eccentric anomaly	E	F	w	A.25
mean anomaly (M)	M = nt	M = nt	M = nt	A.26
	$M = E - e\sin E$	$M = e\sinh F - F$	$M = \frac{1}{3}w^3 + w$	A.27
true anomaly (θ)	$\tan\left(\frac{\theta}{2}\right) = \left(\frac{(1+e)}{(1-e)}\right)^{1/2}\tan\left(\frac{E}{2}\right)$	$\tan\left(\frac{\theta}{2}\right) = \left(\frac{(1+e)}{(e-1)}\right)^{1/2}\tanh^{-1}\left(\frac{F}{2}\right)$	$\tan\left(\frac{\theta}{2}\right) = w$	A.28

In polar coordinates, a planet or comet position (r, θ) at time, t, can be found by:
1. Find the mean motion, n, which is a function of the orbital parameter's, e and q (A.24)
2. Find the mean anomaly, $M = n\,t$ (A.26)
3. Using Newton's method, solve the transcendental equation, Kepler's equation, for the eccentric anomaly, E, F, or w for an ellipse, hyperbola, or parabola, respectively (A.27)
4. Find the true anomaly, θ, using the eccentric anomaly (A.28).
5. Find the radial distance, r, using the equation of the conic (A.1).

The result can then be rotated to the ecliptic (x,y,z) frame [Bate, 2.6: 74-83].

GAS PHASE ION CHEMISTRY AND ION MOBILITY OF PHARMACEUTICAL SUBSTANCES IN COUNTERFEIT FORMULATIONS: TECHNOLOGY FOR MEASUREMENT AND CONFIDENCE OF DETECTION

Jeongmin Lee

ABSTRACT

The health and well-being of populations in certain critical regions of the world are threatened today by the presence of counterfeit pharmaceuticals which are often authentic materials diluted to clinically ineffective levels and sold as authentic medicine. Those paying for the medicine are defrauded while those receiving are given false hope of recovery. Relatively inexpensive and convenient methods to examine pills or formulations for chemical composition are needed in vulnerable communities where counterfeit pharmaceutical trade is abundant even to this day. Existing methods are not completely satisfactory. Measurements and technology based on ion mobility spectrometry (IMS), already proven in military and security venues, provide sensitive and selective measurements with hand-held instrumentation. Preliminary studies suggested that embodiments of IMS instruments could make direct assays of pills possible. There was documentation that these methods would be suitable to detect diluted authentic chemicals. In this investigation, I have calculated that gas phase ion chemistry of formation of key anti-malarial medicines should be favorable over ion chemistry of inert materials of pills. In experimental studies, a laser ionization based method is combined with a mobility spectrometer to determine the limits of detection of 2.5 nanograms or better in a false matrix. Findings confirm the hypothesis and these methods are plausible solutions for detecting counterfeit pharmaceuticals, even in remote locations of the world. There are concerns also about purity of materials purchased through websites and a broader issue of national security of pharmaceuticals with misrepresented manufacture or composition.

Las Cruces High School, Las Cruces jmlee20@yahoo.com

INTRODUCTION

Counterfeit pharmaceuticals contain clinically insufficient amounts of therapeutic substances or, in some instances, only inert materials affecting consumers and legitimate drug manufacturers, including generic brands (Harris, 2014). There are methods to rapidly screen the chemical composition of pills although wide-acceptance and availability are limited by errors in measurements or high costs of technology. Ion mobility spectrometry (IMS) is based on the characterization of gas ions derived from a substances in a weak electric field and supporting gas atmosphere. A combination of physical and chemical principles, IMS provides sophisticated measurements with relatively simple technology. Indeed, hand-held configurations of IMS instruments are used within NATO for battlefield detection of nerve agents; portable units are found in airports worldwide for detecting explosives (Eiceman, 2013). Recently, solid samples were measured using IMS through laser ablation desorption with electro spray ionization of drug neutral vapors and then subsequent spectral analysis (Judge, 2010; Bradya, 2012). The mobility of ions is dependent on shape and charge providing spectral information characteristic of a chemical. Exploratory findings suggested a capability to discover qualitatively inauthentic pharmaceuticals or quantitatively determine medications diluted to clinically insignificant levels.

Malaria and anti-malarial pharmaceuticals. Malaria is a parasitic disease that is transferred by mosquitoes and is commonly treated using by medications that defend the body from contracting the disease, so-called prophylactics. Authentic medicines such as Malarone require consumption for two days before a possible exposure, every day during exposures, and a week after retreating from malaria-carrying vectors. The correct dosage of the active ingredients for adults in Malarone is 250 mg atovaquone and 100 mg proguanil per tablet with a recommended

consumption of 4 tablets per day. Another pharmaceutical, Plaquenil contains hydroxycholoroquine and can be used to treat malarial infections with 200 mg/day of the main ingredient. Handling and ingestion of medicines as pills is made possible with binders or inactive ingredients such hydroxypropyl methylcellulose and starches. A danger is that these or other inert ingredients can be added at point of manufacture to extend profits by extending the mass of pills produced, though at reduced levels of medicinal ingredients. Consequences for users include the loss of resources and health. This particular version of counterfeiting may be seen in quantitative interpretation of findings from ion mobility spectra where lowered concentrations should result in lesser intensity of spectral profiles for active ingredients. The objective of this study is to determine mobility features for ions of two common anti-malarial chemicals and to demonstrate a relationship between the signal strength and the concentration in a pill. These findings and laboratory experiences should permit an evaluation of the capability of ion mobility spectrometry for use in routine counterfeit pill screening and disclose next stages of development (Harris, 2012).

Ion Mobility Spectrometry with Laser Ablation of Solids. The molecular composition of a solid can be accessed through electro spray with laser desorption and ionization (ELDI) where solids are vaporized from a surface and ionized by gas phase ionization chemistry producing protonated molecular forms of a substance (Lubman, 1982; Shiea, 2005). These are passed into an electric field where ions are desolvated and brought to an ion shutter, which is used to inject ions into a second part of the spectrometer, the drift region. Time of drift for ions begins when the ions pass through the ion shutter and ends when they reach the detector. Ions move as swarms and acquire characteristic drift velocities governed by shape, size, and charge (See Figure 1).

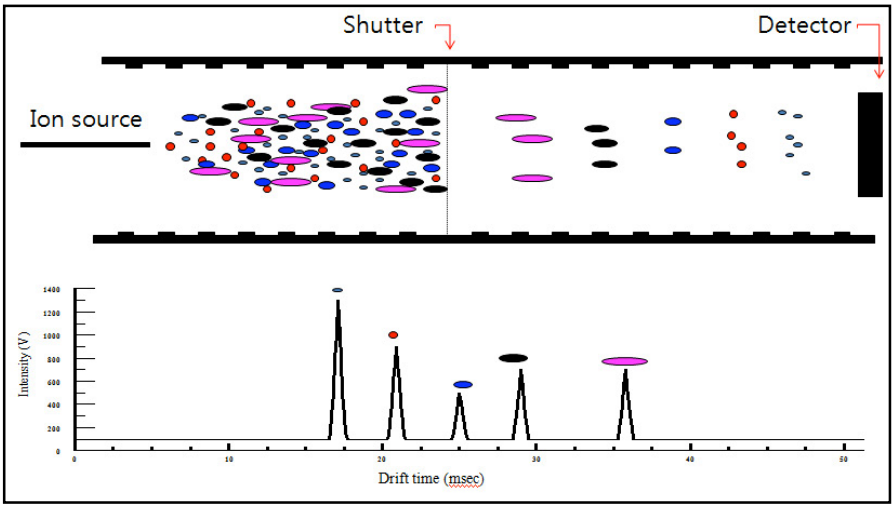

Figure 1. Mobility of Ions in Electric Fields (Up. ions in drift tube with electric field, Down. Spectrum obtain from mobility analysis)

Velocities when normalized for electric field strength are termed mobility coefficients (K) and called reduced mobility coefficients (K_o) when K is further adjusted for ion temperature and pressure. The relationship between K and molecular properties (Eiceman, 2013) is given in Equation 1.

$$K = \frac{3e(2\pi)^{\frac{1}{2}}(1+\alpha)}{16N(\mu k T_{eff})^{\frac{1}{2}}\Omega_D(T_{eff})} \quad (1)$$

The terms are e, charge of electron; N, number density of neutral gas molecules at the measurement; α, correction factor; μ, reduced mass of ion and gas of supporting atmosphere; T_{eff}, the effective temperature of the ion determined by thermal energy and the energy acquired in the electric field; and $\Omega_D(T_{eff})$, the effective collision cross section of the ion at the temperature of the supporting atmosphere. The mobility coefficient is obtained experimentally from peak centers in mobility spectra and is derived from knowledge of the distance the ion travels between the shutter and detector, the ion drift time, and electric field strength.

Uncertainty in these and possible errors have stimulated the use of calibration compounds including 2,6-Di-tertiary-butyl pyridine (2,6-DtBP) so K or K_o values can be derived free of instrument errors.

EXPERIMENTAL

This project used two methods of utilizing ion mobility spectrometry: ELDI, which does not have a prepared sample but rather directly applies the laser on an opened tablet; and electrospray ionization (ESI), which emitted an ion plume from prepared sample solutions with varying degrees of concentration. The experimental setup with the drift tube, electrospray, and laser is shown in Figure 2. The drift tube was modified from standard designs equipped with an electrospray needle and a clean gas chamber to increase convenience in the cleansing of the apparatus between different samples; a laser beam was focused on the sample using a plano-convex lens. Electric fields in the drift tube were 320 V cm^{-1}.The drift gas was purified air. Drift tube temperature was 146°C and drift gas flow was 700 cm^3 min^{-1}. Signals were averaged and stored by a desktop computer equipped with interface card (National Instrument PCI-6023E card) and software (LABVIEW). Acquisition parameters were 10 averages per spectrum with 1800 data points collected per spectrum at a frequency of 24 kHz. Data collection for the limit of detection for the same samples was repeated seven times. The laser was an Nd-YAG (MiniLite II, Continuum, Santa Clara, CA) with frequency quadrupled output (λ = 532 nm). The laser was operated at 10 Hz with a pulse width of < 5 ns. The beam was focused onto a pill or residue using a 10 cm focal length from fused silica lens (Optosigma, Santa Ana, CA). The beam energy was 63.2 μJ/pulse. The focused beam showed a diameter of around 0.3 mm as determined from a photograph of the sampling and ablating a target. The samples that were tested were Plaquenil 200mg tablets and Malarone 250/100mg (atovaquone/proguanil) tablets.

The 2,6-Di-tert-butylpyridine (a standard chemical), ≥98% atovaquone, and ≥98% hydroxlchloroquine sulfate were all from Sigma-Aldrich. Significantly, pills were also ground to a powder by a mortar and pestle and mixed with methanol, which was filtered and analyzed directly by electrospray ionization methods rather than ELDI IMS.

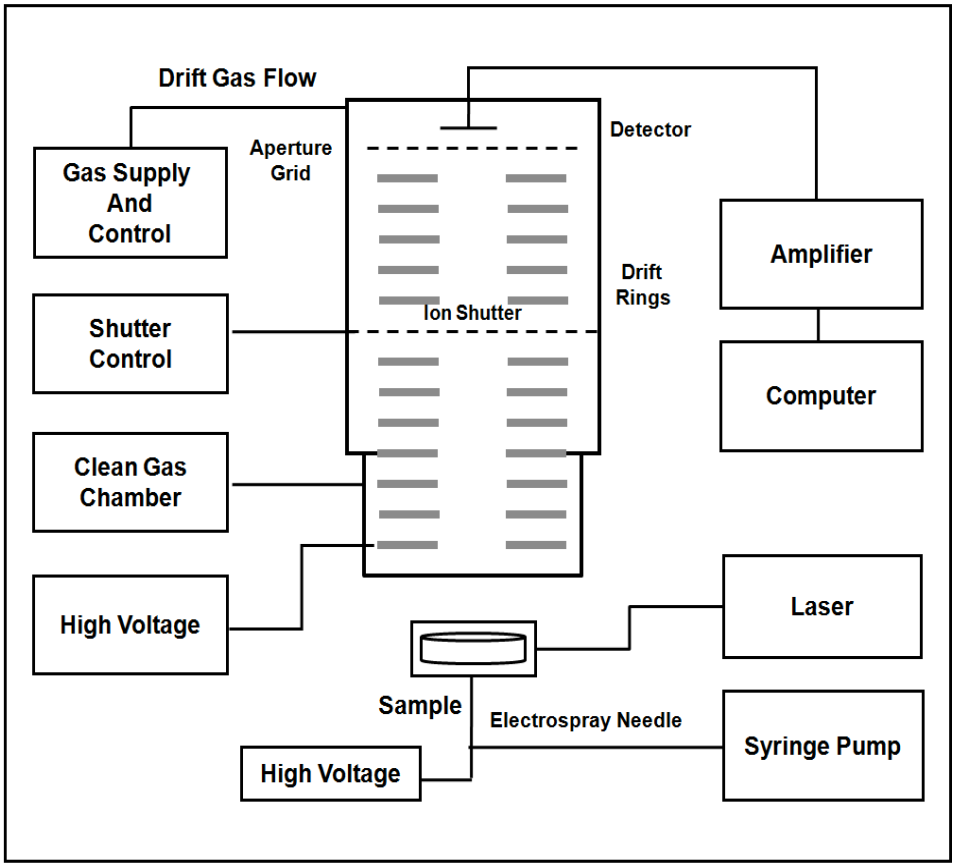

Figure 2. Experimental setup of the ELDI with the utilization of the laser directly vaporizing the sample.

RESULTS AND DISCUSSION

Ion mobility spectra for authentic standards of two widely used anti-malarials are shown in Figures 3 and 4. The chemicals produced single peaks from reactions between neutral molecular forms of each chemical and gas phase protons provided from the electrospray ion source according to Equation 2 yielding protonated monomers of each chemical.

$$M + H^+\cdot(H_2O)_n \longleftrightarrow MH^+\cdot(H_2O)_{n-x} + xH_2O \quad (2)$$

Sample + reactant ion → Product ion + water
neutral → Protonated monomer

Drift times for these ions were 21.38 ms and 20.08 ms for atovaquone and Plaquenil, respectively and reduced mobility coefficients are given in Table 1. When the a pill is accessed through a dry sampling using a laser beam and desorption with ionization indirectly from and ESI source, the findings show minor abundances of the product ion for atovaquone (Figure 5). In contrast, a pill crushed and extracted with solvent, which is then directly analyzed by ESI IMS shows significant intensity, likely due to low amount of chemical available in the limited area of sampling by the laser beam.

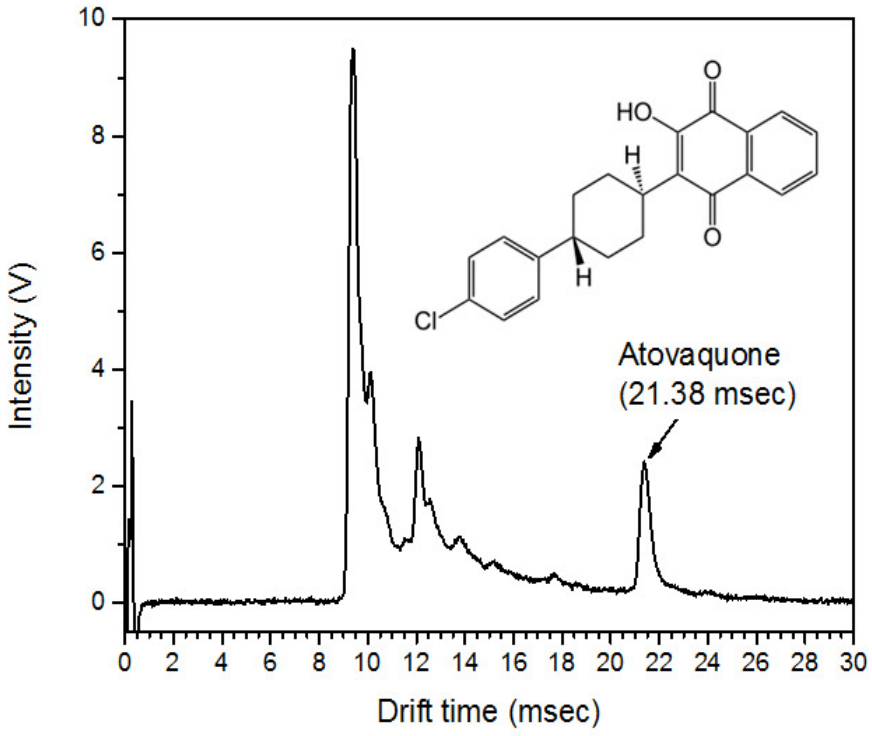

Figure 3. Ion mobility spectrum of solution of Atovaquone, a widely used anti-malarial.

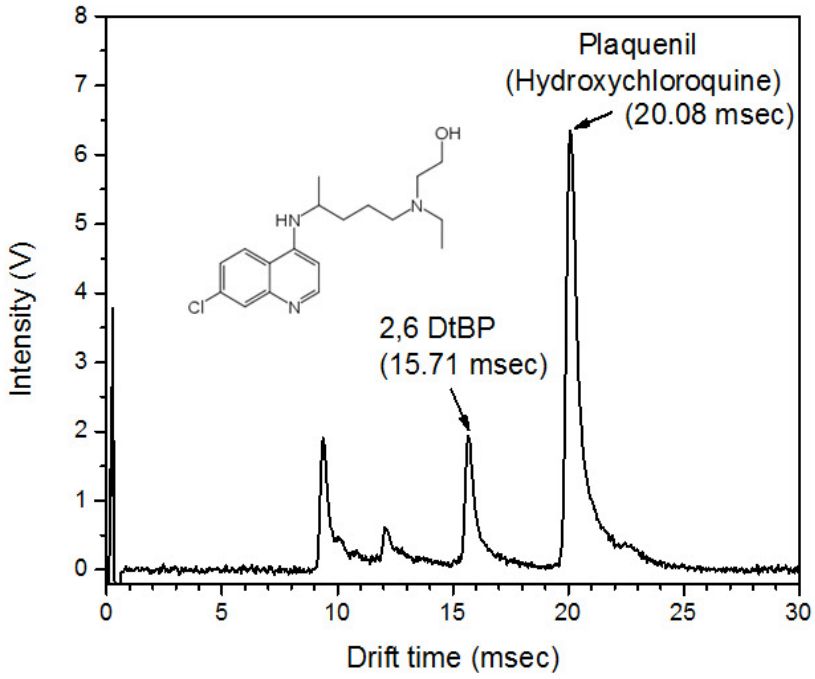

Figure 4. Ion mobility spectrum of solution of Plaquenil, a second widely used anti-malarial.

Table 1. Reduced mobility values for calibration standard, for two authentic chemicals, and for a tentatively identified substance, Proguanil.

Chemical	Reduced mobility ($cm^2\ V^{-1}\ s^{-1}$)
2,6-Di-tert-butylpyridine	1.42
Atovaquone	1.04
Hydroxlchloroquine sulfate	1.11
Proguanil	1.26

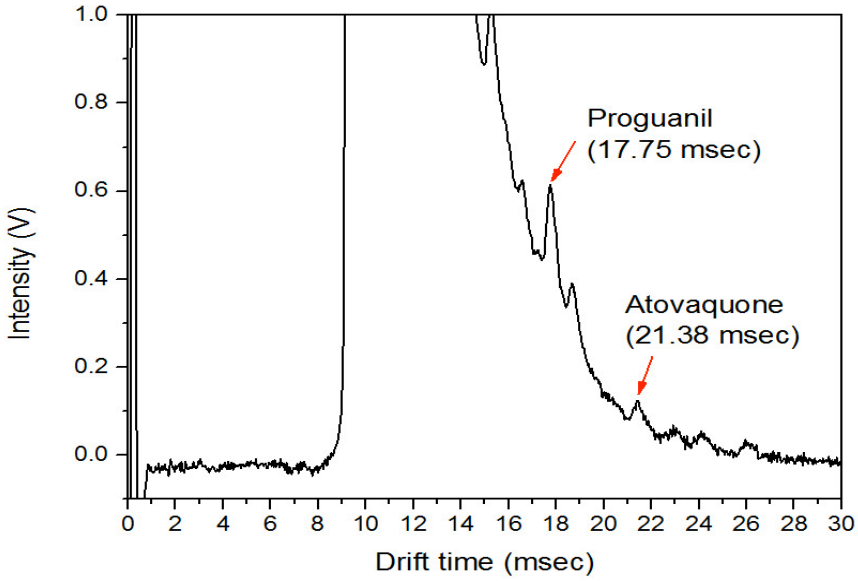

Figure 5. Mobility Spectrum of authentic anti-malarial pill from ELSI IMS analysis, the dry laser sampling method. Note low abundance of Atovaquone.

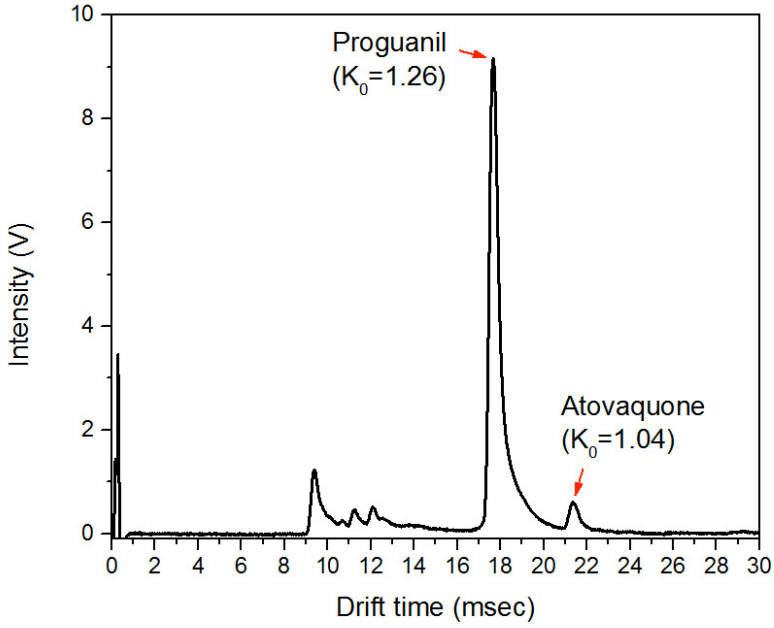

Figure 6. Mobility Spectrum of authentic anti-malarial pill from ESI IMS analysis from methanol extract of pill pulverized before liquid extraction. Note abundance of Atovaquone over baseline noise.

Quantitative Response. In any prior work with ELDI IMS or ESI IMS for these anti-malarial compounds, little has been disclosed on the quantitative response. In Figure 7, the response curves for these substances are shown providing low nanogram limits of detection. The hydroxylchloroquine sulfate has a much larger intensity than atovaquone does. This can be attributed to the fact that hydroxylchloroquine has a higher proton affinity.

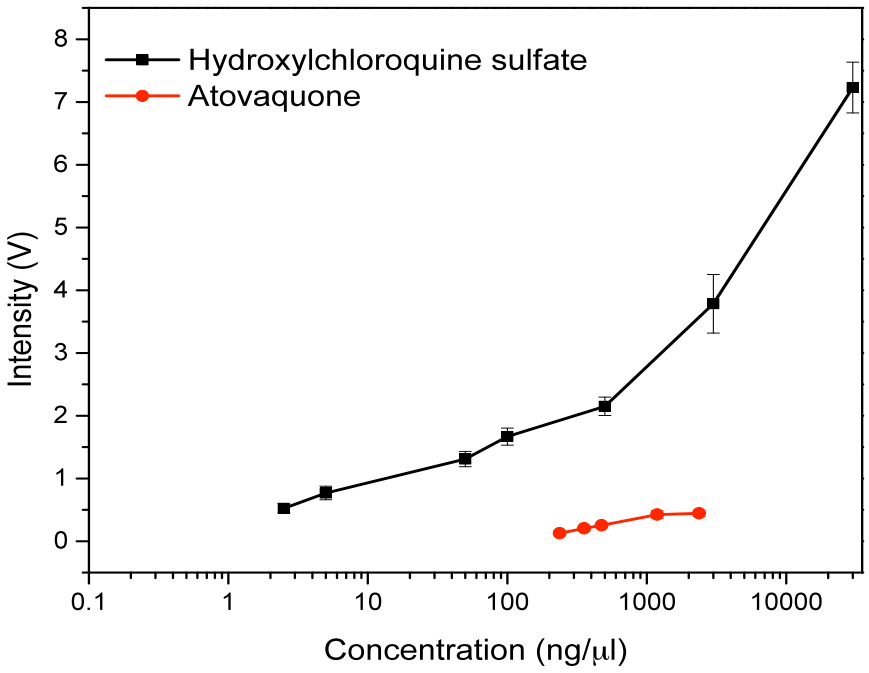

Figure 7. Response curves. The response curves are limited to low nanogram when in theory and practice, response should be observed in the low picogram. This is attributed to poor design and operation of ion source and electric fields in the source region.

CONCLUSIONS

While the mobility behavior of gas phase ions derived from two major anti-malarial chemicals show suitable peaks shape and reduced mobilities have been measured and reported

for the first time, the heterogeneity of pills and low levels in the pill matrix makes the current configuration not suitable for use abroad or even in the US. ESI IMS analysis of extracted pills is plausibly an approach to determine quantitatively the levels of anti-malarial compounds in pharmaceutical preparations.

ACKNOWLEDGEMENTS

I would like to acknowledge the Eiceman Research Group and the Chemistry Department of NMSU for allowing me to experiment with their supply and providing an area to conduct the experiments respectively. Especially, I want to thank Dr. Eiceman for his aid in teaching me and supporting me. The people of the Eiceman Research Group also deserve my appreciation. Finally, I want to thank my own parents.

REFERENCES

1. J. Bradya, P. Flanigan, J. Perez, E. Judge, and R. Levis, "Multidimensional detection of explosives and explosive signatures via laser electrospray mass spectrometry," *SPIE*, vol. 8358, pp. 83580X-1-83580X-9, 2012.
2. J. Dunn, C. Gryniewicz-Ruzicka, J. Kauffman, B. Westenberger, L. Buhse, "Using a portable ion mobility spectrometer to screen dietary supplements for sibutramine," *Journal of Pharmaceutical and Biomedical Analysis.* vol.54, pp. 469-474, 2011.
3. G. Eiceman, Z. Karpas, and H. Hill, Jr., "Ion Mobility Spectrometry," Danvers, MA: *CRC Press*, 2013.
4. E. Judge, J. Brady, D. Dalton, and R. Levis, "Analysis of Pharmaceutical Compounds from Glass, Fabric, Steel, and Wood Surfaces at Atmospheric Pressure Using Spatially Resolved,

Nonresonant Femtosecond Laser Vaporization Electrospray Mass Spectrometry," *Anal. Chem*., vol.82, pp. 3231–3238, 2010.

5. G. Harris, "Medicines Made in India Set Off Safety Worries." *The New York Times.* The New York Times, 14 Feb. 2014. Web. 26 Feb. 2014.
6. G. Harris, S. Graf, R. Knochenmuss, and F. Fernandez, "Coupling laser ablation/desorption electrospray ionization to atmospheric pressure drift tube ion mobility spectrometry for the screening of antimalarial drug quality," *Analyst*., vol.137, pp. 3039-3044, 2012.
7. D. Lubman and M. Kronick, "Plasma Chromatography with Laser-Produced Ions," *Anal. Chem.*, vol.54, pp. 1546-1551, 1982.
8. J. Shiea, M. Huang, H. Hsu, C. Lee, C. Yuan, I. Beech, and J. Sunner, "Electrospray-assisted laser desorption/ionization mass spectrometry for direct ambient analysis of solids," *Rapid Commun. Mass Spectrom*., vol.19, pp. 3701–3704, 2005.

Turbocharger Turbojet

Noah Manz[1]

Abstract

The purpose of this experiment was to see if a jet engine could be built using store bought and home fabricated parts from scrap materials. The prototype is a proof of concept, which should be able to self-sustain without external help. The production of this engine was based around a combustion chamber and turbine and three supporting systems. The three supporting systems functioned independently from each other and consisted of fuel, oil and ignition systems. These systems provide the necessary accommodation to the combustion chamber and turbine for sustained operation of the engine. The combustion chamber consists of an inner and an outer tube. The inner tube, or flame tube, is responsible for the mixing of fuel and air. The outer tube, or combustion liner, channels exhaust gasses towards the turbine and creates a barrier between the exhaust gasses and engine frame and subsystems. The combination of flame tube and combustion liner together form the combustion chamber. Operation of the engine begins by spooling up the turbine with help from the oil system and compressed air source. The air, which turns the compressor turbine wheel, is then channeled down a tube where upon it enters the combustion chamber. Gradually, the fuel valve is opened releasing fuel into the combustion chamber to mix with the air. The piezoelectric ignition system ignites the fuel producing exhaust gasses which under pressure rush to an area of lower pressure, the exhaust turbine. The gasses turn the turbine and then exit the back of the turbocharger as thrust. The exhaust turbine is linked to the compressor turbine via a stainless steel rod. As the exhaust turbine rotates due to the escaping exhaust gasses, it turns the compressor turbine driving more air into the combustion chamber to be ignited. A working prototype was created, but failed to self-sustain.

[1] Farmington High School, Farmington NM 87401 nmanzf35@gmail.com

Introduction

The first operational turbojet engine was created by Frank Whittle, a pilot in the Royal Air Force. Whittle's design incorporated ten combustion chambers rather than one, standard in today's turbojets. This design allowed his engine to fit nicely inside the planes of the day. As jet powered flight evolved, the planes became long and thin like we have today meaning that the engines could do the same. Golley, J. (2010). Jet: *Frank Whittle and the invention of the jet engine*. (5th ed.). London: Datum Publishing. The design for the turbojet in this experiment favors Whittles design meaning that the combustion chamber can be mounted outside of the turbine. An automotive turbocharger was opted for as a turbine, which forced the decision to mount the combustion chamber on the outside of the turbine housing. Just like in Whittle's design, the combustion chamber takes compressed air from the compressor turbine, mixes the air with fuel and ignites it then forcing the exhaust back into the turbine housing to turn the exhaust turbine which in turn, spins the compressor blades which drive more air into the combustion chamber to repeat the process over again. The exhaust gasses that were used to spin the exhaust turbine then exit the back of the engine as thrust propelling the engine and thus whatever it is mounted to in the opposite direction. It is important both in modern turbojet engine and in mine that the fuel mixes with the air so that the fuel has Oxygen to burn with. Davis, M (2014, Jan 20). *The Junkyard Turbojet Engine* retrieved from: http://www.junkyardjet.com/further.html On a modern turbojet, there are steel rings slightly aft of the fuel nozzles that disrupts the flow of air. Gunston, B. (2006) *The Development of Jet and Turbine Aero Engines*. (4th ed.) Sparkford: Haynes Publishing, This creates a swirling effect that mixes the air with the fuel so that it can be ignited. On the engine in this experiment, a similar device was added, but in the form of another tube that would fit inside the combustion chamber. This tube had holes drilled into it at predetermined locations that would channel the flow of air from the compressor turbine between the inside and outside of the tube known as the flame tube. When fuel was injected in the center of the flame tube, the air weaving between the two tubes that together make the combustion chamber, the fuel and air would mix, they could then be ignited to create thrust which would rush to the exhaust turbine. There are many parts of the engine that could have been made better, however, the outcome was due to limited resources and time. The goal of this project was to see if it was possible to create a self-sustaining turbojet engine using an automotive turbocharger.

Engineering Problem

The purpose of this experiment was to see if it was possible to build a turbojet Engine. An engineering process was established whereby;

- The engineering problem was defined
- Background research was conducted on turbojet design and materials
- Design criteria were established based on financial, fabrication and material availability restrictions
- Preliminary designs were created for each of the engines systems and subsystems
- Necessary materials were acquired
- Preliminary designs were built, tested, refined and retested
- All of the tested subsystems were assembled into a final prototype which was then tested

Design Criteria

- The Turbojet will utilize a radial centrifugal compressor and turbine derived from an automobile turbocharger
- The centrifugal compressor design will necessitate an external combustion chamber
- Utilize a readily available, inexpensive, pressurized fuel source
- Utilize readily available materials that can be machined and fabricated easily and inexpensively
- Flux core welding equipment, oxy acetylene cutting equipment were available
- MIG/TIG and plasma arc cutting equipment were unavailable

Methods

1. Acquire turbocharger, frame materials and combustion chamber materials
2. Construct flame tube (Holes drilled and base welded on)
3. Construct combustion liner (construct top and bottom caps, weld onto liner, cut hole for inlet tube, weld on inlet tube)
4. Assemble combustion chamber
5. Attach turbocharger to combustion chamber
6. Acquire materials for combustion chamber mount
7. Fabricate combustion chamber mount
8. Attach combustion chamber and turbocharger to frame

9. Acquire parts for oil system
10. Fabricate mounts for oil system
11. Assemble and mount oil system
12. Acquire parts for ignition system
13. Fabricate mounts for ignition system
14. Assemble and mount ignition system
15. Acquire parts for fuel system
16. Fabricate mounts for fuel system
17. Assemble and mount fuel system
18. Acquire wheels
19. Fabricate mounts for wheels
20. Attach wheels to frame
21. Fabricate control panel
22. Attach control panel and attach ignition coil
23. Test oil system, check for leaks
24. Test fuel system, check for leaks
25. Test ignition system
26. Test completed engine

Turbine and Combustion Chamber

An automotive turbocharger was utilized as the turbine and the compressor. The use of this centrifugal compressor necessitated the construction of an external flame-tube. The flame tube was constructed from ¼“ steel what was fitted with a top and bottom cap to fit the existing turbocharger. A flame tube was fabricated by drilling ½’ holes in a 1/8’ inner sleeve. The flame tube was attached to the compressor via a flexible rubber hose. Since the compressor turbine was taking cold intake air into the compression chamber, the rubber tube was not subjected to extremely high temperatures, with the exception of the attachment point to the combustion chamber. This was continually monitored during operation and never exceeded 160 ^{o}F.

The initial combustion chamber design resulted in too much combustion in the upper portion of the chamber creating high temperatures in the combustion turbine. A redesign was created

utilizing a concept of decreasing flame tube perforation hole size moving higher up the chamber and incorporating a taper at the top of the flame tube to direct hot exhaust gasses into the exhaust turbine. Unfortunately, the shaft on the turbocharger was fractured during bearing replacement and the final combustion chamber design was not able to be tested.

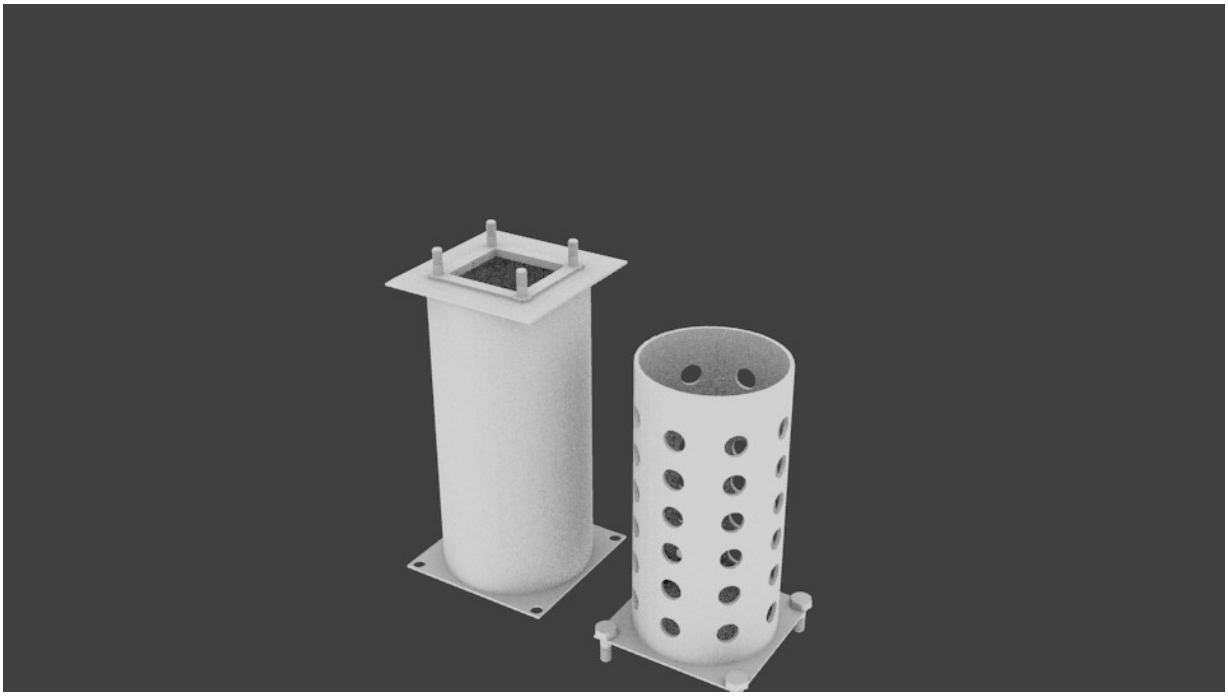

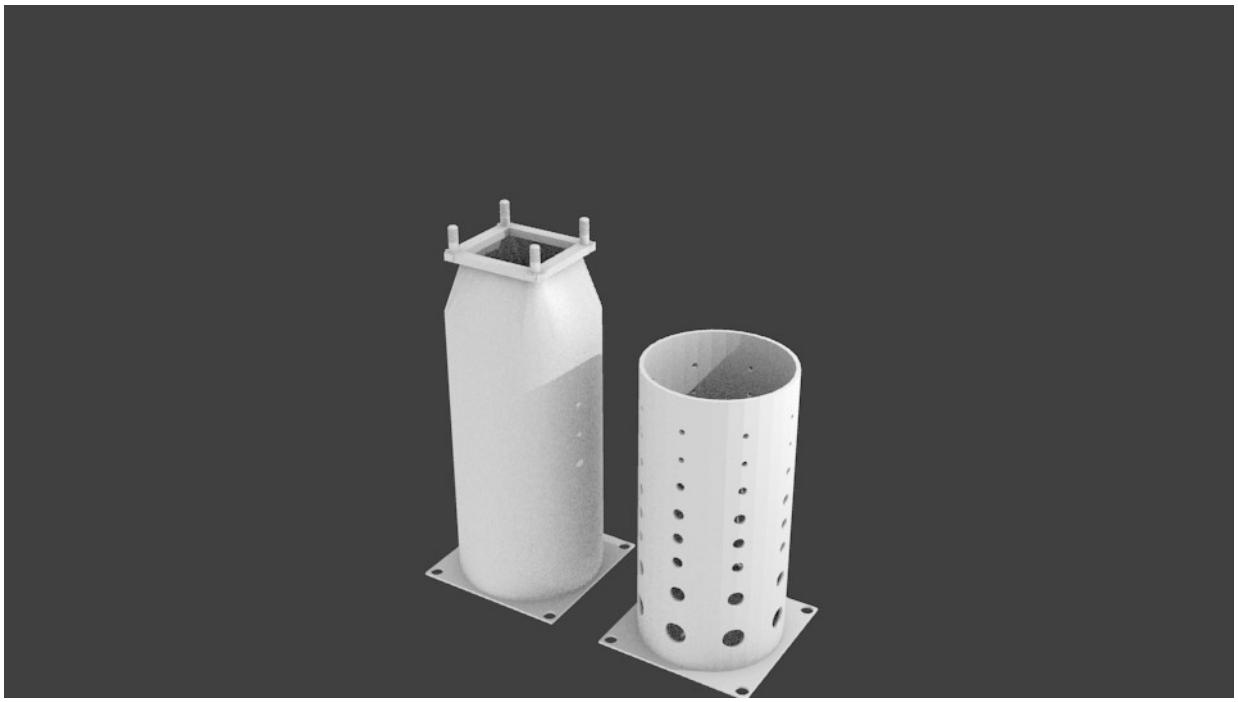

Fuel System

Propane was selected as the initial fuel source due to its being inexpensive, and easily obtained. Propane also is available as a pressurized gas which eliminated the need for a fuel pump and any specially fabricated atomizing nozzles which would be needed for a liquid fuel.

The combustion temperature of propane is approximately 1480 ^{o}C (2696 ^{o}F). Since steel melts at a temp of 1370 ^{o}C (2500^{o}F), the operating temp of the running engine would need to be closely monitored. The ignition temperature of propane 540 ^{o}C (1004 ^{o}F) was also a realistic and achievable goal for the ignition system.

An initial off-the-shelf propane regulator was utilized but this provided insufficient flow. Therefore the system was redesigned utilizing a ball valve regulator which proved capable of delivering sufficient fuel flow and was highly reliable.

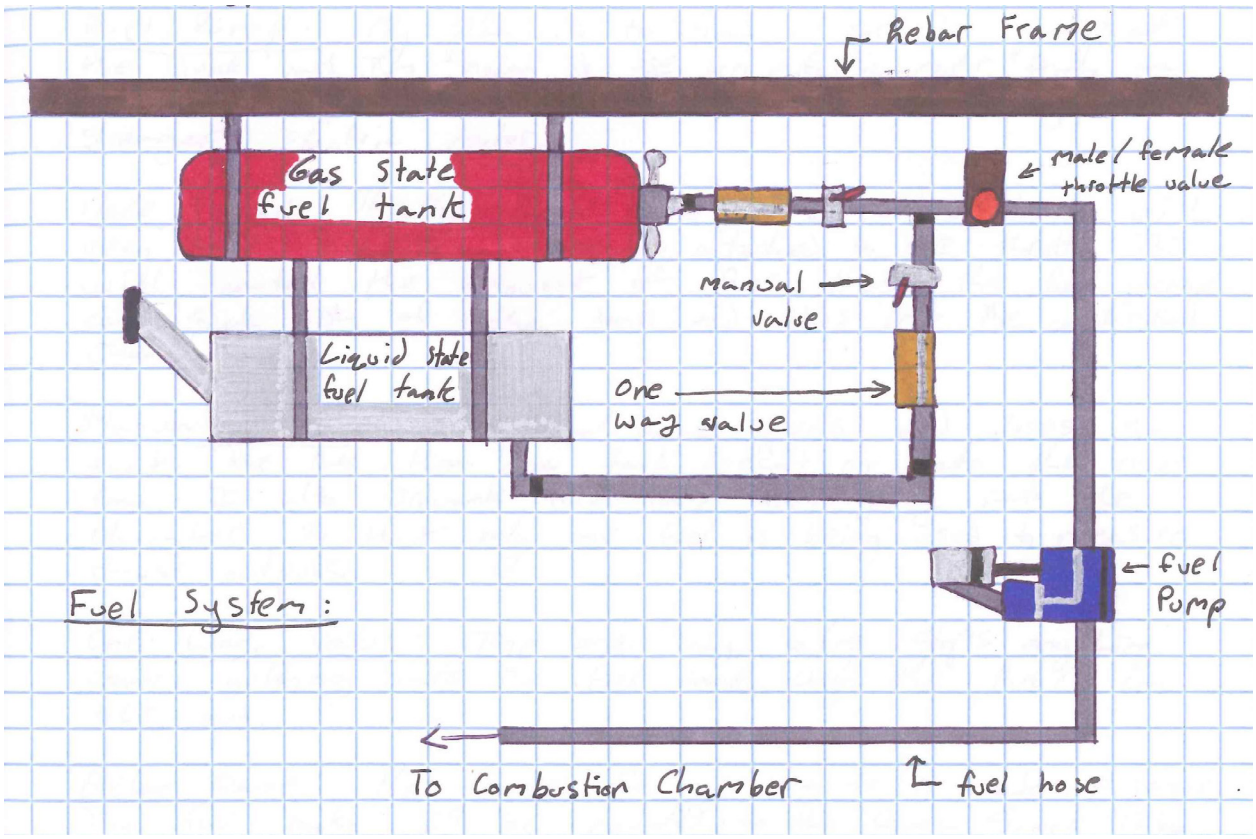

Lubrication System

The preliminary lubrication system design utilized a 120VAC motor to run a centrifugal pump and utilized an external oil reservoir to provide oil volume. A pressure gauge and ball reducer valve were utilized to regulate oil pressure to the turbine bearing.

Initial testing resulted in very high oil pressures. An additional rheostat was installed on the motor to regulate speed and further allow pressure to be regulated. In the end this system worked well with the exception of minor oil leaks.

It is possible that the initial high oil pressures reached in the initial design may have led to the turbine bearing failure which prevented the final testing of the redesigned flame tube.

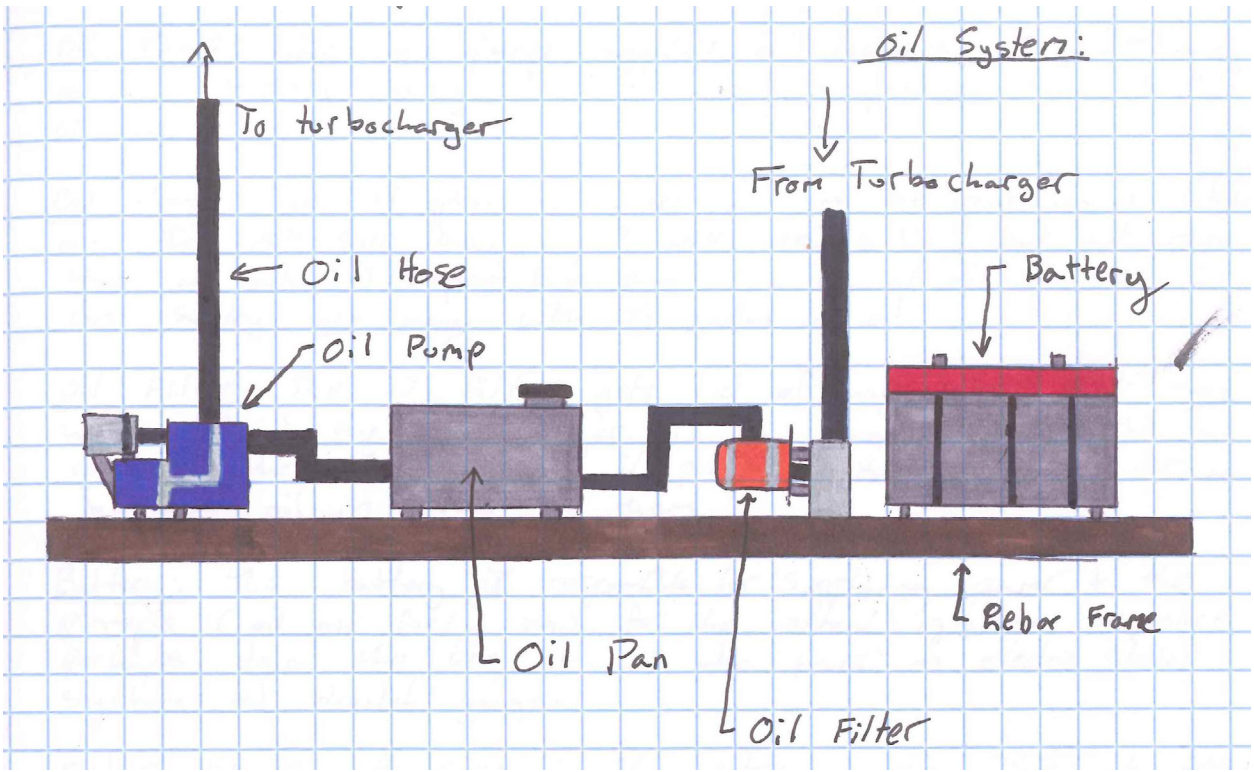

Ignition System

The selection of propane as the fuel required an ignition system which would reach at least 540 ^{o}C (1004 ^{o}F). An automotive glow plug was initially utilized. Although the glow plug was able to ignite the propane, it required a large bulky 12V power supply and also did not prove reliable. A final design was selected which utilized a simple peizo-electric igniter for a propane grill. This design proved efficient and reliable.

Thrust Nozzle

The thrust nozzle creates the exhaust jet (v_e) by turning high pressure, slow velocity gas into lower pressure, high velocity, gas by constricting the gas flow. Utilizing the Ideal gas law;

$$PV = \text{constant}$$

It can be seen that as the pressure decreases exiting the nozzle, the velocity increases.

This increases the engines thrust

- $\mathbf{F_N = (\dot{m}_{air} + \dot{m}_{fuel})v_e - \dot{m}_{air} v}$
    - F_N = net thrust of the turbojet (N)
    - $\dot{m}_{air}$ = the mass flow rate of air flow through the engine (kg/s)
    - $\dot{m}_{fuel}$ = the mass flow rate of fuel entering the engine (kg/s)
    - v_e = the velocity of the exhaust plume (m/s)
    - v= the velocity of the air intake (m/s)
    - $(\dot{m}_{air} + \dot{m}_{fuel})v_e$ = the nozzle gross thrust (F_G)
    - $\dot{m}_{air}$ v= the ram drag of the intake air

The thrust nozzle can be either convergent resulting in subsonic v_e , or convergent-divergent resulting in supersonic v_e

In this project a convergent nozzle design was incorporated due to fabrication limitations. No problems were encountered with this design in testing and no modifications were performed.

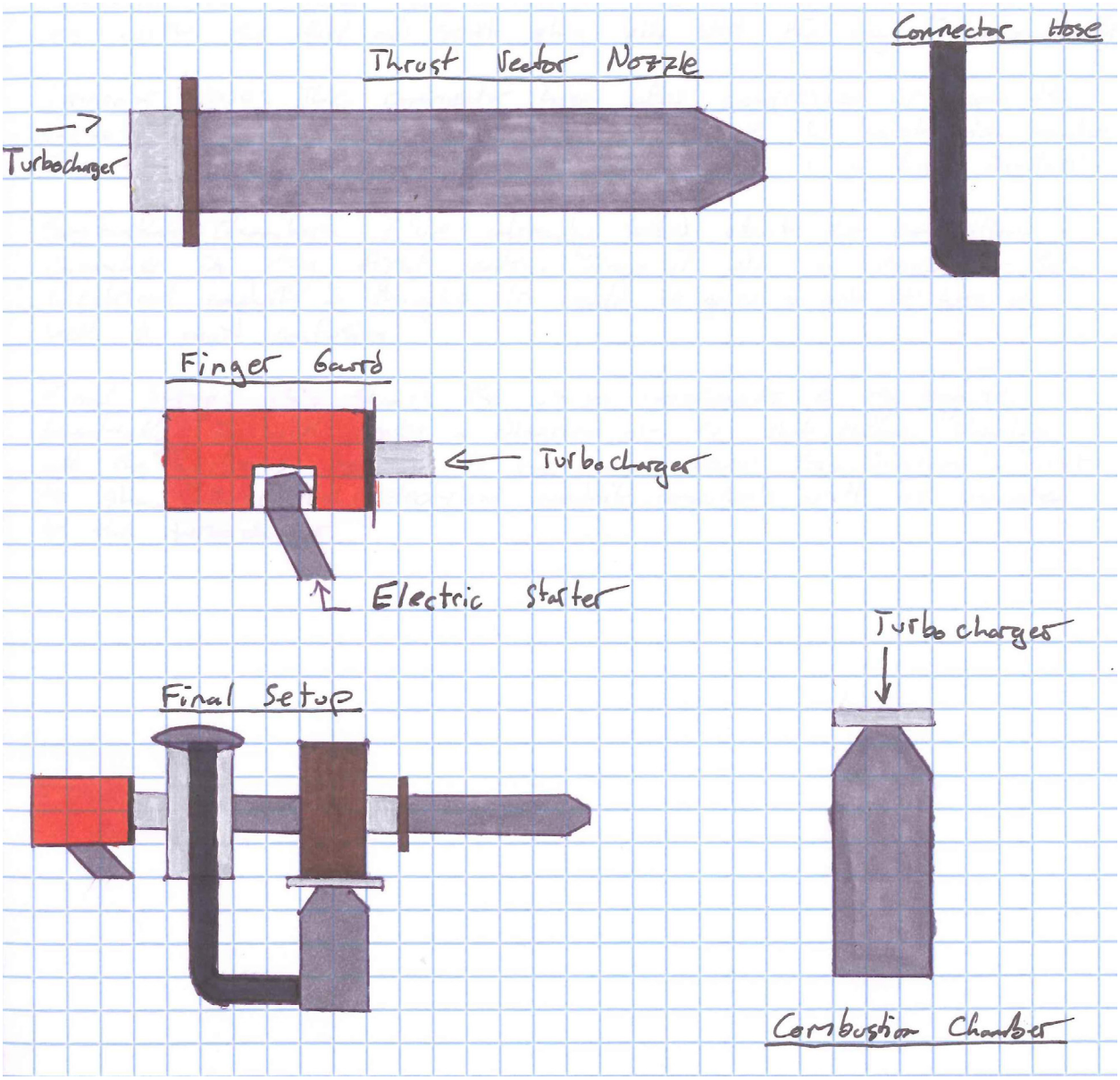
Connector Hose
Thrust Vector Nozzle
Turbocharger
Finger Guard
Turbocharger
Electric Starter
Turbocharger
Final Setup
Combustion Chamber

Starting System

A system to force air through the engine to spool up the turbine and allow flow the engine to light off was designed. Initially a leaf blower was fitted to the inlet. This proved to be bulky and noisy restricting communication between operators during engine operation. A final solution was to utilize the exhaust form a large shop vacuum. This proves sufficient to spool up the turbine and light off the engine.

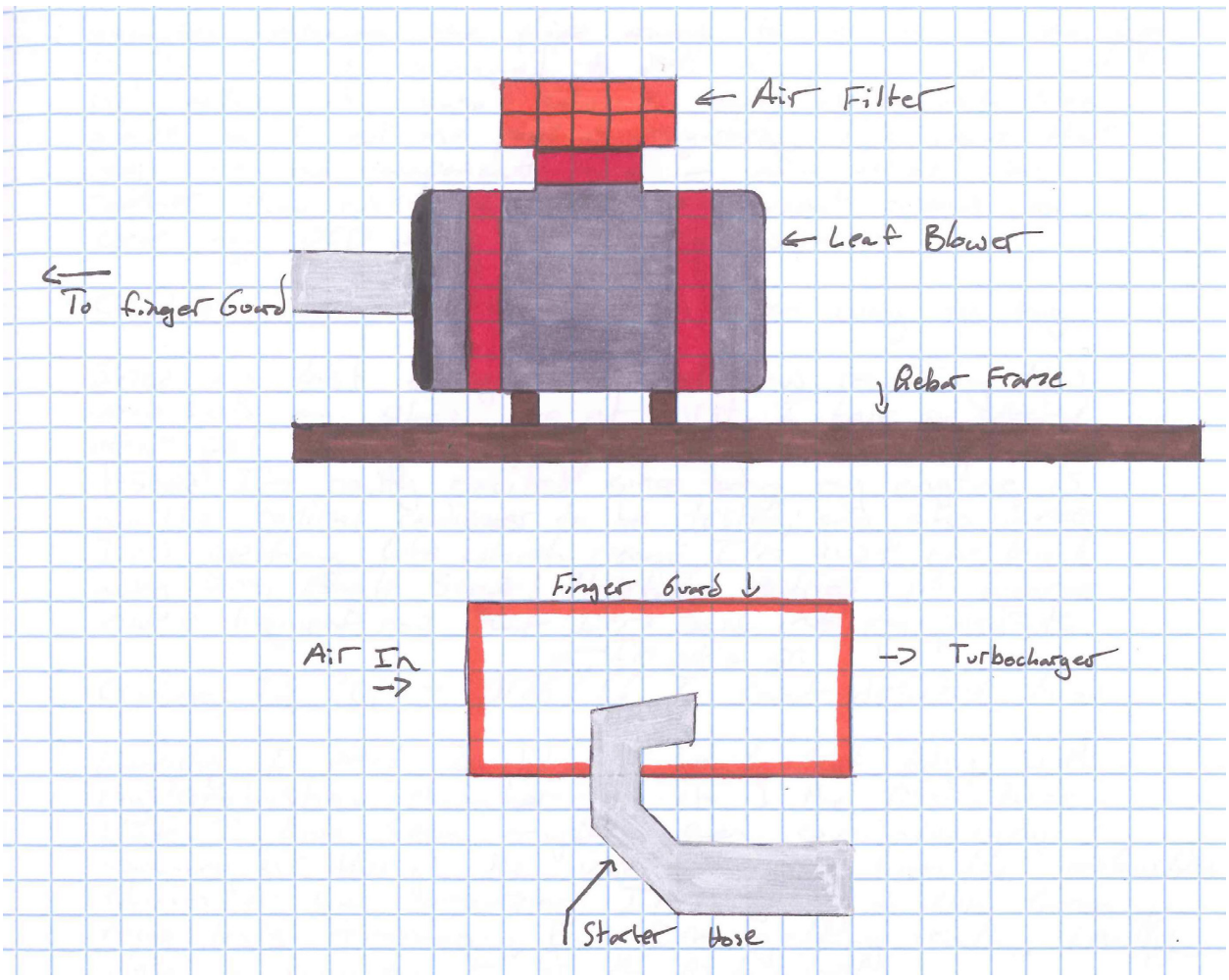

Prototype Results

A final prototype was constructed from the subsystems and successfully run on a number of occasions. The engine required a non-zero intake velocity to remain running, indicating a flaw in the flame tube/combustion chamber design. A new flame tube was designed but was unable to be implemented and tested due to a fracture of the turbocharger shaft during bearing replacement.

Conclusions

It is possible to construct an external flame tube turbojet engine with a centrifugal compressor/turbine assembly utilizing an automotive turbocharger as the turbine.

To further this experiment I would like to:

- Build and implement the redesigned combustion chamber.
- Consider the use of a convergent-divergent thrust nozzle to increase thrust
- Implement varying fuel types (kerosene, hydrogen etc.)
- Consider a larger and more robust turbocharger
- Reevaluate the lubrication system and ensure it is adjusted for the turbocharger bearing oil pressure ratings
- Fabricate a more industrial ignition system.
- Measure design parameters on fully operational engine
    - Thrust - $\mathbf{F_N}$
    - Exhaust velocity - v_e
    - Mass flow rate of air flow through the engine - $\dot{m}_{air}$
    - Fuel mass flow rate - $\dot{m}_{fuel}$

Bibliography

Gunston, Bill. The Development of Jet and Turbine Aero Engines. 4th ed. Sparkford: Haynes Publishing, 2006. Print.

Golley, J. (2010). Jet: Frank Whittle and the invention of the jet engine. (5th ed.). London: Datum Publishing.

Hill, Philip; Peterson, Carl (1992), Mechanics and Thermodynamics of Propulsion (2nd ed.), New York: Addison-Wesley

Chasing the sun – Frank Whittle; PBS

Mattingly, Jack D. (2006). Elements of Propulsion: Gas Turbines and Rockets. AIAA Education Series. Reston, VA: American Institute of Aeronautics and Astronautics.

Encyclopedia Astonautica

Factsheets, Pratt and Whitney J58 Turbojet

Aircraft, Lockheed SR-71 Blackbird

Aircraft Aerodynamics and Design Group. Stanford University.

Acknowledgements

I would like to thank my Father for helping me with this this project and teaching me how to weld, my Physics Teacher, Mr. Watson, for his help and guidance in completing this project, and my Gifted Teacher, Mr. Martinez, for helping me to begin planning this project and for his encouragement and support. Finally, I would like to thank my Grandfather, Dr. Bruno Manz, for much discussion about Physics and Newton's laws of mechanics.

Glossary

Flame tube

- Perforated steel tube designed to allow fuel and air to combine allowing for a combustible mixture to be achieved.
- Houses the fuel inlet and the ignition spark

Combustion Liner

- Outer steel tube which houses the flame tube and contains and focuses exhaust gases forcing them into the exhaust turbine.

Combustion chamber

- Combination of the Flame tube and the Combustion liner.

Axial turbine

- A turbine in which the fluid flow is in the direction of the rotational axis of the turbine.
- Driven by the hot exhaust gasses the axial turbine then drives the compressor by a common shaft

Centrifugal compressor

- A compressor which utilizes the centrifugal force to increase a fluids velocity and compress it. Takes atmospheric air and forces compressed air into the combustion chamber

Fuel system

- Provides and controls combustible material flow to the combustion chamber. In this design, propane was utilized as the fuel

Oil system

- Provides lubrication to the turbine bearings

Ignition system

- Creates spark to ignite fuel. In this design a piezo-electric spark system was utilized

Thrust

- The force created by the exhaust gases based upon Newton's third law (when a system expels accelerated mass in one direction, it will experience a force of equal magnitude in the opposite direction, F=ma)

Appendix: Materials

Item	Quantity
T3T4 Automotive Turbocharger	1
½ Inch Rebar	10 ft
¼ Inch Rebar	13 ft
¼ Inch ID Nylon Tubing	5 ft
6 Inch Diameter Steel Pipe	1 ft
3 Inch Diameter Steel Pipe	9 in
12X18 Inch; Steel Plate	1
16X12 Inch; Steel Plate	1
High Pressure Steel Braided Hose	2
Procon Oil Pump; Centrifugal	1
Electric Motor ¼ HP Carbonate	1
½ Inch Plastic/Acrylic Wheels	4
Metric Thread 14mm Nipple	2
Velcro	6 in
Hose Clamp ¼ Inch/ ½ Inch	16
Hillman Group $^{9}/_{16}$ Inch Washers	50
Teflon Tape ¼ Inch	1 roll
Crown Bolt $^{9}/_{16}$ Inch 5 Coarse Hex Bolt	8
Zip Ties	1 pkge
Plastic Nipple ½ Inch MPT	2
Prime Line ¼ Inch Carriage Bolt With Nut	4
Flat Washer ¼ Inch	100
Galvanized male-male ½ Inch fitting	1
Brass ½ Inch Nipple Barb	6
Steel “L” Bracket $^{1}/_{8}$ Inch	2
Aluminum Plate $^{1}/_{8}$ Inch	1
Item	Quantity

Radiator Hose Flexible 1 ½ Inch (25 Inches)	1
Dynomax Exhaust Pipe	1
Hose Clamp 1 Inch	3
Char Broil Grill Hose and Adaptor	1
Battery Tray	1
Quick Steel	1 pkge
Norpro Stainless Steel 4-$^{3}/_{4}$ Inch Funnel	1
SE Electronic Stepless Rheostat	1
Shrink Wrap	1 pkge
Brinkman Universal Push Button Igniter	1
¼ Liter 2 stroke gas tank	1
Pneumatic plus 15 PSI pressure gauge	1
Mueller $^{3}/_{8}$ Inch Brass NPT Ball Valve	2
Brass ¼ Inch “T” Joint	1
$^{3}/_{8}$ inch X 72 Inch Threaded Rod	1
$^{3}/_{8}$ Inch Hex Nuts	100
$^{3}/_{8}$ Inch Washers	100
Husky 4 Piece Quick Connect Kit	1
JMF 900 Brass Elbow	2
Zenport Zen-Tek Glycerin Filled Pressure Gauge	1
Sharkbite $^{1}/_{2}$X$^{1}/_{2}$Inch Brass MPT Male Adaptor	2

THE NEW MEXICO ACADEMY OF SCIENCE

The New Mexico Academy of Science was founded in 1902 to foster scientific research and scientific cooperation, to increase public awareness of the role of science in human progress and welfare, and to promote science education in New Mexico.

Membership in the Academy is open to anyone interested in science, science education, or the other goals and programs of the Academy. Individuals engaged in scientific research or teaching at all levels are particularly encouraged to become members. Applications for membership as well as more information about the Academy and its programs can be found at http://www.nmas.org.

Contact Information:

The New Mexico Academy of Science
c/o The New Mexico Museum of Natural History and Science
1801 Mountain Road NW
Albuquerque, New Mexico 87104
nmas@nmas.org
http://www.nmas.org

Officers and Executive Board 2014

Officers

President: Dr. Michaela Buenemann
President-Elect: Dr. Jason Jackiewicz
Vice-President: Dr. Shanalyn Kemme
Treasurer: Dr. Vincent Gutschick
Secretary: Mrs. Malva Knoll
Past President: Dr. Kurt Anderson
Director at Large: Ms. Debra Novak
Director-at-Large: Mr. Hal Behl

Directors

Mrs. Jayne C. Aubele; Museum Liason
Mrs. Lynn Brandvold; New Mexico Junior Academy of Science
Mr. John Irwin; NMAS Awards Program
Dr. Marvin Moss; NMAS Lecture Series
Dr. Richard Nygren; National Youth Science Camp
Dr. Hartono Sumali; Outreach

Directors Emeritus

Dr. David Hsi
Mrs. Mona Pomeroy
Dr. Maureen Romine